Institut für Pharmakologie und Klinische Pharmazie

Fachbereich Pharmazie

Voltage-dependence of adrenoceptor activity:

Mechanisms and signal transduction

Dissertation

zur Erlangung des Doktorgrades
der Naturwissenschaften
(Dr. rer. nat.)

dem Fachbereich Pharmazie
der Philipps-Universität Marburg
vorgelegt von

Alexandra Christine Birk

aus Stuttgart

Marburg/Lahn, **2015**

Erstgutachter: Prof. Dr. Moritz Bünemann
Zweitgutachter: Prof. Dr. Jens Kockskämper

Eingereicht am 6. November 2015

Tag der mündlichen Prüfung am 18. Dezember 2015
Hochschulkennziffer: 1180

Table of contents

Abbreviations

[^{3}H]	Tritium
5-HT_{2A} receptor	5-hydroxytryptamine receptor 2A
A	Alanine
a.u.	Arbitrary unit
AC	Adenylyl cyclase
ACh	Acetylcholine
ADP	Adenosine diphosphate
Adr	Adrenaline
ANOVA	Analysis of variance
AP2	Clathrin-adapter protein 2
AR	Adrenoceptor
Arr / Arr3	Arrestin / arrestin 3
BCA	Bicinchoninic acid
BRET	Bioluminescence resonance energy transfer
cAMP	Cyclic adenosine monophosphate
CCh	Carbachol
CCP	Clathrin-coated pit
Cer	Cerulean, variant of CFP
CFP	Cyan fluorescent protein
CHO	Chinese hamster ovary
Cl	Clonidine
CNS	Central nervous system
Cpm	Counts per minute
CS	Cover slips
D	Aspartic acid
D2R	Dopamine D_2 receptor
D2SR	Short splice variant of D2R
DA	Dopamine
DNA	Deoxyribonucleic acid
DOB	Dobutamine
Dpm	Disintegrations per minute
E	Glutamate
E.coli	Escherichia coli

EC50	Half maximal effective concentration
FCS	Fetal calf serum
FRET	Förster resonance energy transfer
GDP	Guanosine diphosphate
GEF	Guanine nucleotide exchange factor
GFP	Green fluorescent protein
GIRK	G protein-coupled inwardly-rectifying potassium channel
GPCR	G protein-coupled receptor
GRK	G protein-coupled receptor kinase
GTP	Guanosine triphosphate
H_3R/H_4R	Histamine $H_{3/4}$ receptor
HEK	Human embryonic kidney
HK	Buffer of high potassium concentration
Iso	Isoprenaline
K	Lysine
L	Leucine
LPA	Lysophosphatidic acid
$M_{1/2/3}AChR$	Muscarinic acetylcholine receptors 1/2/3
MAP kinase	Mitogen-activated protein kinase
$mGluR_{1/3/5}$	Metabotropic glutamate receptor 1/3/5
N	Asparagine
NA	Noradrenaline
ND	Buffer of low potassium concentration
NTP	Nucleoside triphosphate
OH-group	Hydroxyl group
P_2Y_1R	Purinergic P_2Y_1 receptor
PCR	Polymerase chain reaction
PIP_2	phosphatidylinositol 4,5-bisphosphate
PKA	Protein kinase A
PKC	Protein kinase C
PTX	Pertussis toxin
RT	Room temperature
S	Serine
SEM	Standard error of the mean

SNP	Single nucleotide polymorphism
TM	Transmembrane
TXA2	$Thromboxane_{A2}$
V_{50}	Half maximal effective potential
V_M	Membrane potential
W	Tryptophan
Y	Tyrosine
YFP	Yellow fluorescent protein
Yoh	Yohimbine
β_1-AR	β_1-adrenoceptor
β_2-AR	β_2-adrenoceptor
α_{2A}-AR	α_{2A}-adrenoceptor

1 Summary

G protein-coupled receptors comprise a large superfamily of membrane proteins which transmit extracellular stimuli into intracellular responses. Adrenoceptors (AR) belong to the α-group of *Rhodopsin*-family G protein-coupled receptors. Physiological activation of adrenoceptors is mediated by binding of the endogenous catecholamines noradrenaline and adrenaline and leads to the regulation of neuronal, endocrine, cardiovascular, vegetative and metabolic functions. In addition to the classical activation of GPCRs by binding of ligands, experimental evidence has accumulated showing that GPCR activation can be modulated by the membrane potential. In this study adrenoceptors β_1-AR and β_2-AR have been investigated in regard to the modulation of their activity by the membrane potential. Both receptors couple to the stimulatory G_s protein. They were used as model receptors because despite increasing knowledge of voltage-dependent regulation of G_i- and G_q-coupled receptor activity, no data has been published on the voltage-sensitivity of G_s-coupled receptors.

Förster resonance energy transfer (FRET)-based assays were combined with whole-cell patch-clamp in a voltage-clamp mode in order to monitor agonist- and voltage-dependent alterations in either protein conformation or protein-protein interaction. Conformational changes of the receptor molecule upon stimulation with catecholamines in the presence or absence of depolarizing steps were directly monitored using FRET-based intramolecular receptor fusion proteins. By means of the combination of FRET and patch-clamp, voltage-dependence of β_1-AR and to smaller extent β_2-AR activation was shown to be an intrinsic property of these G_s-coupled receptors and was transmitted to downstream signaling. Receptor activity and downstream signaling decreased during depolarization. This expands voltage-dependent GPCRs to the group that couple to stimulatory G proteins. Voltage-dependence of β_1-AR was mainly mediated via an alteration in efficacy of either Iso or Adr and occurred with highest sensitivity at physiological membrane potentials. Regarding Adr this is a unique finding since voltage-dependence of other GPCRs activated by their endogenous ligands were shown to rely on alterations in ligand affinity. Agonist-specificity of voltage-dependence was also apparent as dopamine-induced β_1-AR interaction with arrestin 3 was enhanced during depolarization whereas it was reduced when induced by adrenaline, isoprenaline, noradrenaline or dobutamine. A different binding mode of dopamine might be responsible for these differences.

The second part of this thesis focused on the molecular mechanism underlying voltage-dependence. Mutation of a charged amino acid and a residue involved in agonist binding did not seem to alter voltage-dependence or only yielded inconclusive results. However, the introduction of an additional positive charge in the vicinity of a highly conserved aspartic acid in TM2 ($D^{2.50}$) reduced voltage-dependence of the mutant receptor. We might have identified this aspartic acid as one residue of a voltage-sensor in α_{2A}-AR but further experiments are required in order to corroborate this hypothesis.

Taken together these data expand voltage-dependent GPCRs to the group coupling to G_s proteins. Especially in excitable tissue like the heart, which expresses voltage-dependent β_1-AR the membrane potential could fine-tune adrenoceptor signaling on a time scale within cardiac action potentials and in the presence of endogenous or synthetic catecholamines. On a molecular level we suggest a possible involvement of the highly conserved aspartic acid $D^{2.50}$ in the detection of alterations in the membrane potential in α_{2A}-AR. Whether this conclusion is also transferable to other G protein-coupled receptors remains to be investigated.

Keywords: Förster resonance energy transfer (FRET), G protein-coupled receptor (GPCR), adrenoceptors, voltage-dependence, G_s protein, voltage-sensor, affinity, efficacy, mechanism of voltage-dependence.

2 Zusammenfassung

G Protein-gekoppelte Rezeptoren bilden eine Superfamilie von Membranproteinen, die extrazelluläre Stimuli ins Zellinnere weiterleiten. Adrenozeptoren (AR) sind G Protein-gekoppelte Rezeptoren (GPCRs), die der α-Untergruppe der Rhodopsin-Familie angehören. Die endogenen Katecholamine Noradrenalin und Adrenalin führen über die Aktivierung von Adrenozeptoren zur Regulation verschiedenster neuronaler, endokriner, kardiovaskulärer, vegetativer und metabolischer Funktionen. Zusätzlich zur klassischen Aktivierung von GPCRs durch Agonistenbindung an einen Rezeptor konnte die Regulation der Aktivität durch eine Veränderung des Membranpotentials für eine Reihe G_i- und G_q-gekoppelter Rezeptoren gezeigt werden. Zu Beginn dieser Arbeit war jedoch noch keine Untersuchung zur Spannungsabhängigkeit G_s-gekoppelter Rezeptoren beschrieben. Deshalb wurde in dieser Arbeit die Aktivität der G_s Protein-gekoppelten Adrenozeptoren β_1-AR und β_2-AR hinsichtlich ihrer Modulation durch das Membranpotential untersucht.

Die Kombination Förster-Resonanz-Energie-Transfer (FRET)-basierter Messungen und der *patch-clamp* Methode im *voltage-clamp* Modus ermöglichte die Aufzeichnung agonist- und spannungsabhängiger Änderungen von Proteinkonformationen oder von Protein-Protein-Wechselwirkungen. Es wurden intramolekulare FRET-basierte Rezeptor-Fusionsproteine eingesetzt, um den Einfluss des Membranpotentials auf Bewegungen im aktivierten Rezeptormolekül direkt zu untersuchen. Für die Untersuchung von Protein-Protein-Wechselwirkungen kamen intermolekulare FRET-Sensoren zum Einsatz.

Mithilfe der Kombination aus FRET und elektrophysiologischen Messungen konnte in dieser Arbeit die Spannungsabhängigkeit des β_1-AR gezeigt werden, die sich in einer Aktivitätsabnahme bei Depolarisation äußerte. Auch der eng verwandte β_2-AR zeigte eine depolarisationsabhängige Abnahme der Aktivität, jedoch war diese schwächer ausgeprägt als bei β_1-AR. Die Spannungsabhängigkeit übertrug sich für beide Rezeptoren auch auf die nachgeschaltete Signalkaskade. Diese Ergebnisse erweitern den Kreis spannungsabhängiger Rezeptoren um die Gruppe G_s-gekoppelter Rezeptoren.

Im Falle des β_1-AR wurde die Spannungsabhängigkeit hauptsächlich über eine Änderung der intrinsischen Aktivität der Agonisten Isoprenalin und Adrenalin vermittelt. Dies ist erstaunlich, da bisher die Spannungsabhängigkeit von Rezeptoren, die durch endogene Agonisten aktiviert wurden, nur eine Regulation der Agonistaffinität bekannt war. Es konnte ebenfalls eine agonistspezifische Komponente der β_1-AR Spannungsabhängigkeit ermittelt werden: Mit Dopamin aktivierte Rezeptoren zeigten eine Zunahme ihrer Aktivität während der Depolarisation während die Isoprenalin-,

Noradrenalin-, Adrenalin- und Dobutamin-vermittelte Aktivität bei positiven Membranpotentialen abnahm. Der entgegengesetzten Spannungsabhängigkeit von Dopamin-aktivierten Rezeptoren könnte ein geändertes Bindungsverhalten von Dopamin in der Rezeptorbindetasche zugrunde liegen.

Der zweite Teil dieser Arbeit beschäftigt sich mit der Untersuchung des molekularen Mechanismus, der der Spannungsabhängigkeit zugrunde liegt. Hierfür wurden verschiedene Aminosäuren im spannungsabhängigen α_{2A}-AR mutiert. Die Neutralisation einer geladenen Aminosäure und der Änderung einer Aminosäure, die an der Agonistbindung beteiligt ist, schienen die Spannungsabhängigkeit nicht zu beeinflussen. Jedoch führte das Einbringen einer zusätzlichen, positiven Ladung in die Nähe des hochkonservierten Aspartats $D^{2.50}$ in TM2 zu einer Reduktion der Spannungsabhängigkeit. Diese Aminosäure könnte eine Komponente des Spannungssensors des α_{2A}-AR sein, jedoch sind weitere Experimente nötig, um diese Hypothese zu untermauern.

Zusammengefasst erweitern die in dieser Arbeit vorgestellten Daten die Gruppe der spannungsabhängigen GPCR um jene, die ihr Signal über stimulatorische G_s-Proteine vermitteln. Besonders in erregbaren Geweben wie dem Herzen, das β_1-AR exprimiert, könnte das Membranpotential für eine zusätzliche Feinregulation der Rezeptoraktivität sorgen. Dies könnte sich im zeitlichen Rahmen kardialer Aktionspotentiale abspielen und ohne die Dissoziation des Agonisten vor sich gehen. Auf molekularer Ebene ist eine Beteiligung des hochkonservierten Aspartats in TM2 ($D^{2.50}$) an der Erkennung von Spannungsänderungen der Plasmamembran im α_{2A}-AR denkbar. Ob sich dies auch auf andere spannungsabhängige GPCRs übertragen lässt, bleibt zu ermitteln.

Stichworte: Försterresonanzenergietransfer (FRET), G Protein-gekoppelte Rezeptoren, Adrenozeptoren, Spannungsabhängigkeit, G_s Protein, Spannungssensor, intrinsische Aktivität, Affinität, Mechanismus der Spannungsabhängigkeit.

3 Introduction

A plasma membrane surrounds all living cells and separates the cytoplasm from the extracellular environment. It is a bilayer formed by amphiphilic phospholipids and embedded proteins and acts as a barrier for charged molecules. Different concentrations of ions within the cell or the extracellular space separated by the plasma membrane cause a gradient. Electrodiffusion along this gradient leads to a charge separation and to the generation of the membrane potential. The strong electrical field that arises from the charge separation across the very thin plasma membrane can be used by membrane proteins to generate their functions or to allosterically alter their function. Voltage-gated ion channels are prototypical for membrane proteins whose activity is regulated by the membrane potential. A stretch of basic amino acids in one transmembrane (TM) domain of each subunit moves through the membrane upon alterations in its potential causing conformational changes in the ion channel molecule. The membrane potential also influences the activity of voltage-dependent phosphatases or of some ion carriers and pumps (Molleman, 2003; Bezanilla, 2008). Within the last 12 years evidence has accumulated that also the activity of agonist-occupied G protein-coupled receptors (GPCRs) can be modulated by the membrane potential (V_M). This voltage-dependence of GPCRs, using the example of adrenoceptors (ARs), will be the topic of this study.

3.1 G protein-coupled receptors

The human genome encodes for over 800 different G protein-coupled receptors which are phylogenetically divided into five different receptor families with several subgroups: The *Rhodopsin-*, the *Secretin-*, the *Glutamate-,* the *Adhesion-* and the *Frizzled/TAS2-* receptor families (Takeda et al., 2002; Fredriksson et al., 2003; Katritch et al., 2013). A diversity of ligands including amines, peptides, glycoproteins, ions and proteases as well as exogenous stimuli like light or organic odors are able to activate GPCRs leading to GPCR-mediated cellular responses (Takeda et al., 2002; Fredriksson et al., 2003). As GPCRs control a variety of signal transduction processes in the human body they are targets for about 36% of drugs listed in the DrugBank (Rask-Andersen et al., 2011).

Biochemical and theoretical studies as well as a low resolution projection map of rhodopsin suggested common structural features for GPCRs (Baldwin, 1994). 15 years ago the crystal structure of bovine rhodopsin was solved and a few years later solved again with higher resolution (Palczewski, 2000; Li et al., 2004; Okada et al., 2004). Since then

technological progress enabled the crystallization of more GPCRs in both active and inactive states ((Tate and Schertler, 2009) reviewed in (Katritch et al., 2013)).

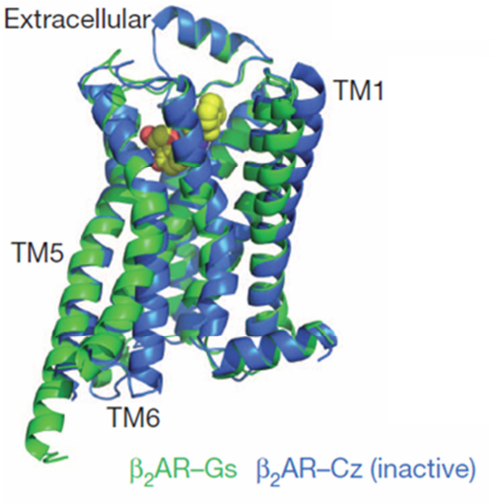

Figure 1: Inactive and active state crystal structures of the β_2-adrenoceptor.
The active (green) and inactive (blue) structures of an engineered β_2-adrenoceptor are overlaid in their side views and show the seven transmembrane helices and parts of the extra- and intracellular loops. The active structure was obtained as a ternary complex of the agonist-bound receptor and the nucleotide-free G_s protein heterotrimer. The inactive structure was obtained in the presence of carazolol (Cz). The ligand is shown as yellow spheres. Activation-dependent structural changes are most prominent in the intracellular parts of transmembrane domains five and six (Rasmussen et al., 2011a).

These crystal structures confirmed that GPCRs share a common structure of seven transmembrane α-helices, connected by intra- and extracellular loops of variable length, an extracellular amino and an intracellular carboxyl terminus (Figure 1). Because of the seven TM bundle, GPCRs are also referred to as 7-TM or heptahelical receptors (Huber et al., 2008). Although GPCRs share this common structure, the overall sequence homology is low (Gether, 2000).

3.1.1 G protein coupled receptors transduce extracellular stimuli into intracellular signals

Activation of GPCRs and further signal transduction is a multistep process which is initiated by the binding of a ligand to the receptor or induced by photons in case of rhodopsin. An orthosteric ligand binding pocket is located inside the TM-bundle in most GPCRs whereas others bind there ligands at their amino termini (Baldwin, 1994; Fredriksson et al., 2003). Ligand binding to the receptor initiates conformational changes in the receptor molecule starting at the ligand binding site and expanding via the transmembrane helices with several conformational intermediates (Kobilka and Deupi, 2007; Hofmann et al., 2009). The most prominent transmembrane movements seen between crystal structures of the inactive β_2-AR and active β_2-AR in complex with the G_s

protein are an outward movement of TM6 and an extension of the cytoplasmic end of TM5 (Figure 1).

Movements of TM5 and TM6 open a cleft on the cytosolic side of the receptor in which the Gα-subunit's carboxyl terminus can interact with its binding moieties (Figure 2, (Rasmussen et al., 2011a)). The conformational changes and intermediates, however, vary between receptors and can also vary within one receptor when activated by different ligands (Kobilka and Deupi, 2007). In a ternary complex consisting of the agonist, the receptor and the G protein, the receptor is stabilized in its fully activated state (Rasmussen et al., 2011b).

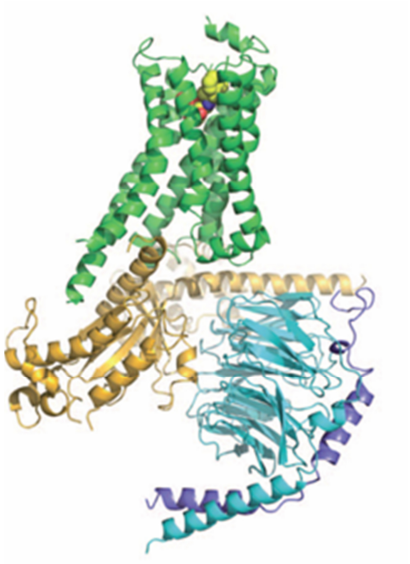

Figure 2: The ternary complex of an agonist-occupied β_2-adrenoceptor and a stimulatory G protein. The agonist-activated β_2-AR (agonist: yellow spheres, receptor: green) is shown in complex with the stimulatory G_s protein with its α- (orange), β- (cyan) and γ- (purple) subunits (modified from (Rasmussen et al., 2011a)).

3.1.1.1 The G protein cycle

Upon activation of a GPCR by a ligand, membrane-bound heterotrimeric G proteins are recruited to the receptor (Figure 3). These heterotrimeric G proteins consist of a Gα-, a Gβ- and a Gγ-subunit and so far 23 different Gα-, 5 Gβ- and 14 Gγ-subunits have been identified in humans. Gα-subunits are divided into the four long known classes $G\alpha_s$, $G\alpha_i$, $G\alpha_q$ and $G\alpha_{12}$ based on sequence homology and are further subdivided into 2-4 groups each. Gβ and Gγ solely function as heterodimers and the dimer will be referred to as βγ-subunit or simply βγ. Due to the number of different Gβ- and Gγ-subunits many functional dimer combinations can be formed (Simon et al., 1991; McCudden et al., 2005; Milligan and Kostenis, 2006; Oldham and Hamm, 2008).

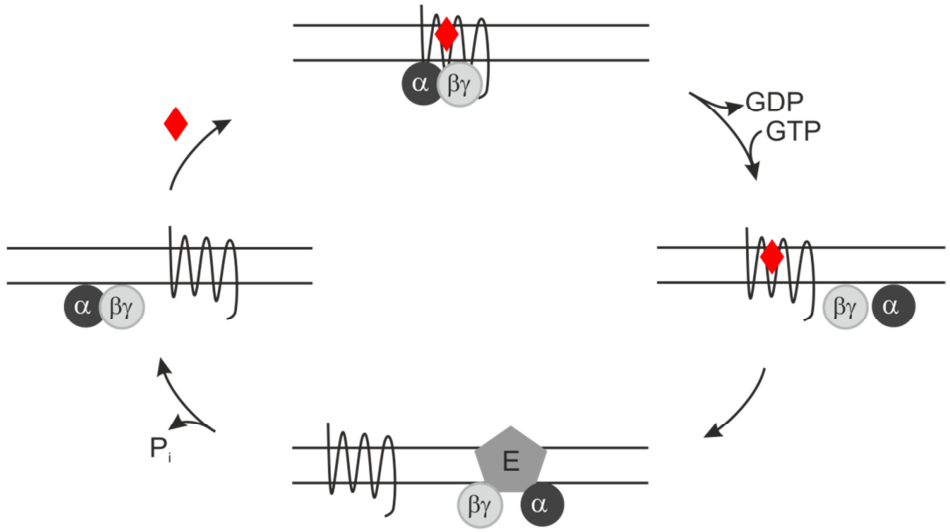

Figure 3: The G protein cycle.
The schematic shows different steps of the G protein cycle. Binding of a ligand (red diamond) to a receptor induces interaction of the heterotrimeric G protein (βγ is represented as one gray sphere only) with the activated receptors. The activated G protein dissociates from the receptor upon nucleotide exchange and an activating conformational change (depicted as a rearrangement of the α- and βγ-subunits). The α- and βγ-subunits interact with effectors (gray pentagon, E) upon activation. Hydrolysis of GTP by the α-subunit's GTPase activity terminates the G protein cycle.

Activated GPCRs serve as a guanine nucleotide exchange factor (GEF): They facilitate the exchange of GDP to GTP in the associated G protein by favoring a conformational change in the Gα-subunit's Ras domain which leads to G protein activation and dissociation from the receptor (Figure 3, (Tuteja, 2009; Dror et al., 2015)). The nucleotide exchange in the Gα-subunit marks the rate-limiting step of G protein-mediated signaling (Oldham and Hamm, 2007). A conformational change within the G protein, induced by the nucleotide exchange, was believed to cause dissociation of the GTP-bound Gα from the constitutive heterodimeric βγ-subunit (Hofmann et al., 2009). However, for the G_i protein a conformational rearrangement of the subunits upon activation rather than their dissociation has been described. In Förster resonance energy transfer (FRET)-based assays monitoring G_i protein activation an increase in FRET was detected upon receptor stimulation. If the subunits dissociated from each other, FRET would have decreased due to an increasing distance between the donor and acceptor fluorophore (5.3.3.1, (Bünemann et al., 2003)). Similar findings were observed in measurements that relied on bioluminescence resonance energy transfer (BRET) (Galés et al., 2006). A conserved region in the α-helical domain of G_i protein subtypes seemed to be required for the activation-dependent increase in FRET between fluorescently labeled $G\alpha_i$ and Gβγ-subunits (Frank et al., 2005). A decrease in FRET between fluorescently labeled α and βγ of the G_s protein upon receptor stimulation does not necessarily point towards subunit dissociation but could also result from a structural rearrangement leading to fluorophore orientations which do not favor energy

transfer (Hein et al., 2006) A dissociation of the subunits can be induced by binding of G protein effectors to the heterotrimeric complex (Figure 3, personal communication with Dr. Eva-Lisa Bodmann and Anna-Lena Krett and (Wolters, 2014)).

Upon G protein activation both α- and βγ-subunits transfer the signal to distinct intracellular effectors like enzymes or ion channels which in turn modulate diverse signaling pathways for example via the generation of second messengers. The G protein cycle is completed with the hydrolysis of GTP to GDP by the inherent GTPase activity of the Gα-subunit and the subsequent reassociation or deactivating rearrangement of the subunits (Figure 3, reviewed in (Wettschureck and Offermanns, 2005; Milligan and Kostenis, 2006; Oldham and Hamm, 2008; Reiter et al., 2012)). In addition to signaling via GPCRs located at the plasma membrane, a second phase of G protein-dependent signaling was suggested to arise from internalized GPCRs located on early endosomes (Irannejad et al., 2013).

Besides signaling through G proteins, several other protein families can also interact with activated GPCRs in a G protein-independent way. These include for example PDZ domain-containing proteins (Bockaert et al., 2004), non-receptor and receptor tyrosine kinases (Marrero et al., 1995; Sun et al., 2007), G protein-coupled receptor kinases (GRKs) and arrestins (Arr) (Pierce et al., 2002; Reiter et al., 2012). A large variety of allosteric modulators like ions, lipids, some drugs or the membrane potential can additionally alter GPCR activity and signaling (Christopoulos, 2002; Ben-Chaim et al., 2003; Katritch et al., 2014).

3.1.2 G protein-coupled receptor homologous desensitization and internalization is mediated by G protein-coupled receptor kinases and arrestins

GPCR-mediated signaling needs to be tightly regulated in order to maintain proper cell function. Apart from the recruitment of G proteins, activated GPCRs also represent targets for GRKs which phosphorylate serine and threonine residues in the C-terminus of GPCRs as a first step of homologous desensitization, i.e. desensitization of agonist-occupied receptors (Figure 4, (Pierce and Lefkowitz, 2001; Pierce et al., 2002; Krasel et al., 2005)). However, a new study has also described phosphorylation of unstimulated GPCRs by GRKs of the GRK4 family (Li et al., 2015). A second form of desensitization, the heterologous desensitization, which occurs independently of agonist occupancy of the receptor, is induced by protein kinase A (PKA)- and protein kinase C (PKC)-mediated receptor phosphorylation (Pierce and Lefkowitz, 2001) but will not be described in detail here.

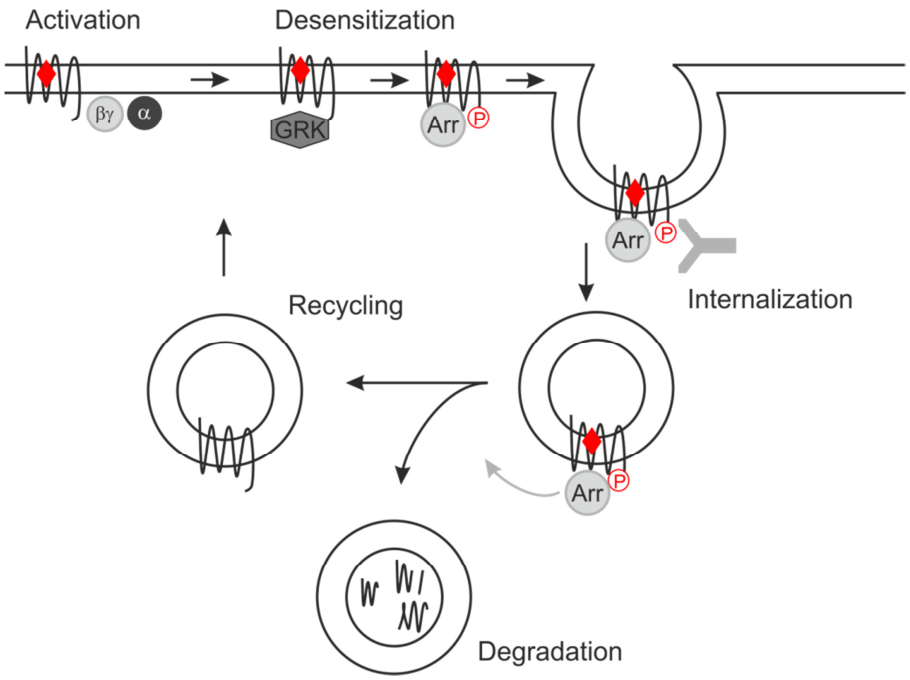

Figure 4: G protein-coupled receptor homologous desensitization and internalization.
Members of the G protein-coupled receptor kinase 2 family (gray hexagon) phosphorylate agonist-occupied receptors. Arrestins translocate to agonist-activated and phosphorylated receptors and the complex accumulates in clathrin-coated pits (clathrin: gray, Y-shaped). Arrestin dissociates from internalized receptors or only transiently interacts with receptors at the plasma membrane. Receptors are either dephosphorylated and cycle back to the membrane or will be degraded in lysosomes.

3.1.2.1 G protein-coupled receptor kinases

GRKs are a family of serine/threonine kinases with seven members (GRK1-7). The expression of GRK1 and 7 is restricted to the retina and GRK4 is mainly expressed in the brain, kidneys and testes. GRK2, GRK3, GRK5 and GRK6, in contrast, are ubiquitously expressed (Pierce et al., 2002; Shenoy and Lefkowitz, 2003). The GRK subtypes also differ in their localization within the cell. GRK2, GRK3 and GRK5 are cytosolic proteins. Translocation to the membrane of GRK2 and GRK3 is facilitated by the binding of the βγ-subunit of G proteins to the GRK's c-terminal PH-domain. The membrane association of GRK5, in contrast, is promoted by phosphatidylinositol 4,5-bisphosphate (PIP_2). A constant tethering to the plasma membrane of GRK1, GRK7, GRK4 and GRK6 is achieved by farnesylation of the first two and palmitoylation of the latter two GRK subtypes (Pitcher et al., 1992, 1996; Stoffel et al., 1994; Shenoy and Lefkowitz, 2003). Phosphorylation of GPCRs by GRKs as a first step of desensitization was described to be strictly activation-dependent (Gurevich et al., 2012). Interaction of GRK2 with active β_2-AR activates GRK2 which makes activated β_2-ARs targets for and allosteric activators of GRKs (Chen et al., 1993). Strict activation-dependent phosphorylation was shown for GRK2 and GRK3 (Benovic et al., 1987; Krasel et al., 2005; Li et al., 2015). However,

GRK5 and GRK6 of the GRK4 family also phosphorylated unstimulated receptors which resulted in arrestin recruitment to the inactive but phosphorylated receptors (Li et al., 2015). Desensitization by GRKs can also occur in a phosphorylation-independent manner as shown for the metabotropic glutamate receptor (mGluR) type 5 in neurons (Ribeiro et al., 2009).

3.1.2.2 Arrestins

GRK-mediated receptor phosphorylation is then followed by the second step of homologous desensitization: The translocation of arrestins from the cytosol to the membrane and their interaction with the phosphorylated receptor (Figure 4, (Barak et al., 1997; Shenoy and Lefkowitz, 2005)). Activation of the receptors and phosphorylation of agonist-occupied receptors by GRKs of the GRK2 family is required for high affinity arrestin binding to the receptor (Krasel et al., 2005; Violin et al., 2006). In a FRET-based assay monitoring β_2-AR interaction with arrestin 3, functional GRK2 was necessary in order to detect an increase in FRET, i.e. to induce receptor-arrestin interaction. Expression of a dominant negative form of GRK2 abolished the agonist-evoked FRET signal observed in the presence of functional GRK2 (Krasel et al., 2005).

Arrestins form a small family of four proteins, two of which are expressed ubiquitously (Arr 2 and Arr 3) whereas Arr 1 and Arr 4 are considered visual arrestins and localize to rods and cones, respectively. Arrestins terminate G protein-mediated signaling by sterically hindering G protein-receptor interaction, they induce signaling for example via Src-family kinases and initiate internalization of most GPCRs via clathrin-coated pits (CCPs) (Luttrell et al., 1999; Krasel et al., 2005; Shenoy and Lefkowitz, 2005). With a binding motif for clathrin near the arrestin C-terminus, arrestins can directly interact with the clathrin heavy chain (Goodman et al., 1996; Krupnick et al., 1997). In addition direct interaction with the clathrin-adapter protein 2 (AP2) has also been shown and is also required for arrestin-mediated endocytosis. Arrestins therefore directly link (ligand-activated) phosphorylated receptors to the internalization machinery to induce clathrin-mediated endocytosis. Endocytosis can then lead to receptor resensitization and recycling back to the plasma membrane or to lysosomal degradation (Figure 4, (Laporte et al., 1999, 2000; Ferguson, 2001; Shenoy and Lefkowitz, 2003; Ribas et al., 2007)).

3.1.3 Adrenoceptors

Adrenoceptors are GPCRs physiologically activated by the endogenous ligands noradrenaline and adrenaline and belong to the α-group of the *Rhodopsin*-family, which is

the largest family of GPCRs with about 670 members (Fredriksson et al., 2003). Based on their physiologic actions, on anatomical grounds and, later, on molecular cloning of the receptors, adrenoceptors were subdivided into three α_1-ARs, three α_2-ARs and three β-ARs. Adrenoceptors regulate a variety of functions in the neuronal, endocrine, cardiovascular, vegetative system. Single nucleotide polymorphisms (SNPs) in the genes for different subtypes can result in variations in receptor function and responsiveness to medical treatment among individuals (Kirstein and Insel, 2004; Hein, 2006; Ahles and Engelhardt, 2014). The adrenoceptors α_{2A}-AR, β_1-AR and β_2-AR were used in this study to investigate the voltage-dependent regulation of receptor activity.

3.1.3.1 α_{2A}-adrenoceptors

Activation of α_2-ARs induces coupling of G_i-proteins to the receptors' third intracellular loop resulting in their activation. A decrease in cyclic adenosine monophosphate (cAMP) concentration through the inhibition of adenylyl cyclases (ACs) via the $G\alpha_i$-subunit follows G protein activation. The βγ-subunit in turn inhibits voltage-gated Ca^{2+}-channels and activates GIRK-channels. Additionally, activation of signaling via mitogen-activated protein (MAP) kinases and phospholipases has been shown (Docherty, 1998; Saunders and Limbird, 1999; Hein, 2006). α_2-ARs are involved in the regulation of, for example, neurotransmitter release, platelet aggregation or blood pressure (Knaus et al., 2007). The subtype A of α_2-ARs (α_{2A}-ARs) is found pre-and postsynaptically in the peripheral and central nervous system as well as in non-neuronal tissue. Presynaptic α_{2A}-ARs in sympathetic nerves control neurotransmitter release and thereby regulate the sympathetic innervation of the heart and of noradrenergic neurons in the central nervous system (CNS). They are also involved in the regulation of vascular smooth muscle cell contraction but central effects predominate (Docherty, 1998; Hein et al., 1999).

An extensive study has elaborated on the voltage-dependence of α_{2A}-ARs, which is an intrinsic property of the receptor molecule and independent of G_i protein binding (Rinne et al., 2013). In the present thesis, the α_{2A}-AR has been used to further investigate the molecular mechanism of GPCR voltage-dependence by site-directed mutagenesis.

3.1.3.2 β_1- and β_2-adrenoceptors

β-adrenoceptors regulate many physiological processes in the cardiovascular system, the airways, the uterine system and the peripheral metabolism. Receptor activation increases, for example, the heart rate and contractility (β_1-AR) or leads to the relaxation of smooth muscle cells (β_2-AR) (Kirstein and Insel, 2004; Hein, 2006) which makes them

important targets in the treatment of cardiovascular diseases or asthma, respectively (Frishman, 2013; Ortega, 2014). Both β_1-AR and β_2-AR have also been found to be expressed in the brain were they are involved in the retrieval of memory, the control of melanin circadian rhythm and the central regulation of the sympathetic tone (Hein, 2006). The third β-AR isoform, β_3-adrenoceptors, will not be discussed here.

In contrast to α_2-ARs, β-adrenoceptors couple to stimulatory G_s proteins which induce cAMP production via the stimulation of ACs. In cardiomyocytes, elevated cAMP-levels activate PKA which phosphorylates various effectors like L-type Ca^{2+}-channels and sarcoplasmic reticulum-located ryanodine receptors which ultimately increases the intracellular Ca^{2+} concentration. β-ARs themselves are also targets of PKA and desensitize upon PKA phosphorylation (Lymperopoulos et al., 2013).

3.2 Voltage-dependence of G protein-coupled receptors

The regulation of GPCR activity by the membrane potential has gained increasing interest since the first documentations of voltage-regulation of muscarinic acetylcholine (ACh) receptor 2 (M_2AChR) activity in 2003 (Ben-Chaim et al., 2003). Since then several other GPCRs of the *Rhodopsin*- and *Glutamate*-receptor family have been shown to be voltage-dependent. Voltage-dependence is transmitted from the receptor molecule to downstream signaling which was detected as altered G protein-activated inwardly rectifying channel (GIRK) activation, Ca^{2+} signaling, G protein activation or receptor-arrestin interaction (for example (Martinez-Pinna et al., 2004; Sahlholm et al., 2012; Rinne et al., 2013)).

Two important parameters have to be considered when describing the pharmacology of a drug: Its affinity and efficacy. The affinity is a measure of how well a substance binds to its molecular target, in this study its receptor. Efficacy describes how well this substance is able to induce a biological response through binding to its target (Huber et al., 2008). The intrinsic efficacy describes the direct effect of a compound on the receptor molecule itself, i.e. its ability to activate the receptor (Kenakin, 1984). Regulation of receptor activity by the membrane potential could be achieved through alterations in efficacy and/or affinity. Both has been demonstrated indirectly or directly for several GPCRs. Depolarization-dependent effects on efficacy have been suggested for purinergic P_2Y_1 receptors (P_2Y_1R), muscarinic M_2 acetylcholine receptors (M_2AChR) stimulated with pilocarpine and dopaminergic D_2 receptors (D_2R) (Gurung et al., 2008; Navarro-Polanco et al., 2011; Sahlholm et al., 2011). However, direct evidence for a reduction in efficacy during depolarization has only been published for clonidine-activated α_{2A}-ARs (Rinne et al.,

2013). Potentiation of Ca^{2+} signaling at depolarization not only occurred during P_2Y_1R stimulation with adenosine diphosphate (ADP) but also in the presence of competitive antagonists (Gurung et al., 2008). Ca^{2+} signaling evoked by stimulation of the lysophosphatidic acid (LPA) receptor was also potentiated during depolarization (Martinez-Pinna et al., 2010). Agonist binding was increased during depolarization at the muscarinic M_1AChR and the $mGluR_1$ while it was decreased at M_2AChR and $mGluR_3$ (Ben-Chaim et al., 2003; Ohana et al., 2006). A decrease in agonist affinity was also determined to underlie voltage-dependence of noradrenaline-stimulated α_{2A}-AR using a FRET-based intramolecular fusion protein of this receptor (α_{2A}-AR-cam, (Vilardaga et al., 2003; Rinne et al., 2013)). A minor right shift in concentration-response curves for histamine-induced GIRK activation via H_3R and less pronounced via H_4 at depolarization indicated voltage-sensitivity of these receptors as well (Sahlholm et al., 2012). In addition to alterations in affinity/efficacy also an agonist-specific voltage-sensitivity was present at M_2AChR, H_4R, at the short splice-variant of D_2R ($D_{2S}R$), at α_{2A}-AR and, as will be seen in this study, at the β_1-AR (Navarro-Polanco et al., 2011; Sahlholm et al., 2011, 2012; Rinne et al., 2013; Birk et al., 2015). So far only few GPCRs have been identified which lack detectable voltage-dependence. To my knowledge these are the dopamine D_3 receptor (Sahlholm et al., 2008a) and the adenosine A_{2A} receptor ($A_{2A}R$) (personal communication with Prof. Bünemann and Prof. Rinne).

In voltage-gated ion channels gating currents arise from the movement of a voltage-sensor upon alterations in the membrane potential. This voltage-sensor is located in the fourth transmembrane segment (S4) and is comprised of positively charged, basic amino acids (Aggarwal and MacKinnon, 1996; Seoh et al., 1996). Movement of the charged segment upon alterations in the membrane potential translates into a conformational change in the ion channel thereby changing channel conductance and open probability. Other mechanisms by which membrane proteins could react to altered potentials with a conformational change include movement of ions localized in cavities within the proteins or reorientation of dipole-containing residues (Bezanilla, 2000, 2008). An important finding in the research of voltage-dependence of GPCRs was the detection of gating currents in M_2AChR (Ben-Chaim et al., 2006). Measurements of gating currents in M_2AChR and of voltage-dependent conformational changes in the α_{2A}-AR-cam suggested that voltage-dependence is an intrinsic property of the receptor molecule (Ben-Chaim et al., 2006; Navarro-Polanco et al., 2011; Rinne et al., 2013). This was also supported by a close correlation between depolarization-induced charge movement (gating charges) and

agonist binding to M_2AChR. Voltage-dependent conformational changes in the binding pocket of this receptor detected by site-directed fluorescence labeling also correlated well with charge movement and suggested voltage-dependence to reside at the receptor level (Dekel et al., 2012). However, a similar structure to the S4-segment or other structures which could function as a voltage-sensor are not obviously present in GPCRs (Bezanilla, 2008). Therefore the mechanism by which GPCRs sense alterations in the membrane potential remains unclear.

3.2.1 The mechanism of voltage-dependence of G protein-coupled receptors

Since the publication of first experimental evidence for a voltage-dependent regulation of GPCR activity, it was the aim to elucidate the underlying mechanism. The mode of agonist binding within the binding pocket of GPCRs was recently shown to effect direction of voltage-dependence of muscarinic receptors. Interaction with an asparagine residue in TM6 determined whether receptor activation was enhance or reduced during depolarization (Rinne et al., 2015). Gating currents measured in the M_2AChR pointed to the existence of a voltage-sensor which is, most likely, charged or is at least expected to contain (a) dipole(s) (Bezanilla, 2000; Ben-Chaim et al., 2006; Navarro-Polanco et al., 2011). In the prototypical voltage-gated Shaker K^+ channel the voltage-sensor consists of a segment containing several basic amino acids. The amount of charge moved per channel was calculated to be 13 e_0, which causes a steep voltage-dependence of these channels (Bezanilla, 2008). Compared to voltage-gated ion channels the steepness of GPCR voltage-sensitivity is shallower. Current-voltage relations or FRET response-voltage relations yielded similar numbers of charges moved across the membrane: $z=0.76\ e_0$ in M_1AChR, $z=0.55$ or $0.85\ e_0$ in M_2AChR, and $z=0.5\ e_0$ in α_{2A}-AR (Ben-Chaim et al., 2006; Navarro-Polanco et al., 2011; Rinne et al., 2013, 2015). Voltage-dependence resided within the range of physiological membrane potentials with a half maximal effective potential (V_{50}) of V_{50}=-53 mV (M_1AChR, (Rinne et al., 2015)), V_{50}=-44 mV or -67 mV (M_2AChR, (Ben-Chaim et al., 2006; Navarro-Polanco et al., 2011)) and V_{50}=-20 mV (α_{2A}-AR, (Rinne et al., 2013)). In order to sense alterations in the membrane potential it is also likely that the voltage-sensor would reside within the transmembrane region where the electrical field is strongest. Using mutational studies research groups set off to identify (residues of) the GPCR voltage-sensor.

3.2.1.1 Mutation of a conserved motif and charged amino acids

Site-directed mutagenesis has been performed of conserved micro domains or charged amino acids conserved among *Rhodopsin*-family GPCRs within the TM domains or in receptor sections close to the plasma membrane. In the muscarinic M_2AChR, the most studied GPCR in terms of voltage-sensitivity, several mutations have been inserted. An early study suggested that the DRY-motif in TM3, which is highly conserved among *Rhodopsin*-family GPCRs, would be (part of) the voltage sensor (Gether, 2000; Ben-Chaim et al., 2006). Residues of the DRY-motif are involved in the so called *ionic lock* through ionic bonds with a glutamate and threonine in TM6 which stabilizes GPCRs in their inactive state. Mutations of the ionic lock residues increases basal activity of many GPCRs (Palczewski, 2000; Kobilka and Deupi, 2007). Mutation of the charged aspartic acid and arginine residues of the DRY-motif to asparagine (NNY-mutant) diminished gating charges and voltage-dependent radioligand binding (Ben-Chaim et al., 2006). However, a later study could not reproduce these findings and showed gating currents also in the NNY-mutant (Navarro-Polanco et al., 2011). Mutation of the corresponding amino acids in the α_{2A}-AR did not abolish voltage-sensitivity in this receptor either (unpublished data). A charge-neutralizing mutation of a glutamate in TM6 ($E^{6.30}A$) involved in the ionic lock in dopamine D_2 receptors did not remove or alter the receptors' voltage-dependence, neither did a corresponding mutation ($D^{6.30}A$) in histamine H_3 receptors (Sahlholm et al., 2012). This argued against an involvement of these conserved and/or charged amino acids in the GPCR voltage-sensing process.

3.2.1.2 Mutation of amino acids involved in sodium coordination

Crystal structures of β_1-AR and the A_{2A} revealed a binding site for a sodium ion which is coordinated by amino acids highly conserved among the *Rhodopsin*-family GPCRs, namely $D^{2.50}$ and $S^{3.39}$ (Ballesteros-Weinstein numbering in superscript (Ballesteros and Weinstein, 1995)), together with three structural water molecules (Mirzadegan et al., 2003; Liu et al., 2012; Gutiérrez-De-Terán et al., 2013; Miller-Gallacher et al., 2014). In addition, the also highly conserved amino acids $N^{1.50}$, $W^{6.48}$, $N^{7.45}$, $N^{7.49}$ and $Y^{7.53}$ form a larger network of hydrogen bonds with and around the sodium coordination pocket (Liu et al., 2012). Several studies have addressed the allosteric modulation of agonist binding and receptor function by sodium ions especially in *Rhodopsin*-family GPCRs (reviewed in (Katritch et al., 2014)). Sodium binding to its binding pocket stabilizes receptors in their inactive state. A dramatic change of the pocket upon agonist binding might lead to the release of the ion to the cytoplasm which would be facilitated especially by the movement

of TM6 and TM7 during activation. The ionic current resulting from the sodium translocation could be involved in GPCR voltage-dependence and could contribute to the gating currents (Katritch et al., 2014). Mutation of the sodium-coordinating $D^{2.50}$ to alanine ($D^{2.50}A$) in M_2AChRs greatly reduced receptor membrane expression. Therefore, the authors were not able to investigate an involvement of this mutant in voltage-sensing (Navarro-Polanco et al., 2011). The corresponding aspartic acid was mutated in the α_{2A}-adrenoceptor to investigate its role in voltage-dependence.

Despite many mutagenesis studies and a lot of effort that has been put into the identification of a GPCR voltage-sensor, it remains unidentified.

3.3 Aim of the study

GPCRs comprise a large superfamily of membrane proteins whose activation by a large variety of extracellular stimuli translates into intracellular signaling via heterotrimeric G proteins or other interaction partners. Besides the ability to bind chemically diverse ligands, intrinsic voltage-dependence was demonstrated for several G_i- and G_q-coupled receptors of the *Rhodopsin*- and *Glutamate*-receptor families. The membrane potential was shown to alter ligand binding, activation and/or downstream signaling of receptors like $M_{1/2}$AChR, D_2R, mGlu$R_{1/3}$, $H_{3/4}$R, α_{2A}-AR, P_2Y_1 or LPA receptors. When the work for this study began, there have been no reports on whether also G_s-coupled receptors exhibit voltage-dependence. Thus, the aim of this work was to investigate voltage-dependence of G_s-coupled receptors using β_1-AR and β_2-AR as model receptors. FRET measurements in single living cells were combined with whole-cell patch clamp in the voltage-clamp mode to determine the influence of membrane potential alterations on receptor activation. With intramolecular FRET-based fusion proteins of both β_1-AR and β_2-AR I aimed to detect voltage-dependent conformational changes in the receptor molecules which would indicate an intrinsic voltage-dependence. Whether voltage-sensitivity was transmitted to downstream signaling was answered using FRET assays monitoring G protein activation or the interaction of receptors and G proteins or receptors and arrestin 3. Analysis of deactivation kinetics as well as of concentration-dependence of voltage-sensitivity helped to quantify the contribution of altered agonist affinity or efficacy to β-AR voltage-dependence.

The mechanism how GPCRs sense alterations in the membrane potential is unclear. GPCRs do not possess a similar motif to S4-segments which act as voltage-sensors in voltage-gated ion channels. In order to elucidate the mechanism by which GPCRs detect alterations in the membrane potential, mutagenesis studies mainly at the M_2AChR have

been carried out in search of a GPCR voltage-sensor. Neither mutation of amino acids in the binding pocket nor of a conserved sequence motif identified the voltage-sensor but only led to allosteric modulation of voltage-dependence. As yet, the search for the voltage-sensor has not been successful. Therefore, we engaged in the search of amino acids involved in the detection of membrane potential alterations with mutants of the FRET-based intramolecular fusion protein of α_{2A}-AR.

4 Materials

4.1 Technical equipment

4.1.1 General technical equipment

Accu-jet pro	BRAND GMBH + CO KG, Wertheim
Digital Sonifier	Branson Ultrasonics Corp., Danbury, USA
Feinwaage 770 (precision balance)	KERN & Sohn, Balingen-Frommern
FiveEasy pH meter	Mettler Toledo, Gießen
FLUOstar OPTIMA	BMG Labtech, Ortenberg
Freezer (-80°C) FORMA 900 Series	Thermo Scientific, Waltham, USA
Freezer Premium NoFrost	Liebherr, Biberach a. d. Riss
Fridge Profiline	Liebherr, Biberach a. d. Riss
Heat sterilization Heraeus Oven	Thermo Scientific, Waltham, USA
Heraeus Fresco 17 Centrifuge	Thermo Scientific, Waltham, USA
Heraeus Megafuge 16R Centrifuge	Thermo Scientific, Waltham, USA
Horizontal shaker 3015	GFL, Burgwedel
Ice flaker F100 Compact	Icematic, Düsseldorf
Incubator APT.line™ C150	Binder, Tuttlingen
Magnetic stirrer MR Hei-Standard	Heidolph Instruments, Schwabach
Microwave R-202	SHARP Electronics, Hamburg
Nano photometer	Implen, München
Pipette Gilson Pipetman	Gilson, Limburg-Offheim
Steam sterilization VX-95	Systec GmbH, Linden
Sterile workflow LabGard ES NU-437 Class II, Type A2 Biosafety Cabinet	NuAire, Plymouth, USA
Sterile workflow SK 1200	BDK, Sonnenbühl-Genkingen
Thermocycler	SensoQuest, Göttingen
Thermomixer comfort	Eppendorf, Hamburg
Ultra Clear UV plus (ultra-filtered water device)	SG, Hamburg
Vortex – Genie 2	Scientific Industries, Bohemia, USA

4.1.2 Technical equipment for FRET measurements

100x oil immersion objective A-Plan	Zeiss, Oberkochen
Air-cushioned optical table	Newport Corp., Stahnsdorf
Attofluor	Invitrogen, Darmstadt
Dichroic beam splitter DCLP 460	*Chroma* Technology, Bellows Falls, USA
Dichroic beam splitter DCLP 515	*Chroma* Technology, Bellows Falls, USA
Dual-emission photometry system	*TILL Photonics, Gräfelfing*
Emission filter CFP D480/40M	*Chroma* Technology, Bellows Falls, USA
Emission filter YFP HQ535/30M	*Chroma* Technology, Bellows Falls, USA
EPC-10 amplifier	HEKA Elektronik Dr. Schulze GmbH, Lambrecht
Excitation filter ET 436/20x	*Chroma* Technology, Bellows Falls, USA
Inverted microscope Axiovert 135	Zeiss, Oberkochen
Micromanipulator MMJ	Märzhäuser, Wetzlar
Perfusion system ALA VC3-8SP	ALA Scientific Instruments, Farmingdale, USA
Polychrome V light source	TILL Photonics, Gräfelfing

4.1.3 Technical equipment for electrophysiological measurements

2.0 mm square box filament, 2.0 mm wide	Science Products GmbH, Hofheim am Taunus
Air-cushioned optical table	Newport Corporation, Stahnsdorf
EPC-10 amplifier	HEKA Elektronik Dr. Schulze GmbH, Lambrecht
Micromanipulator MHW	Narishige, London, UK
Puller P-87	Sutter Instruments, Navato, USA

4.1.4 Other technical equipment

1600TR scintillation counter	Packard Instruments, Downers Grove, USA

Axoclamp 2B amplifier	Axon Instruments, Union City, USA
DMI 6000B epifluorescence microscope DFC360 FX camera	Leica, Wetzlar
LS-2800 scintillation counter	Beckman Coulter, Krefeld

4.2 Consumables

Borosilicate glass capillaries GC 150 F-10	Harvard Apparatus, Holliston, USA
Cell culture dishes 6 cm, 10 cm (coated)	Greiner, Solingen
Cell culture plate 6-well (coated)	Sarstedt, Nümbrecht
Cover slips (diameter 24 or 25mm)	VWR, Darmstadt
GF/C glass fiber filters	Whatman, Dassel
MicroFil	World Precision Instruments, Sarasota, USA
Parafilm	Brand, Wertheim
Pasteur pipets	Hartenstein, Würzburg
PCR-Tubes 0,2 mL	Brand, Wertheim
Petri dishes (uncoated)	Hartenstein, Würzburg
Pipet tips 10 µL, 200 µL, 1000 µL	Greiner, Solingen
Reaction tubes 1,5mL	Hartenstein, Würzburg
Reaction tubes 15 mL und 50 mL	Greiner, Solingen

4.3 Chemicals

[^{3}H]-clonidine hydrochloride	Perkin Elmer, Waltham, USA
[^{3}H]-noradrenaline hydrochloride	Perkin Elmer, Waltham, USA
Adrenaline hydrochloride	Sigma-Aldrich, Steinheim
Agar	AppliChem, Darmstadt
Ampicillin	AppliChem, Darmstadt
Calcium chloride	Sigma-Aldrich, Steinheim
cOmplete ULTRA Tablets, Mini, EDTA-free EASY pack (protease inhibitor cocktail)	Roche, Mannheim
Desoxyribonucleotides (dNTPs)	New England Biolabs, Frankfurt
Dimethyl sulfoxide	Sigma-Aldrich, Steinheim
DMEM high glucose (4,5 g/L)	Capricorn, Ebsdorfergrund
Dobutamine hydrochloride	Alfa Aesar, Lancashire, UK
Dopamine hydrochloride	Sigma-Aldrich, Steinheim

EDTA	Sigma-Aldrich, Steinheim
Effectene Transfection Reagent	Qiagen, Hilden
EGTA	Sigma-Aldrich, Steinheim
Ethanol absolute	Roth, Karlsruhe
Ethidium bromide	Promega, Mannheim
FCS superior	Biochrom, Berlin
G418 Sulphate	PAA, Pasching
HEPES	Sigma-Aldrich, Steinheim
Immersol 518F Immersion oil	Zeiss, Oberkochen
Isopropanol	Roth, Karlsuhe
Isoproterenol	Sigma-Aldrich, Steinheim
Kanamycin sulfate	Roth, Karlsuhe
LB-Medium-powder according to Lennox	AppliChem, Darmstadt
LE Agarose	Biozym Scientific, Hessisch Oldendorf
L-glutamine 200 mM	Biochrom, Berlin
Magnesium chloride	Sigma-Aldrich, Steinheim
Noradrenalin bitartrate	Sigma-Aldrich, Steinheim
Opti-Fluor Scintillation liquid	Packard Instruments, Downers Grove, USA
Paraformaldehyde (PFA)	Sigma-Aldrich, Steinheim
PBS	Biochrom, Berlin
Penicillin/Streptomycin (10.000 U/mL; 10 mg/mL)	Biochrom, Berlin
Poly-L-lysine hydrobromide	Sigma-Aldrich, Steinheim
Potassium acetate	Sigma-Aldrich, Steinheim
potassium chloride	Sigma-Aldrich, Steinheim
sodium chloride	Sigma-Aldrich, Steinheim
Tris	Sigma-Aldrich, Steinheim
Trypsin/EDTA (1:250)	Biochrom, Berlin
VECTASHIELD	Vector Laboratories Inc., Burlingame, USA
Yohimbine hydrochloride	Sigma-Aldrich, Steinheim

4.4 Enzymes

Dpn1	New England Biolabs, Frankfurt
Pfu DNA polymerase	Promega, Mannheim
Phusion high-fidelity DNA polymerase	New England Biolabs, Frankfurt
RNAse A	Roth, Karlsruhe

4.5 Plasmids

Plasmid	Species	Origin
CFP-Arr3	bovine	Cornelius Krasel
CFP-$G\gamma_2$	human	(Hein et al., 2005)
GRK2	human	(Winstel et al., 1996)
$G\alpha_s$-wt	rat	(Hein et al., 2006)
$G\alpha_s$-YFP	human	(Hein et al., 2006)
$G\beta_1$-wt	human	(Bünemann et al., 2003)
α_{2A}-AR wt	mouse	(Bünemann et al., 2003)
α_{2A}-AR-cam	mouse	(Vilardaga et al., 2003)
α_{2A}-AR-YFP	mouse	(Hein et al., 2005)
β_1-AR wt	human	Bünemann lab
β_1-AR-sensor (Arg389)	human	Provided by Prof. Stefan Engelhardt (Rochais et al., 2007)
β_1-AR-YFP (Arg 389)	human	mutated to Arg389 during this thesis (Birk et al., 2015)
β_2-AR-sensor	human	kindly provided by Prof. Stefan Engelhardt (Ahles et al., 2011)
β_2-AR-YFP	human	Bünemann lab

4.6 Primers for Quick Change® Mutagenesis

Beta1 G389R for	CAAGGCCTTCCAGAGACTGCTCTGCTGC
Beta1 G389R rev	GCAGCAGAGCAGTCTCTGGAAGGCCTTG
α_{2A}-L75K, D79A-cam	CCAAGGCCTCAGCGGCCATCCTGGTGGCCACG

Other mutated receptor-sensor constructs discussed in this thesis have been constructed by Anna-Lena Krett.

4.7 Kits

Plasmid Midi Kit	Qiagen, Hilden

QIAquick Gel Extraction Kit	Qiagen, Hilden
mMessage mMaschine transcription kit	Ambion, Kaufungen
Pierce BCA Protein Kit	Thermo Scientific, Waltham, USA

4.8 Software and Databases

ApE -A plasmid Editor	M. Wayne Davis
BLAST	http://blast.ncbi.nlm.nih.gov/Blast.cgi
Corel Draw X5	Corel Corporation, Ottawa, Canada
Fluorescence Spectra Viewer	http://www.thermofisher.com/de/de/home/life-science/cell-analysis/labeling-chemistry/fluorescence-spectraviewer.html
GPCRDB	www.gpcr.org/7tm/
GraphPad Prism 5	GraphPad Software, La Jolla, USA
IUPHAR	www.guidetopharmacology.org
Mendeley Desktop	Mendeley, London, UK
Microsoft Office Professional Plus 2010	Microsoft, Redmond, USA
Optima	BMG Labtech, Ortenberg
OriginPro 8.5.0 SR1	OriginLab Corporation, Northampton, USA
Patchmaster 2.5	HEKA Elektronik Dr. Schulze GmbH, Lambrecht
Primer X	www.bioinformatics.org/primerx
Pubmed	www.ncbi.nlm.nih.gov/pubmed

4.9 *E.coli* strain and cell lines

The chemically competent *E.coli* strain DH5α was used for plasmid amplification. Experiments were performed in HEK 293 or HEK 293T cells.

4.10 Buffers and Media

Standard buffers and media are listed here. Buffers which are specific to only one method are mentioned in the corresponding section. Ultra-filtered water was used in all buffers (H_2O from here on).

FRET-buffer, pH 7,3

137 mM NaCl
5.4 mM KCl
10 mM HEPES
1 mM $MgCl_2$

LB medium

20 g LB medium powder according to Lennox
in 1 L H_2O
autoclaved

Internal solution

100 mM potassium aspartate
40 mM KCl
5 mM NaCl
7 mM $MgCl_2$
20 mM HEPES
10 mM EGTA
25µM GTP
5 mM sodium ATP

Cell culture medium

500 mL Dulbecco's Modified Eagle's Medium high glucose
10% (v/v) fetal calf serum
2 mM L-glutamine
100 U/mL penicillin
0.1 mg/mL streptomycin

5 Methods

5.1 Cell culture

5.1.1 Cultivation of human embryonic kidney 293 cells

The human embryonic kidney (HEK) cell-lines HEK 293 and HEK 293T were used in this study. They were cultured in an incubator at 37°C, 90-95% humidity and 5.0% CO_2. Cells were grown in DMEM (Dusbecco's Modified Eagle's Medium high glucose) supplemented with 10% (v/v) fetal calf serum (FCS), 2 mM L-glutamine, 100 U/mL penicillin and 0.1 mg/mL streptomycin. For stably transfected cell lines the additional selection antibiotic G418 (0.5mg/mL) was added to the culture medium.

HEK 293T cells were passaged three times, stably transfected HEK 293 cells two times per week. Trypsin/EDTA (0.05/0.02% in Dulbecco's PBS without Mg^{2+}/Ca^{2+}) incubation for one minute helped to detach the adherent cells from the culture plate. Trypsin activity was stopped by the addition of new medium which was also used to wash the detached cells from the dish. Centrifugation for 3 min at 1000 rpm (Heraeus Fresco 17 centrifuge) pelleted the cells which were then resuspended in medium and seeded onto new culture dishes at an appropriate density.

5.1.2 Transient transfection of HEK 293T cells with *Effectene*

To transfect cells, DNA is introduced into eukaryotic cells. Depending on whether the introduced DNA integrates into the cell's genome or only resides in the cytosol as a circular plasmid, the transfection is stable or transient, respectively. Spontaneous integration into the genome, i.e. stable transfection, occurs only to a small percentage which is why most of the cells lose transfected plasmids during mitosis.

At least 8 hours before transfection, HEK 293T cells were split onto 6 cm dishes in a density that resulted in about 50% confluency at the time of transfection. Transfection of HEK 293T cells was achieved with *Effectene transfection reagent* (Qiagen), a non-liposomal lipid formulation, following Qiagen instructions. Experiments were conducted on the second day after transfection.

5.1.3 Transfer of transfected cells onto poly-L-lysine coated glass cover slips

For fluorescence microscopy experiments transfected cells were transferred onto glass coverslips (CS) the day before the experiment. To allow stable adherence of the transfected cells during the measurements in which they were constantly superfused, CS were coated with poly-L-lysine. Cover slips were sterilized with 70% ethanol and put upright into the

wells of 6-well-plates until the ethanol evaporated. After sterilization the CS were incubated with 100 µL poly-L-lysine for 30 min. The excessive poly-L-lysine was removed and the cover slips were washed with PBS. Transfected cells were split onto the CS in a low density that allowed single cell FRET measurements the following day.

5.2 Molecular Biology

5.2.1 Transformation of *E. coli*

To amplify plasmid DNA in *E.coli* (DH5α strain), chemically competent *E.coli* were transformed. A mix of 100 µL competent *E.coli*, 20 µL 5x potassium-calcium-magnesium (KCM) buffer, 80 µL H_2O and 0.2-2 µg plasmid DNA was incubated on ice for 20 minutes. A 10 minutes incubation time at room temperature (RT) followed. 1 mL LB medium was added to the mixture and the bacteria were grown shaking at 37°C for 50 minutes (Thermomixer comfort, Eppendorf). The bacterial culture was then plated on an antibiotic-containing agar plate (ampicillin or kanamycin) and cultured overnight at 37°C. As the plasmids contain resistance genes against either of the two antibiotics, only bacteria that took up the plasmid DNA survived on the agar plate and formed colonies overnight.

5x KCM-Puffer
500 mM KCl
150 mM $CaCl_2$
250 mM $MgCl_2$

5.2.2 Plasmid preparation from *E. coli*

Medium-scale plasmid preparation (Midi preparation, 100 mL *E.coli* overnight cultures) was done using the Qiagen Plasmid Midi Kit following the manufacturer's instructions. This kit is based on the alkaline lysis method (Birnboim and Doly, 1979). The DNA pellet was resuspended in H_2O and stored at -20°C.

Small-scale preparation (Mini preparation) was carried out using a protocol modified from Birnboim and Doly and self-made buffers but no purification columns. 1.5 mL out of 5 mL overnight cultures were centrifuged for 2 min at 13,300rpm (Heraeus Fresco 17 Centrifuge used for all centrifugations, Thermo scientific) and resuspended in 100 µL resuspension buffer. 2 µL RNAseA were added to ensure RNA digestion and to increase DNA purity. 200 µL lysis buffer were added to lyse the bacteria. A 3-5 min incubation time at RT ensured bacterial lysis. Addition of 150 µL neutralization buffer neutralized the pH and precipitated proteins and bacterial genomic DNA during a 5 min incubation on ice.

In the following centrifugation (10 min, 13,300 rpm) the precipitate was pelleted. The plasmid DNA containing supernatant was mixed with 450 µL isopropanol and incubated for 5 min to precipitate the plasmid DNA which was then pelleted by centrifugation (10 min, 12,000 rpm). The pellet was washed with 70% ethanol, air-dried and resuspended in H_2O. DNA from Mini preparations was only used in control digestions as its purity was not sufficient for sequencing, cloning, transformation or transfection. In order to use Mini preparation DNA for one of these purposes it was purified using the Qiaquick Gel Extraction Kit (Qiagen) following the manufacturer's protocol.

Resuspension buffer	**Lysis buffer**	**Neutralization buffer**
50 mM glucose	0.2 M NaOH	3 M potassium aspartate
10 mM EDTA	1% (w/v) SDS	11% (v/v) acetic acid (96%)
25 mM Tris(base)	in H_2O	in H_2O
pH 8.0, in H_2O		

5.2.3 Measurement of DNA concentration

DNA concentrations were measured with a Nano photometer (Implen). Since all DNA solution were prepared with H_2O, it served as a blank in the measurements. To determine the concentration of each sample, the absorbance at 280 nm and 320 nm was measured relative to the absorbance of the blank value.

5.2.4 Quick Change® site-directed mutagenesis

Site-specific mutations like base exchanges in double-stranded plasmids leading to amino acid exchange in the encoded protein can be achieved by PCR-based *QuickChange® site-directed mutagenesis* (Braman et al., 1996). Primers for this method carry a mismatch to the parental plasmid strand approximately in their center. Aside from this mismatch both primers are complimentary to one of the parental plasmid strands. Compared to a conventional PCR reaction, the whole double-stranded plasmid is amplified during the mutagenesis. For this reason the elongation phase is greatly prolonged and a polymerase with proof reading capacity is necessary to avoid additional, unwanted mutations. Reactions were performed with *Phusion* high-fidelity DNA-polymerase and the following components were included in the reaction tube:

Phusion

10 µL 5x GC buffer

25-50 ng DNA template

0,2 µL 5‘-mutagenesis primer (100 pmol/µL)

(0,2 µL 3‘-mutagenesis primer (100 pmol/µL))*

2 µL dNTP-mix

0.5-1 µL **Phusion** polymerase

(3.5 µL DMSO)*

ad 50 µL H_2O

* Components in parentheses where only present in some of the mutagenesis reactions.

The mutagenesis reaction was performed in a thermocycler (SensoQuest) in 16 or 35 cycles. Before the first cycle and as a first step of each cycle, the mixture was heated to 95°C or 98°C for 30 s (up to 4 min before first cycle) to denature the double-stranded plasmid. This strand separation allowed primer binding to the single strands during the annealing phase. The annealing temperature depended on the primer sequence, ranged between 56°C and 60°C and was set for 30 s. After primer annealing the temperature was increased to the optimum working temperature of the polymerases (72°C). During this 5-11 min elongation phase the plasmid strands were replicated. After elongation the temperature increased to 95°C/98°C again and the next cycle started. After the last cycle the elongation temperature was set for another 10 min to allow elongation of unfinished strands.

To separate new, mutated strands from template strands a digestion of the PCR mix with the endonuclease Dpn1 followed. Dpn1 specifically digests methylated DNA, i.e. the parental template DNA, but not the unmethylated strands produced during the PCR reaction. To increase digestion efficiency, an ethanol precipitation of the PCR-DNA preceded Dpn1-digestion. *E.coli* were transformed with 5 µL of the reaction mix. After DNA preparation the success of the mutagenesis was controlled by sequencing.

5.2.5 Sequencing

Mutated and cloned plasmid DNAs (100 µg/µL, in H_2O) were sent for sequencing to Eurofins Genomics. Sequencing was carried out using standard primers CMVfw and/or pcDNA3rev as the constructs resided in a pcDNA3 backbone vector. To verify the G389R mutation in β_1-AR-YFP, the standard sequencing primer EGFPN1rev was used.

5.3 Radio-ligand binding

Radio-ligand binding assays were performed in intact *Xenopus leavis* oocytes expressing α_{2A}-AR to investigate voltage-dependent agonist binding. In cell membranes of HEK 293 cells α_{2A}-AR density was measured.

5.3.1 Radio-ligand binding in oocytes

5.3.1.1 Buffers for oocyte culture and binding experiments

Oocytes were cultured in standard oocyte culture medium (NDE). The membrane potentials of about -88 mV and +5 mV were induced by solutions of low (ND) and high (HK) potassium concentration, respectively (Ben-Chaim et al., 2003, 2006).

ND96 (ND)	**Enriched ND96 (NDE)**	**ND 0 Ca^{2+}**	**High K^+ (HK)**
96 mM NaCl	**ND96**	96 mM NaCl	2 mM NaCl
2 mM KCl	+2.5 mM Na^+-pyruvate	2 mM KCl	96 mM KCl
1 mM $MgCl_2$	+100U/mL penicillin	1 mM $MgCl_2$	1 mM $MgCl_2$
1 mM $CaCl_2$	+100 µg/mL streptomycin	5 mM HEPES	1 mM $CaCl_2$
5 mM HEPES			5 mM HEPES

The pH of these solutions was adjusted to pH 7.4 with NaOH (ND96, NDE, ND 0 Ca^{2+}) or KOH (HK).

5.3.1.2 Preparation of cRNA and injection of cRNA into oocytes

Injection of *Xenopus laevis* oocytes was performed with cRNA of the α_{2A}-AR and the two GIRK channel subunits GIRK1 and GIRK2. Linear cDNA encoding for the α_{2A}-AR or the two GIRK subunits was transcribed in the following mix using the mMessage mMachine™ transcription kit (Ambion) according to the included protocol:

10 µL	2x NTP/CAP
2 µL	10x reaction buffer
1 µg	linear template DNA
2 µL	T7 polymerase

cRNAs of α_{2A}-AR (5ng/oocyte) and the two GIRK subunits (200pg/oocyte each) were injected into the oocytes one day after oocyte preparation in Ca^{2+}-free ND96 solution (ND 0 Ca^{2+}). Control oocytes to estimate unspecific binding were not injected with cRNA. Injected and untreated oocytes were cultured at 18°C in NDE solution which was changed daily.

5.3.1.3 Two-electrode voltage-clamp

Three to five days after cRNA injection GIRK currents were measured using the two-electrode voltage-clamp technique (Axoclam 2B amplifier, Axon Instruments) to check for α_{2A}-AR expression. Recording electrodes (15-40 MΩ) were pulled in a vertical puller, injecting electrodes (0.9-2 MΩ) in a horizontal puller both from 1.5 mm glass capillaries (Hilgenberg, Malsfeld). Both electrodes were filled with 500 mM KCl. An oocyte was immobilized in a small chamber filled with ND96 solution and both pipettes were inserted for current measurements. ND96 was replaced by 48 mM K^+ solution (HK:H_2O 1:1) via a gravity perfusion system to measure GIRK currents. To check for α_{2A}-AR expression, the oocyte was then superfused with 48 mM K^+ solution containing 10 µM noradrenaline. Batches of oocytes showing an increase in GIRK currents upon stimulation with noradrenaline were used for radio-ligand binding experiments.

5.3.1.4 Binding assay

[^{3}H]-NA binding (specific activity 48.4 Ci/mmol) to α_{2A}-AR expressing oocytes was measured in intact oocytes at two membrane potential induced by solutions of different potassium concentration 3-5 days after cRNA injection. One oocyte at a time was incubated either in ND or HK solution containing a given concentration of [^{3}H]-NA for 30 s. Using a glass pipette inserted into a standard 200 µL pipette tip the oocyte was transferred from the radio ligand solution into a special washing device (Ben-Chaim et al., 2003) filled with 4 mL ligand free ND or HK solution (the same solution as the [^{3}H]-NA containing one). Within 2 seconds the oocyte sank to the ground of the conical washing chamber and was removed from it. The oocyte was placed into a vial which was then filled with 3 mL scintillation liquid (Opti-Fluor, Packard Instruments). Radioactivity was counted in a LS-2800 scintillation counter (Beckman). Oocytes which have not been injected with cRNA were measured in the same way alternating with injected ones to determine the amount of nonspecific binding of [^{3}H]-NA.

The average of nonspecific binding in each set of experiments was subtracted from the total binding of individual oocytes to calculate specific binding. Specific binding of the injected oocytes was then averaged and displayed as average±SEM. Only when specific binding could be detected in measurements in ND solution, binding experiments in HK solution were performed.

5.3.2 Measurement of α_{2A}-AR density in membranes of HEK 293 cells

To estimate α_{2A}-AR density in transiently transfected HEK 293 cells, [^{3}H]-clonidine hydrochloride ([^{3}H]-Cl) (specific activity 57.8 Ci/mmol) binding to cell membranes prepared from these cells was measured.

5.3.2.1 Membrane preparation

Receptor expressing cells cultured in 10 cm culture dishes were washed once with PBS and detached from the dish with a cell scraper in 1 mL buffer (in mM: 150 NaCl, 20 NaH_2PO_4 H_2O, 3 $MgCl_2$, 1 EDTA and 1 tablet protease inhibitor cocktail (Roche) per 10 mL buffer, pH 7.4). Cells were pelleted by centrifugation for 1 hour at 13,300 rpm at 4°C (Heraeus Fresco 17 Centrifuge). Pellets were resuspended in resuspension buffer (in mM: 100 NaCl, 20 Tris base, pH 7.4) and sonified. Protein concentration was determined using a Pierce^{TM} BCA Protein Assay kit (Thermo Scientific) following the manufacturer's instructions.

5.3.2.2 Radio-ligand binding

Total [^{3}H]-Cl binding was performed in triplicates. To determine unspecific binding to transfected cells 10 µM cold yohimbine hydrochloride (Yoh) was added to the [^{3}H]-Cl binding mix and was measured in duplicates. 25 µL membrane preparation was incubated with either [^{3}H]-Cl or [^{3}H]-Cl+Yoh both in resuspension buffer shaking over night at 4°C. GF/C glass fiber filters (Whatman) were used to separate bound and unbound ligand by vacuum filtration. Filters were washed four times with ice-cold 50 mM Tris base (pH 7.4), transferred to vials containing 2 mL scintillation liquid and radioactivity was counted in a Packard1600TR beta counter. Counts per minute (cpm) measured by the beta counter were transformed into disintegrations per minute (dpm) using the following formula:

$$dpm = (cpm_{sample} - cpm_{background})/\text{detector efficiency}$$

The detector efficiency for [^{3}H] was 20%. The average unspecific binding detected in duplicates in the presence of cold Yoh was subtracted from the total binding value of each sample to calculate specific binding. Specific binding of triplicate values was then averaged and the amount of receptor in each membrane sample was calculated using the specific mol/dpm factor of [^{3}H]-Cl ($7.79*10^{-18}$ mol/dpm). BCA data were used to determine the amount of protein per 25 µL membrane preparation and the receptor density (pmol receptor/mg membrane protein) was calculated.

Data of three transfections of α_{2A}-AR together with Epac1-camps and AC5 were pooled. Untransfected cells were also measured in triplicates with [^{3}H]-Cl or in duplicates with

[^{3}H]-Cl+Yoh to confirm specific binding of [^{3}H]-Cl to α_{2A}-AR. No specific binding was detected in untransfected cells. The density of α_{2A}-AR was 10.98±0.9 pmol/mg membrane protein.

5.3.3 Förster resonance energy transfer measurements in single living cells

Cells transiently or stably expressing the fluorescently labeled proteins under investigation were split onto poly-L-lysine coated cover slips the day before the measurements (5.1.3). FRET measurements were conducted in single living cells the following day.

5.3.3.1 Theoretical background

Based on theories of Jean Perrin, Theodor Förster described the transition of electron excitation energy between two similar molecules in solution (Förster, 1948), a process we today call Förster or fluorescence resonance energy transfer, short FRET.

FRET can occur between two fluorophores when an excited donor fluorophore transmits its energy radiation-free onto an acceptor fluorophore. This acceptor can either transmit the energy to yet another acceptor or emit it as light. There are three main prerequisites for this transfer to happen (Lohse et al., 2012): 1) The transition dipole orientation should ideally be parallel. 2) The donor emission and acceptor excitation spectra need to overlap (Figure 5). The most frequently used FRET pair consists of the donor CFP and the acceptor YFP. The fluorophores are spectral variants of the green fluorescent protein (GFP) found in the jellyfish *Aequorea Victoria* (Prasher et al., 1992; Heim and Tsien, 1996). An excitation wavelength of 430 nm in the FRET measurements performed in this study mainly excited CFP (Figure 5). CFP could then transfer its energy to YFP if 3) the distance between the fluorophores relative to each other is within 1-100Å. This makes FRET an ideal tool to study protein-protein interaction (intermolecular FRET) or to monitor protein conformational changes (intramolecular FRET) in living cells.

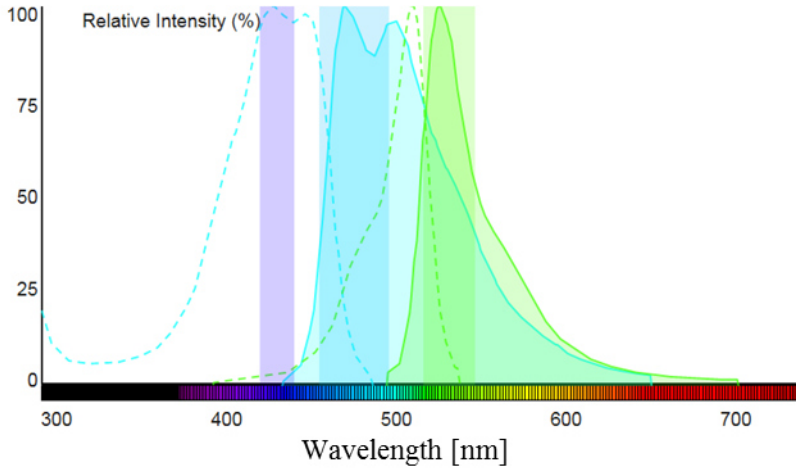

Figure 5: Excitation and emission spectra of CFP and YFP.
Excitation (dashed curves) and emission (solid lines) spectra of CFP (blue) and YFP (green) are shown. The overlap of CFP emission (solid blue) and YFP excitation (dashed green) is nicely visible. Purple, light blue and green rectangles correspond to the bandwidths of the excitation, CFP emission and YFP emission filters, respectively. The image was modified from an image produced with the Thermo Fisher Scientific Fluorescence Spectra Viewer.

There are several ways to measure FRET. In this study the FRET approach of sensitized emission (simply called FRET in this thesis) was used in which the acceptor emits light after excitation by a donor via FRET (Lohse et al., 2012). Measurements of sensitized emission usually include correction of the total YFP emission by two factors: "direct excitation" of the acceptor by the donor excitation wavelength and "bleed through" of the donor emission into the acceptor emission channel both due to spectral overlap (Berney and Danuser, 2003). In this thesis corrections of the YFP emission could not be carried out. Combination of FRET measurements with electrophysiology did not allow measurement of total YFP emission after each measurement which would be needed to calculate the actual YFP emission after subtraction of bleed-through and direct excitation.

5.3.3.2 Preparation of agonist solutions

Stock solutions of a concentration of 10 mM were prepared for all agonists by weighing in a defined amount of each substance and dissolving it in the appropriate amount of FRET buffer. Dissolving of dobutamine (DOB) was achieved by gentle shaking and warming to 40°C (Thermomixer comfort). Ascorbic acid was added to each solution to prevent oxidation. Stock solutions of isoprenaline (Iso), noradrenaline (NA) and DOB were stored at -20°C and used repeatedly whereas solutions of adrenaline (Adr) and dopamine (DA) were prepared freshly on each measuring day. Stock solutions were then used to prepare 10 mL of the desired agonist concentration in FRET buffer (4.10) for FRET measurements.

5.3.3.3 Förster resonance energy transfer measurements (sensitized emission)

On the measuring day cover slips were mounted in an Attofluor cell chamber (Invitrogen), washed twice with FRET buffer and covered with FRET buffer. Measurements were conducted at room temperature on an inverted Axiovert 135 (Zeiss) microscope equipped with a 100x-A-Plan oil immersion objective (Zeiss) and a dual-emission photometric system (TILL Photonics). Transfected cells expressing both fluorophore-labeled proteins at their appropriate location within the cell were selected in a dual excitation mode. In the FRET measurement mode cells were excited with a wavelength of 430 nm (excitation filter ET 436/20x, DCLP 460 nm, Chroma Technology), a frequency of 2.5 Hz or 5 Hz and an illumination time of 5 ms with a polychrome V light source (TILL Photonics). Emission intensities of both fluorophores (F_{535}, F_{480}; DLCP 515, emission filter CFP D480/40M and YFP HQ535/30M, all Chroma Technology) were detected separately by high-resolution photodiodes (TILL Photonics). An analogue-digital converter included in the EPC-10 amplifier (HEKA) converted fluorescence intensity signals into digital data which were stored on a computer using Patchmaster software 2.42 (HEKA). To investigate agonist-mediated changes in FRET, cells were continuously superfused with buffer or buffer containing agonist by a pressurized perfusion system VC3-8SP (ALA Scientific Instruments) which enabled solution exchange in less than 10 ms. A black bar in each graph labeled with the concentration and type of agonist indicated the duration of agonist application.

5.3.3.4 F_{535}, F_{480}, F_{535}/F_{480}

As the emission intensity was not corrected in the FRET measurements, single channel fluorescence intensities are labeled according to the specifications of the emission filters (D480/40M and HQ535/30M) in the setup: F_{480} and F_{535} correspond to the channels, in which mostly donor and acceptor emissions were measured, respectively (Figure 5). The acceptor-over-donor emission ratio was calculated (F_{535}/F_{480}) and is simply referred to as ‘ratio’ in this thesis.

5.4 Control of the membrane potential by patch-clamp electrophysiology

Ionic currents across the plasma membrane or the plasma membrane potential can be measured by means of patch-clamp electrophysiology in the voltage-clamp or current-clamp mode, respectively (Hamill et al., 1981). In this study the membrane potential of cells expressing fluorescently labeled proteins suited for FRET (5.3.3.1) was set to desired values using patch-clamp in the voltage-clamp mode. A patch pipette filled with internal

solution (similar ionic composition as cytosol, 4.10) was positioned close to the cell membrane with a micromanipulator under optical control. By the application of slight suction a tight seal between patch pipette and the plasma membrane (giga seal) was achieved. Further suction opened the plasma membrane patch within the pipette without breaking the seal (whole-cell configuration). By means of a patch amplifier (EPC-10, HEKA) set to voltage-clamp mode the membrane potential (V_M) was controlled.

5.5 FRET measurements under direct control of the membrane potential

A combination of FRET measurements and the patch-clamp technique in a voltage-clamp mode was used to investigate conformational changes in a receptor molecule as well as alterations in protein-protein interaction due to variations in the plasma membrane potential. Figure 6 illustrates a cell transfected with an intramolecular receptor fusion protein in the whole-cell configuration. On each day of experiments borosilicate glass capillaries (GC150F-10, Harvard Apparatus) were pulled into patch pipettes (resistance of 4-8 MΩ) using a horizontal P-87 pipette puller (Sutter Instruments). Starting from a holding potential of -90 mV the membrane potential was switched to one or various test potentials by means of the EPC-10 patch amplifier (HEKA). The course of the membrane potential during measurements is indicated as a black rectangular pulse bar below each measurement. Simultaneously, cells were excited and the fluorescence intensities were recorded (5.3.3.3).

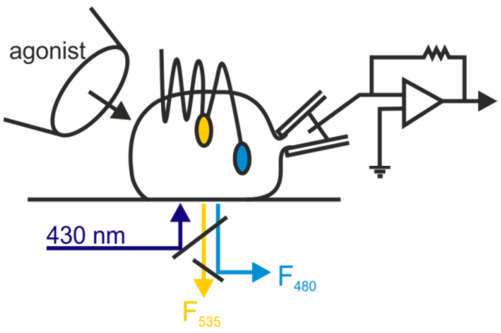

Figure 6: Schematic of combined FRET and electrophysiology measurements.
A cell expressing an intramolecular receptor fusion protein is excited with a wavelength of 430 nm (dark blue) and donor (F_{480}, light blue) and acceptor (F_{535}, yellow) emissions were recorded. Simultaneously, cells were superfused with buffer or agonist-containing buffer with a pressurized perfusion system (left) and the membrane potential was controlled in whole-cell voltage-clamp configuration (patch pipette and amplifier, right).

5.6 Data evaluation and statistics

Emission intensities at 480±20 nm (D480/40M) and at 535±15 nm (HQ535/30M) were recorded with Patchmaster software 2.42 which also calculated the ratio of F_{535}/F_{480}. Raw data were exported as AscII files and evaluated using OriginPro 8.5.0 SR1 (OriginLab Corp.) or GraphPad Prism 5 (GraphPad Software Inc.). All data in the study are presented either as individual experiments or averaged data ±standard error of the mean (SEM). The number of measurements per condition is stated as *n=x* in the figure legends.

5.6.1 Correction for photo bleaching

Fluorophores are harmed by high intensity light pulses which leads to a decrease in fluorescence over time. This photo bleaching occurred in all FRET measurements but to a different degree depending on the excitation frequency and needed to be corrected for. Pronounced photo bleaching was present in 5Hz measurements of the FRET-based intramolecular fusion proteins β_1-AR-sensor, β_2-AR-sensor and α_{2A}-AR-cam as well as their mutant forms. Correction for bleaching was achieved by subtraction of a mono-exponential curve (dashed line) from the original acceptor-over-donor emission ratio as shown in a representative measurement of the β_1-AR-sensor stimulated with 10 µM Adr (Figure 7, upper layer). The corrected ratio trace was then normalized to the starting value prior to agonist stimulation (Figure 7, lower layer) or to the maximal agonist-induced FRET amplitude (e.g. Figure 8C, D). Photo bleaching also occurred during 5 Hz measurements of receptor-G protein interaction and G protein activation and was corrected in the same manner as shown in Figure 7.

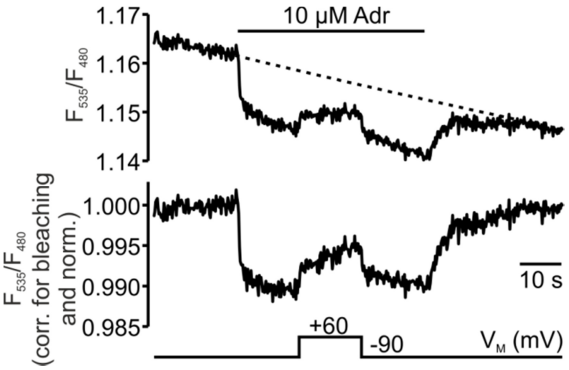

Figure 7: Correction for photo bleaching.
In a representative measurement, a cell transiently transfected with the FRET-based β_1-AR intramolecular fusion protein was stimulated with 10 µM Adr. The ratio (F_{535}/F_{480}) is shown before (above) and after (below) correction for photo bleaching by subtraction of a mono-exponential curve (dashed line, τ=574 s). The bleach corrected ratio was normalized to the initial FRET value before stimulation. A black bar with agonist labeling above the ratio trace indicates the duration of Adr application. The time scale appears as a black bar. The bar below the trace shows the course of membrane potential (holding potential: -90 mV; test potential: +60 mV).

5.6.2 Normalization

In order to average data of different cells despite differences in initial acceptor-over-donor emission ratio values, ratios of individual measurements were normalized. In FRET assays with high initial FRET (measurements of receptor activation or G protein activation) the bleach corrected ratios were normalized by dividing F_{535}/F_{480} by the average FRET value before agonist stimulation (F_{535}/F_{480} (norm.)). In FRET assays which show an increase of FRET upon agonist stimulation (receptor-G protein FRET, receptor-arrestin FRET), the (bleach corrected) ratio was calculated as $\Delta(F_{535}/F_{480})$: The average FRET value before stimulation was subtracted from the ratio values at every given point. To compare deactivation kinetics, ratios were normalized to their maximal response. For this normalization $\Delta(F_{535}/F_{480})$ at every given time was divided by the maximum agonist-

induced FRET response ($\Delta(F_{535}/F_{480})/\Delta(F_{535}/F_{480})_{max}$) and is indicated as F_{535}/F_{480} (norm to max.).

5.6.3 Deactivation kinetics

To perform evaluations of deactivation kinetics, the following mono-exponential function was fit to the appropriate section of individual experiments or the averaged data of 'n' experiments using GraphPad Prism or Origin:

$$Y=A*e^{(-k/x)}+Y_0,$$

where Y_0 is the Y value at x=0 s, A is the size of the signal and k the rate constant in s^{-1}. The sections reached from the time-point of agonist withdrawal or start of depolarization to the plateau after washout or during depolarization. K_{off} values and standard errors were directly determined by GraphPad Prism with the equation mentioned here.

5.6.4 Concentration-response curves

Data for concentration-response curves were collected in a similar way to normal FRET measurements or FRET measurements in combination with patch-clamp. For a concentration-response curve of DA at the β_1-AR, cells were stimulated with increasing concentrations of DA without washout between the different concentrations. FRET responses induced by different concentrations were normalized to the maximal FRET response by the highest agonist concentration. A concentration-response curve for Iso-induced β_1-AR-arrestin 3 interaction at two different potentials (-90 mV and +45 mV) was obtained in clamped cells stimulated with one test concentration and a reference concentration after washout of the first concentration. The test concentrations varied between cells whereas the reference concentration was the same. A switch between the holding potential and depolarization was performed in order to measure the Iso-induced FRET response during both potentials. Amplitudes at both potentials during stimulation with the test concentration were normalized to the amplitude of the reference concentration at rest (A_{+45}/A_{rest} or A_{-90}/A_{rest}).

A concentration-response curve was fit using the following function in GraphPad Prism ("dose-response, variable slope"):

$$Y=Bottom+(Top-Bottom)/(1+10^{((logEC50-x)*Hill\ Slope)}),$$

in which bottom/top are the values of the bottom/top plateau, x is the logarithm of the concentration, Y is the relative response amplitude, logEC50 is the x value when the response is 50% and the Hill Slope marks the steepness of the curve. The equation allowed for a variable slope.

5.6.5 Statistical tests

To test for statistical significant differences between conditions the following statistical tests were performed in GraphPad Prism or Origin: One way ANOVA with Bonferroni´s multiple comparison test to compare more than two conditions with each other; paired or unpaired Student's t-test to compare two different conditions of paired or unpaired observations, respectively; extra sum of squares F-test for fit comparison.

6 Results

6.1 The β_1-adrenoceptor activity is voltage-sensitive

In recent years voltage-sensitivity of a number of class A and C GPCRs coupling to G_i- or G_q-proteins has been reported (reviewed in (Mahaut-Smith et al., 2008)). But whether this regulation of receptor activation by the membrane potential also occurs in GPCRs coupling to the stimulatory G_s-protein has not yet been investigated. The β_1-AR was used as a model G_s-coupled receptor to measure receptor activity as a function of the membrane potential. Ratiometric FRET measurements combined with patch-clamp electrophysiology were performed in HEK 293 cells which either stably or transiently expressed an intramolecular FRET-based fusion protein of β_1-AR (β_1-AR sensor (Rochais et al., 2007)). The crystal structure of the active state of the closely related β_2-AR showed a rotation and large outward movement of TM6 compared to the inactive state (Rasmussen et al., 2007, 2011b). With the intramolecular β_1-AR sensor this activating conformational change can be monitored: The outward movement of TM6 upon agonist application leads to an increase in distance between the donor (Cer) and acceptor (YFP) fluorophores fused to the c-terminus and inserted into the third intracellular loop, respectively (Figure 8A). Thus, donor emission (blue) increased while acceptor emission (yellow) decreased during stimulation of the β_1-AR sensor with 10 µM adrenaline (Adr) resulting in a decrease in acceptor-over-donor emission ratio (black trace, from here on only referred to as ratio or F_{535}/F_{480}) (Figure 8B, D) which reflects receptor activation (Rochais et al., 2007). Also stimulation with isoprenaline, another full agonist at the receptor (Bond et al., 2015), decreased the ratio, i.e. activated the receptor. This decrease was reversible upon washout of both ligands, indicating deactivation of the receptor (Figure 8B, C, D). Different concentrations of Iso and Adr were used to account for differences in affinities towards the β_1-AR (Bond et al., 2015). When the membrane potential was depolarized from a holding potential of -90 mV to +60 mV during agonist application, the ratio increased very rapidly. This depolarization-induced change in ratio was reversible upon repolarization of the membrane to the former holding potential of -90 mV (Figure 8B, C, D).

To verify that the changes in energy transfer induced by this large depolarizing step arose from a conformational change of the receptor molecule and not due to unspecific alteration of fluorophore emission, cells expressing the β_1-AR sensor were subjected to depolarization in the absence of agonists (Figure 8E).

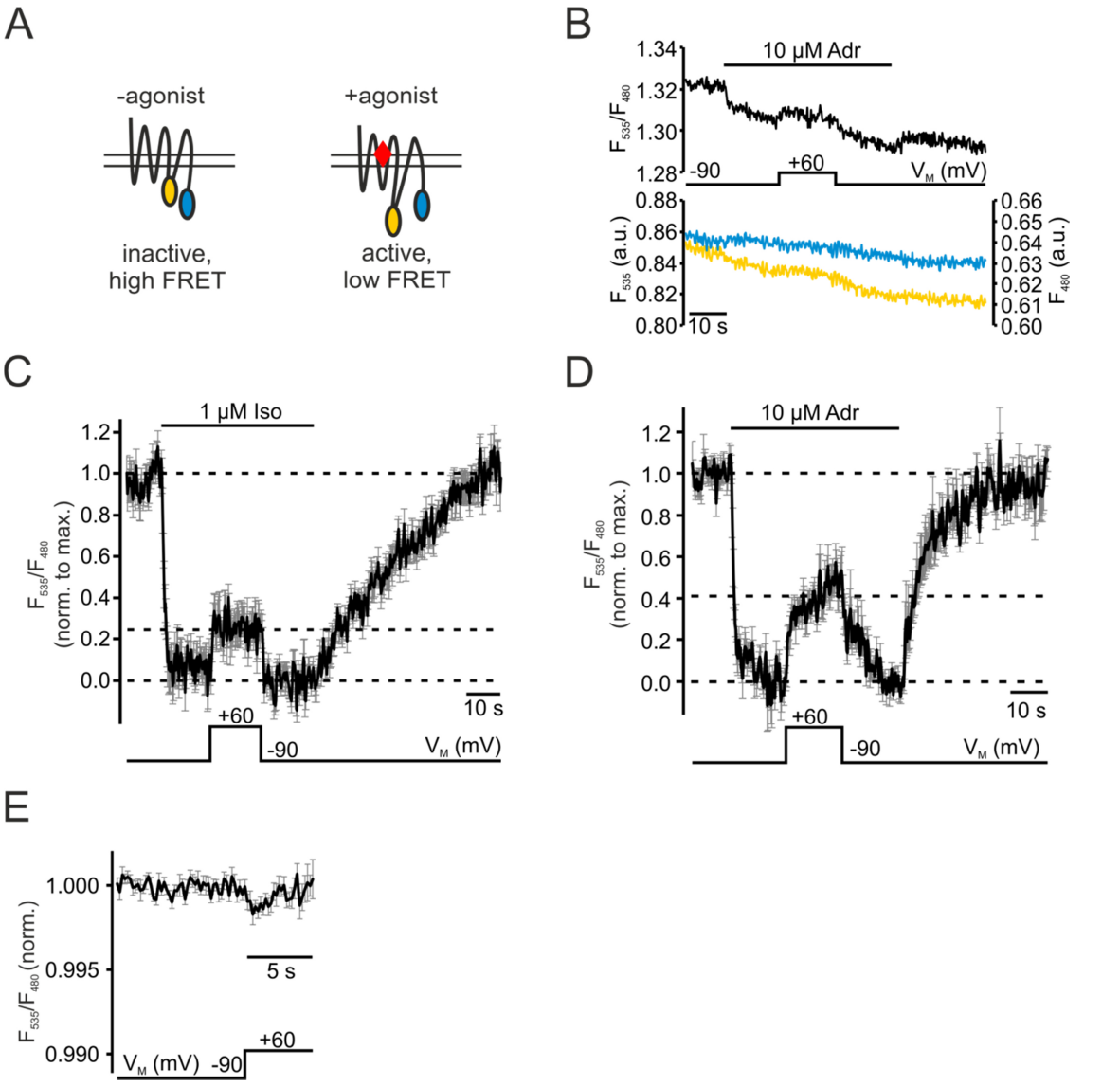

Figure 8: Membrane potential modulates agonist-induced β_1-AR-sensor activity.
In all figures, a black bar above measurements indicates the length and type of agonist application. The time scale is given as a black bar with a time in seconds in each graph. In cells subjected to voltage-clamp the applied change in membrane potential is indicated as a square pulse below the traces. In figures showing single fluorophore emission traces, the blue and yellow traces corresponds to donor (F_{480}) and acceptor (F_{535}) emission intensities, respectively. Blue and yellow ovals represent CFP and YFP fluorophores, respectively, a red diamond indicates the presence of an agonist. A small schematic of the FRET assay used is given in the first subfigure in which it was measured.
A: An intramolecular FRET-based fusion protein of the β_1-AR displays high initial FRET in unstimulated conditions. Stimulation with an agonist (red diamond) induces a decrease in FRET. Cells transiently (*B, D*) or stably (*C, E)* expressed the β_1-AR-sensor. *B*: A representative measurement of a transiently transfected cell shows the course of YFP (yellow) and CFP (blue) emission and the acceptor-over-donor emission ratio (from here on termed "ratio", black) stimulated with 10 µM Adr. The cell was subjected to whole-cell voltage-clamp and the membrane potential was switched from the holding potential (-90 mV) to depolarization (+45 mV) during agonist application. *C, D, E:* Measurments were corrected for photo bleaching, normalized and smoothed using 5-point Savitzky-Golay-smoothing before calculation of the average±SEM. *C and D:* Cells were stimulated with 1 µM Iso (*A*) or 10 µM Adr (*B*), clamped to a holding potential of -90 mV and subjected to a depolarizing pulse to +60 mV during agonist application. Individual traces were normalized to the maximal agonist-induced change in FRET signal before averaging (average±SEM, *A*: n=9; *B:* n=8). Dashed lines indicate how amplitudes were measured for Figure 9. *E:* Cells were subjected to a depolarizing pulse to +60 mV in the absence of agonist. Individual measurements were normalized to the value prior to depolarization, then averaged (average±SEM, n=7). Alterations in the ratio induced by depolarization did not reach statistical significance (p=0.22).

In unstimulated cells depolarization did not alter the ratio, i.e. did not cause a conformational change in the receptor molecule and did not unspecifically alter fluorophore emission (Figure 8E). As the FRET signal of unstimulated β_1-AR-sensors was unaltered during depolarization, the reduction in FRET amplitude (i.e. the agonist-evoked FRET signal) by depolarization in stimulated cells could be interpreted as voltage-induced receptor deactivation.

These initial data showed that the voltage-sensitivity is an intrinsic property of β_1-AR. Its activity is modulated by the membrane potential in such a way that depolarization deactivates the receptor. It can also be appreciated from these averaged measurements that deactivation by depolarization seemed to occur with much faster kinetics than deactivation by agonist withdrawal. This phenomenon points towards a change in agonist efficacy playing a role in voltage-sensitivity of β_1-ARs and will be described in detail in section 6.1.4.

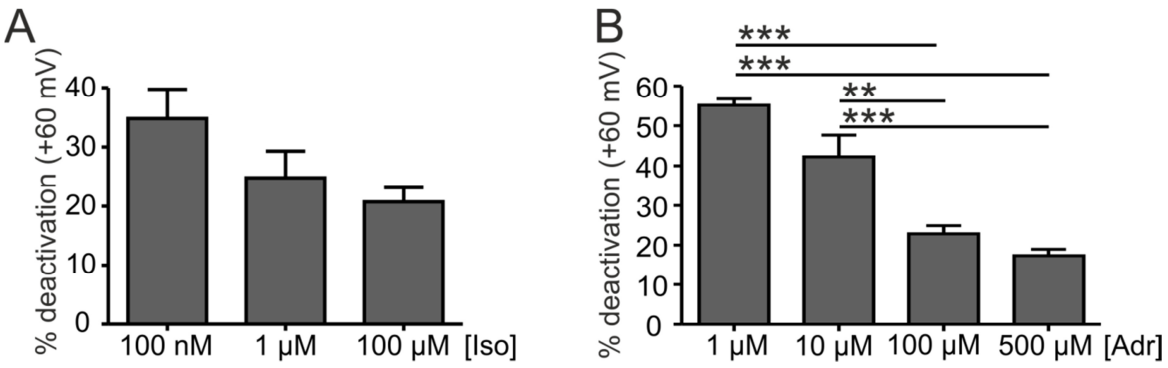

Figure 9: Saturation of β_1-AR with agonist does not abolish depolarization-mediated receptor deactivation.
A and *B:* The effect of depolarization on the β_1-AR-sensor activity induced by stimulation with different sub- or saturating concentrations of Iso (*A,* n=8-11) or Adr (*B,* n=5-8) was quantified for measurements similar to those in Figure 8*C* and 4*D*. The dashed lines in Figure 8*A* and 1*B* indicate the baselines for the calculation of FRET amplitudes in the individual measurements. The quotient of FRET amplitudes during depolarization and during the holding potential was calculated in % and subtracted from 100% to obtain the percentage of depolarization-induced receptor deactivation. One way ANOVA with Bonferroni's multiple comparison test was used to test for statistical significance. **: $p<0.01$; ***: $p<0.001$.

Voltage-sensitivity of several GPCRs has been shown to act through alterations in agonist affinity (Ben-Chaim et al., 2003, 2006; Ohana et al., 2006; Rinne et al., 2013). One would assume that if only a reduction in agonist affinity underlay voltage-sensitivity of β_1-AR as well, stimulation with saturating concentrations of agonist would abolish depolarization-mediated deactivation similarly as described for the α_{2A}-AR (Rinne et al., 2013). This was not the case for Iso- or Adr-stimulated β_1-AR in cells subjected to depolarization (Figure 9). To quantify the degree of voltage-induced deactivation, cells were stimulated with sub- or saturating concentrations of either Iso or Adr in

measurements similar to those in Figure 8C and D. Agonist-induced alterations in FRET (from here on FRET amplitudes) were measured before and during the depolarizing step to +60 mV in the individual measurements normalized to their maximal agonist-induced FRET amplitude (see dashed lines in Figure 8C, D). The relation of the latter over the former amplitude was calculated, subtracted from 1, calculated as percent deactivation and averaged over the given number of individual measurements (Figure 9). There was no significant difference in deactivation by depolarization when cells were activated by concentrations of Iso ranging from 100 nM to 100 µM (Figure 9A). Although increasing concentrations of Adr significantly reduced the depolarization-mediated deactivation, about 20% deactivation remained even when cells were stimulated with 500 µM Adr (Figure 9B). Depolarization induced stronger deactivation in cells stimulated with non-saturating concentrations of Adr compared to non-saturating concentrations of Iso (compare about 55% deactivation to about 35% deactivation during depolarization and application of 1 µM Adr and 100 nM Iso, respectively). The remaining fraction of about 20% deactivation by depolarization during receptor saturation, however, was comparable in Iso- and Adr-stimulated cells (Figure 9A, B).

These data indicate that a reduction in agonist affinity which seemed more pronounced in Adr- than in Iso-stimulated cells contributes to the effect of voltage-dependence. However, the remaining effect of depolarization on receptor activity even in saturation points towards a contribution of altered agonist efficacy to β_1-AR voltage-dependence, which is similar for Iso and Adr.

6.1.1 G protein signaling is attenuated by depolarization

With the β_1-AR sensor we were able to monitor depolarization-dependent conformational changes of the agonist-stimulated receptor which reflected receptor deactivation. Apart from voltage-dependent changes in agonist binding other voltage-dependent GPCRs also showed altered downstream signaling upon depolarization (for example (Martinez-Pinna et al., 2005; Ohana et al., 2006; Sahlholm et al., 2011; Rinne et al., 2013, 2015)). But would depolarizing steps also influence downstream signaling of β_1-AR? To answer this question we used FRET assays which monitored the G protein axis of β_1-AR signaling. To analyze voltage-dependence of G_s protein activation, FRET was measured between the YFP-labeled $G\alpha_s$ and CFP-$G\gamma_2$ subunits under co-transfection of non-fluorescent β_1-AR and $G\beta_1$ subunit (Hein et al., 2006). In its inactive state the fluorescently labeled heterotrimeric G protein exhibits high initial FRET. Upon receptor activation the G protein interacts with active receptors and undergoes an activating conformational change which reduces the

affinity of the subunits to one another and to the receptor. A decrease in the energy transfer between CFP-Gγ_2 and Gα_s-YFP, i.e. a decrease in FRET, represents G protein activation (Figure 10A). Activation of the G_s protein by 30 nM Adr strongly activated the G_s protein. Opposing courses of donor and acceptor emissions calculated into a decrease in acceptor-over-donor ratio during agonist stimulation (Figure 10B). Depolarization to +60 mV reversibly reduced the agonist-evoked FRET response. Stimulation with 0.3 nM Iso led to a ratio decrease in a single experiment which slowly recovered after withdrawal of the agonist (Figure 10C). Depolarization of the membrane to +60 mV deactivated the G protein almost completely despite continuous activation of β_1-AR. After repolarization of the membrane the inhibition of G protein activation was abolished (Figure 10C).

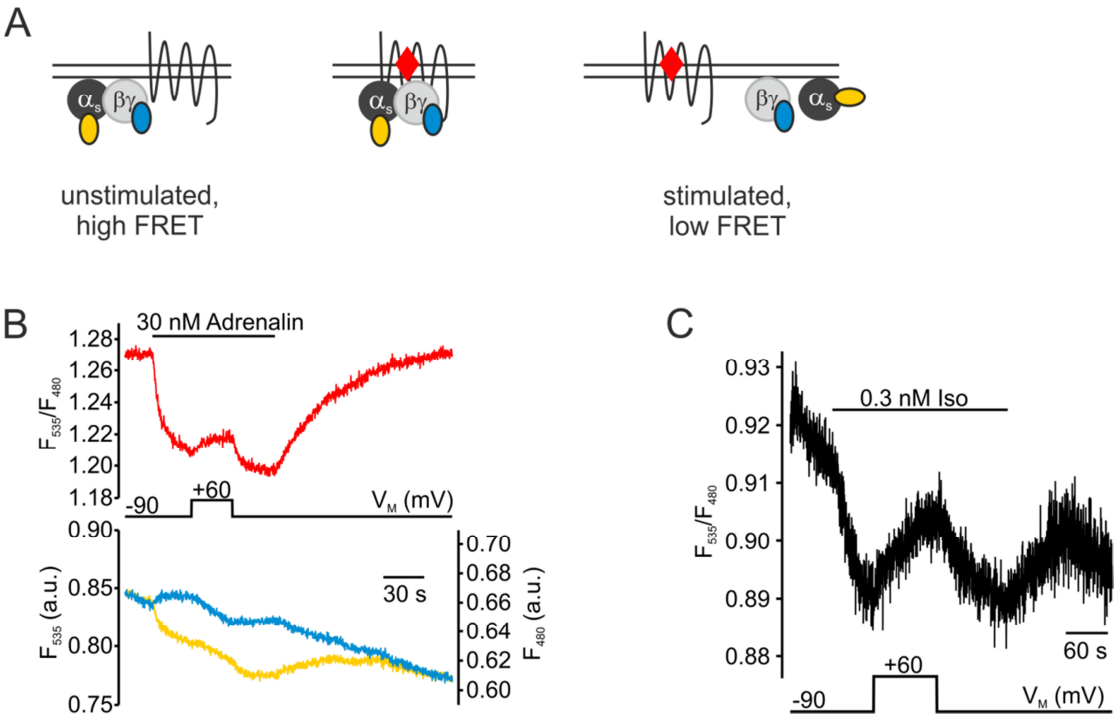

Figure 10: Signal transmission through G proteins is weakened during depolarization.
G_s protein activation has been measured in cells transfected with YFP-labeled Gα_s, CFP-Gγ and non-fluorescent β_1-AR and Gβ_1. *A*: High initial FRET occurs in the absence of agonists. Upon stimulation the G protein interacts with the receptor. This enables G protein activation by a conformational change in the G protein which is indicated by a reduction in FRET. *B*: One of three successful experiments is shown in which cells were stimulated with 30 nM Adr. Individual traces of CFP and YFP emission run in opposing directions upon agonist stimulation and during depolarization to +60 mV indicating specific FRET. *C*: A single experiment of a cell stimulated with 0.3 nM Iso and depolarized to +60 mV during stimulation is shown.

Due to differences in expression levels of the constructs among cells variations occurred in response to agonist stimulation. Many cells did not show agonist-evoked responses whereas in others G protein activation was saturated. Amplification of the signal at the level of G proteins and fast saturation of the system proved the measurements of voltage-dependent G_s protein activation to be difficult. Therefore, only a few of many experimental

attempts succeeded and the results obtained have to be considered preliminary. It appears, however, as if G protein activation was also hampered during depolarization. More (high quality) experiments with low agonist concentrations will be necessary before a conclusive interpretation of the data is possible.

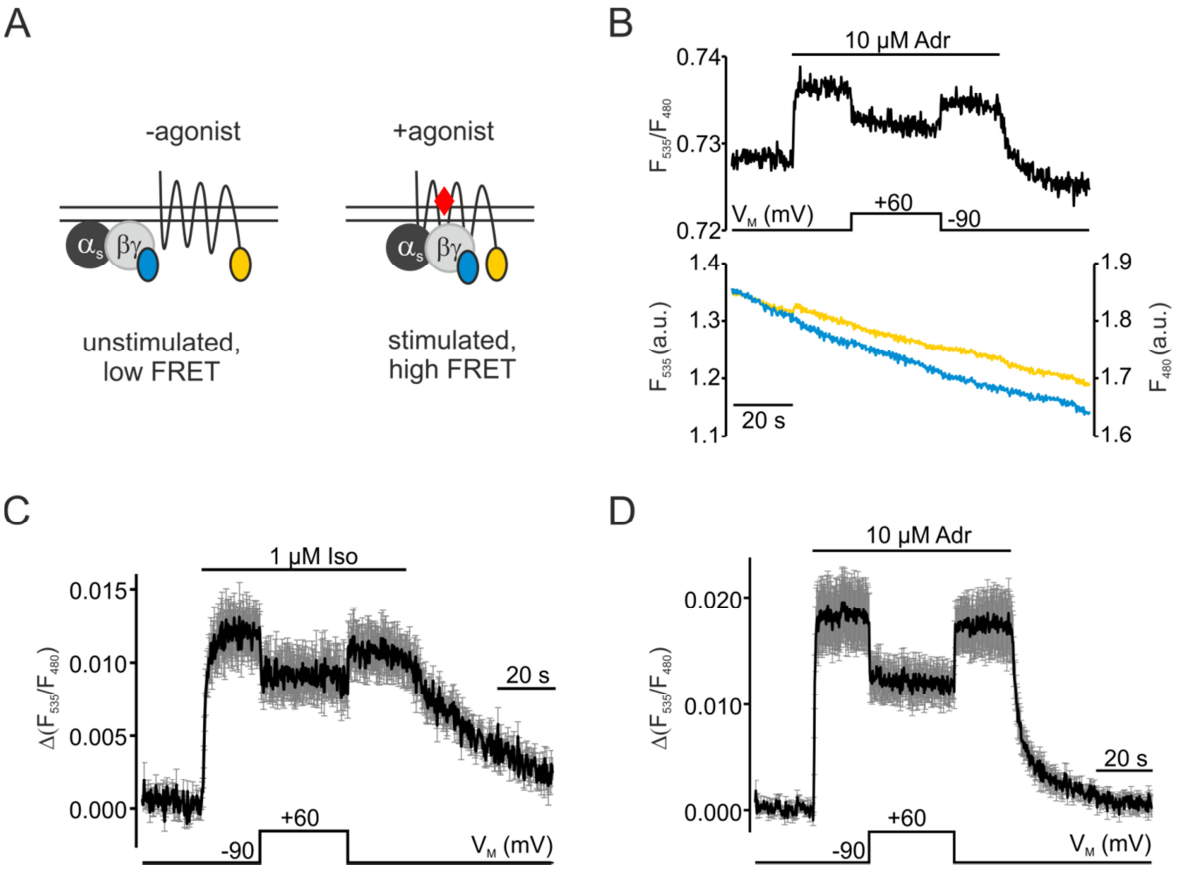

Figure 11: Depolarization rapidly diminishes receptor-G protein interaction.
A: The interaction between β_1-AR and the Gs protein was monitored with a FRET assay between YFP-labeled β_1-AR (β_1-AR-YFP) and the CFP-labeled $G\gamma_2$-subunit (CFP-Gγ) in the presence of unlabeled G protein subunits $G\alpha_s$ and $G\beta_1$. Before stimulation, the receptor-G protein interaction assay displays low FRET. Stimulation of the receptor leads to the interaction of receptors and G proteins which results in an increase in FRET. *B:* Stimulation with 10 µM Adr enhanced energy transfer from CFP to YFP indicated by an increase YFP and a decrease in CFP emission intensity. Only minor alterations however to opposing directions are visible in the single emission traces. Those calculate into an increase in the ratio of acceptor-over-donor emission intensity. Depolarization to +60 mV was performed during Adr-stimulation. *C and D:* Cells stimulated with 1 µM Iso (*A*: n=7) or 10 µM Adr (*B*: n=7) were depolarized to +60 mV during stimulation. Individual measurements were corrected for bleaching before the averages were calculated (average±SEM).

As a reduction in agonist efficacy seemed to contribute to receptor deactivation during depolarization we aimed to investigate this effect also downstream of the receptor. Due to the signal amplification at the level of G proteins, the FRET assay monitoring G protein activation was not suitable for the investigation of alterations in agonist efficacy (Lohse et al., 2003). Therefore, we measured the interaction of β_1-AR and the heterotrimeric G_s protein by means of FRET. Cells were transfected with YFP-labeled β_1-AR (β_1-AR-

YFP), CFP-labeled $G\gamma_2$ subunit (CFP-Gγ) and unlabeled $G\alpha_s$ and $G\beta_1$ subunits (Hein et al., 2006). Stimulation with agonist triggers the interaction of receptor and the heterotrimeric G protein which can be detected by an increase in FRET (Figure 11A). YFP emission increased upon stimulation with 10 µM Adr while CFP emission slightly decreased resulting in an increase in acceptor-over-donor emission ratio (Figure 11B). Depolarization rapidly and reversibly diminished the interaction between β_1-AR and G protein induced by Adr (Figure 11B). The average data of cells stimulated with 1 µM Iso (Figure 11C) or 10 µM Adr (Figure 11D) also showed the interaction of receptor and G protein indicated by an increase in FRET. Withdrawal of the agonists terminated the interaction and the ratio decreased to baseline levels. During both Iso- and Adr-stimulation a depolarizing step to +60 mV quickly reduced the ratio, i.e. attenuated the interaction between receptor and G protein, which was reversible upon repolarization to the holding potential of -90 mV. Adr-stimulated cells were slightly more sensitive to the positive membrane potential than Iso-stimulated cells. The average reduction of receptor-G protein interaction by depolarization was 33.8±5% (Adr) and 28.2±5% (Iso). As seen for the β_1-AR sensor deactivation, also the depolarization-induced weakening of receptor-G protein interaction occurred with faster kinetics than the disruption of interaction by washout of the ligands indicating a reduction in agonist efficacy (6.1.4).

6.1.2 Depolarization weakens β_1-adrenoceptor-arrestin 3 interaction

In addition to G proteins, arrestins play an important role in GPCR signaling and desensitization. Therefore, it was interesting to find out whether depolarization also influenced the interaction of arrestin 3 with β_1-AR. A FRET-based assay with β_1-AR-YFP, N-terminally CFP-labeled arrestin 3 (CFP-Arr3) and unlabeled GPCR kinase 2 (GRK2) was used (Ahles et al., 2015) which will be referred to as the arrestin FRET assay. GRKs phosphorylate receptors in a ligand-dependent manner (Krasel et al., 2005) which is necessary for the recruitment of and interaction with arrestins (Lohse, 1993). A ratio increase reflects the interaction of β_1-AR and arrestin 3 upon ligand activation and GRK phosphorylation (Figure 12A). Single emission intensity traces of a cell stimulated with 100 nM Iso nicely show opposing courses upon agonist application: CFP intensity decreased as it transferred its energy onto YFP resulting in an increased YFP emission (Figure 12B). Upon agonist removal YFP intensity decreased while CFP intensity increased which was caused by arrestin 3 dissociation from the receptor. As seen for the interaction measurement of β_1-AR and G_s protein, β_1-AR-arrestin 3 interaction was disrupted during depolarization indicated by a decrease in the Iso-evoked FRET amplitude

(Figure 12B). Averaged data showed that the interaction of β_1-AR and Arr3 evoked by either Iso (100 nM, Figure 12C) or Adr (1 µM, Figure 12D) was weakened by a depolarizing step to +45 mV. Reduction of the depolarization step from +60 mV to +45 mV compared to the measurements before helped to stably control the membrane potential over these longer-term recordings. The β_1-AR-Arr3 complex disruption by depolarization also seemed faster than disruption kinetics by agonist withdrawal; a similar finding as for measurements at the receptor level and G protein-receptor interaction (6.1, 6.1.1, 6.1.4).

Especially in cells stimulated with Iso it was apparent that the FRET signal was not fully reversible after ligand washout (Figure 12B, C). This is, presumably, due to the accumulation of β_1-AR-Arr3 complexes in clathrin-coated pits (CCPs) which prevented the disruption of their interaction by ligand washout. Only a fraction of receptors and arrestins are still able to dissociate upon ligand washout which resulted in an elevated baseline at the end of the measurements. The degree of recovery in Adr-stimulated cells was better than in Iso-stimulated cells but also incomplete (Figure 12D). A lower affinity of Adr towards β_1-AR compared to Iso resulting in faster dissociation rates allowed shorter measurement protocols. In a shorter time less β_1-AR-Arr3 complexes could accumulate leading to a better reversibility of the FRET signal upon Adr washout.

To quantify the reduction in FRET induced by depolarization, amplitudes at -90 mV and +45 mV were measured. The amplitudes at +45 mV were measured from the baseline to the ratio during depolarization in each individual measurement. At the same time-point the reference amplitude at -90 mV in each cell was measured: Ratio values before and after the depolarizing step were linearly connected (indicated by dashed lines in Figure 12C and D) and the -90 mV amplitude was measured between the baseline and the connecting straight line at the same time-point as the amplitude at +45 mV. In non-saturating conditions, depolarization weakened the interaction between arrestin 3 and β_1-AR by about 30% in Iso- and Adr-stimulated cells (Figure 12E). This loss of interaction was significantly smaller when saturating concentrations of Iso and Adr were used. When stimulated with 100 nM and 10 µM Iso, the depolarization effect was significantly reduced from 31.0±2.2% to 16.9±1.6% ($p<0.001$), respectively, i.e. by about two-fold. The weakening of interaction by depolarization dropped significantly from 32.3±1.2% to 8.3±1.2% ($p<0.001$), i.e. by about a factor of four, in cells stimulated with 1 µM Adr and 100 µM Adr, respectively.

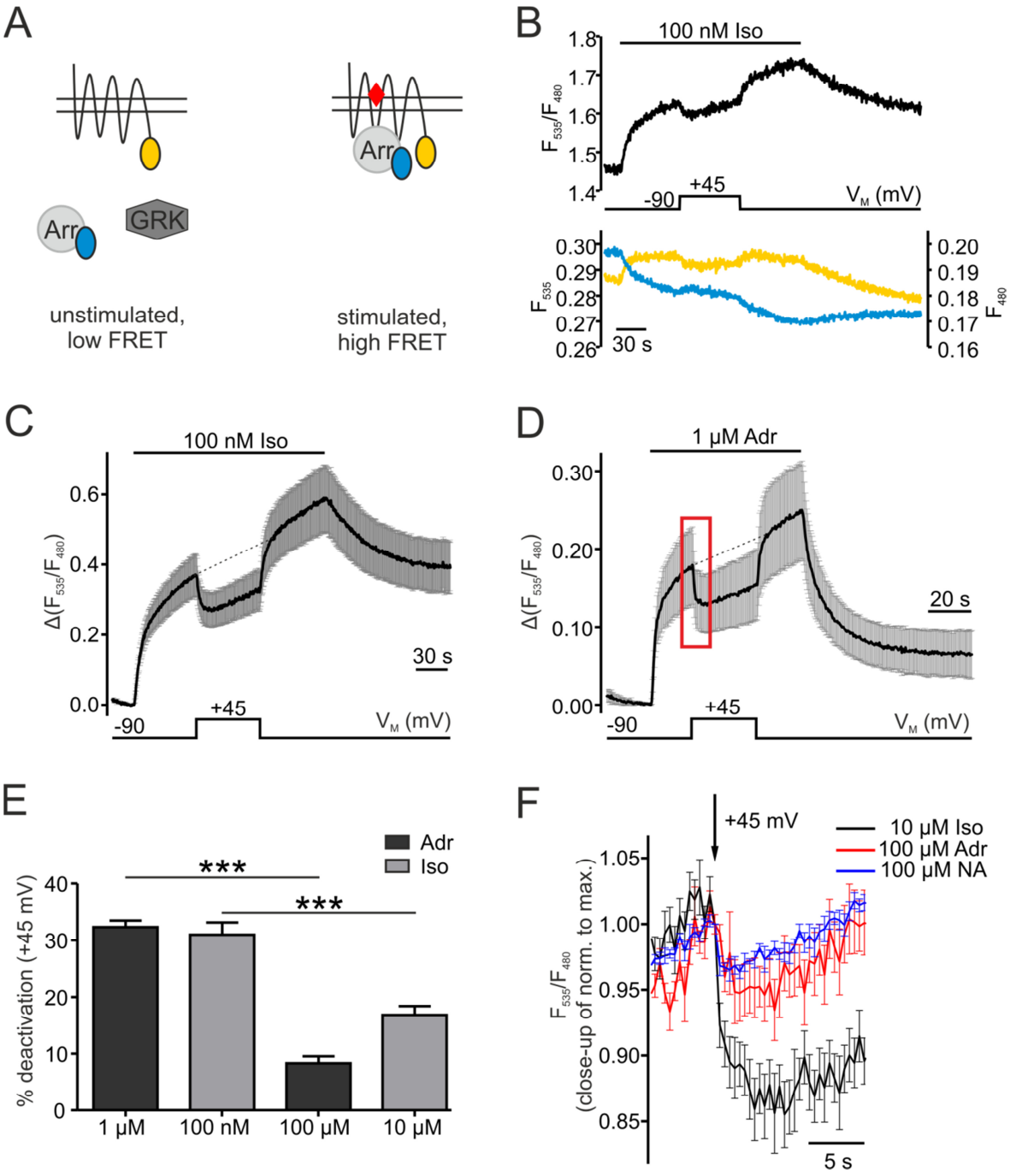

Figure 12: Depolarization weakens the interaction between β_1-AR and arrestin 3.
A: To analyze the interaction of β_1-AR and arrestin 3, cells were transfected with β_1-AR-YFP and CFP-labeled arrestin 3 together with non-fluorescent GRK2. Arrestin and GRK2 reside in the cytosol of unstimulated cells which results in low FRET. Stimulation of the receptor causes translocation of GRK2 and arrestin 3 to the membrane and interaction with the receptor. This agonist-induced interaction can be measured as an increase in FRET. As from now on FRET assays investigating this interaction between arrestin and the receptor will be called arrestin FRET assay or arrestin FRET. *B:* Opposing directions of CFP and YFP emission intensity due to FRET can be detected in a representative measurement upon stimulation of β_1-AR with 100 nM Iso. Depolarization to +45 mV reduces energy transfer from CFP to YFP, resulting in a decrease in FRET and indicating dissociation of arrestin from the receptor. *C and D*: Averages±SEM of cells stimulated with 100 nM Iso (*C*: n=8) and 1 µM Adr (*D*: n=6) and subjected to a depolarizing pulse to +45 mV. The red box in *D* marks the section of data used for the close-up in *F*. *E*: Data points before and after depolarization of individual measurements under saturating and non-saturating concentrations of agonist were linearly connected as depicted by dashed lines in *C* and *D*. Amplitudes at rest and during depolarization were measured to calculate %-deactivation by depolarization (Iso: 100 nM and 10 µM, n=8; Adr: 1 µM, n=10 and 100 µM, n=8). Amplitudes were measured as follows: +45 mV amplitude: baseline to curve; -90 mV amplitude: baseline to dashed line at the same time point. The calculation of %-deactivation

was performed as described in Figure 9. Statistical significance was confirmed by one way ANOVA with Bonferroni's multiple comparison test. ***: p<0.001. *F*: Measurements with saturating concentrations of Iso (10 µM, black trace, n=8), Adr (100 µM, red trace, n=8) and NA (100 µM, blue trace, n=8) were normalized to the maximal agonist-evoked FRET response prior to the depolarizing step and averaged. An overlay of the section indicated by the red box in *B* of each average is shown. The black arrow marks the time point at which the membrane potential was depolarized from -90 mV to +60 mV.

The remaining effect of depolarization on β_1-AR-arrestin 3-interaction induced by saturating agonist concentrations together with the faster deactivation kinetics upon depolarization again points towards an alteration in agonist efficacy during depolarization. This is consistent with the measurements of the β_1-AR sensor and of β_1-AR-G protein interaction and will be analyzed together in chapter 6.1.4.

Apart from adrenaline, β_1-ARs are also activated by the endogenous full agonist noradrenaline, which has the same affinity towards β_1-AR as Adr (Bond et al., 2015). Arrestin 3 also interacted with the β_1-AR upon stimulation with NA. Depolarization weakened this interaction induced by 100 µM NA (saturation) to a comparable degree as seen for Adr (Figure 12F). As no apparent differences in voltage-dependence between the two endogenous full agonists were detected, further experiments only compare the effect of depolarization on β_1-AR stimulated with Iso and Adr.

Depolarization-induced deactivation of β_1-AR was not only detected at the receptor level but was also transmitted to downstream signaling. The interaction of β_1-AR and G protein or arrestin 3 was weakened by depolarization through a reduction in agonist affinity and efficacy. The proportion to which reduction in affinity or efficacy contribute to the phenomenon of voltage-dependence will be addressed in chapters 6.1.4, 6.1.5 and 6.1.6.

6.1.3 Voltage-dependence occurs within the physiological range of the membrane potential

As a next step it was important to determine whether the observed voltage-dependence of β_1-AR occured within the physiological range of V_M. The arrestin FRET assay was used to measure the relation of β_1-AR-arrestin 3 interaction and V_M. During stimulation with a non-saturating concentration of agonist, the membrane potential was switched stepwise to several different potentials. A representative measurement of a cell stimulated with 1 µM Adr showed differential alterations in the FRET amplitude induced by different potentials (Figure 13A). Hyperpolarization to -120 mV enhanced the interaction between β_1-AR and arrestin 3 while stepwise depolarization gradually reduced it. The FRET amplitudes at a given test potential and the corresponding amplitude at -90 mV (baseline to dashed line at the same time point) were measured. Amplitudes were calculated as a percentage of the

response at -90 mV and plotted against the membrane potential. The data calculated in this manner were then fit to a Boltzmann equation (Figure 13B).

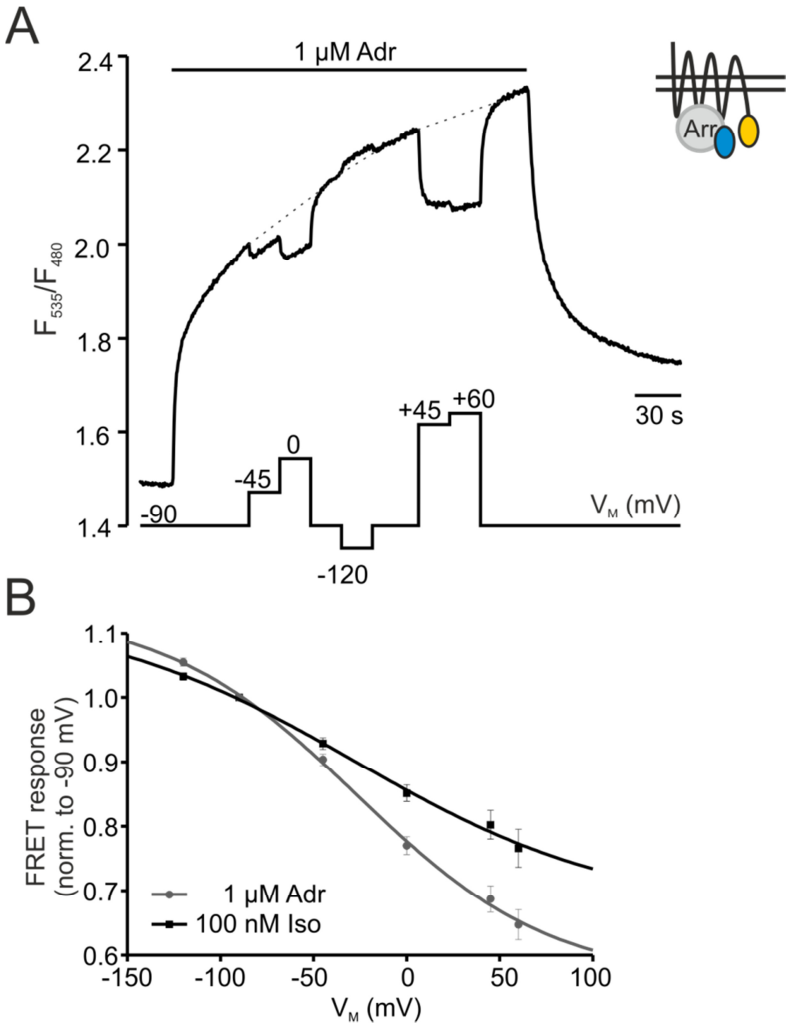

Figure 13: Voltage-dependence of β_1-AR occurs within the physiological range of membrane potential. *A*: A representative measurement of a cell transfected with the arrestin-FRET assay (inset) demonstrates how data for a FRET response-V_M-plot were obtained. During stimulation with 1 µM Adr the membrane potential is switched between the holding potential of -90 mV and various other potentials. Amplitudes were measured during every VM-step, calculated as a percentage of the corresponding amplitude at -90 mV (measured from the baseline to the dashed line at the same time point) and plotted against V_M (*B*). *B*: A Boltzmann equation was fit to the FRET response-V_M-data of Iso- and Adr-stimulated cells (Iso: black, n=14, R^2=0.99; Adr: gray, n=11, R^2=0.99). Half maximal effective potentials were V_{50}=-28±22 mV (Iso) and V_{50}=-27±8 mV and the amount of charge moved was z=0.36 e_0 (Iso) and z=0.49 e_0 (Adr).

The fits of Iso and Adr data yielded similar half maximal effective potentials of β_1-AR-arrestin 3 interaction (Iso: $V_{0.5}$=-28±22 mV and Adr: $V_{0.5}$=-27±8 mV). From the slope of a Boltzmann fit it is also possible to calculate the amount of charges moved across the membrane ("gating charge" in ion channels). These z-scores were z=0.36 e_0 and z=0.49 e_0 for Iso and Adr, respectively. The z-scores indicated that one charge moved across about half the membrane in Adr-stimulation and a bit less in Iso-stimulation. The z-score corresponding to the Iso curve was comparably small due to the shallower Boltzmann

curve. Both the half maximal effective potential and the calculated z-scores for β_1-AR voltage-dependence are in line with data obtained at M_1AChR, M_2AChR and α_{2A}-AR (3.2.1 and 7.1; (Ben-Chaim et al., 2006; Navarro-Polanco et al., 2011; Rinne et al., 2013, 2015)).

Half maximal effective potentials for the interaction of receptors and arrestins obtained from the Boltzmann fit showed that voltage-dependence of the β_1-AR lies within the physiological range of membrane potential.

6.1.4 Off-kinetics indicate a major contribution of altered agonist efficacy to β_1-adrenoceptor voltage-dependence

Differences in deactivation kinetics induced by depolarization compared to ligand withdrawal were visible in measurements on the β_1-AR receptor level. They were also seen in measurements analyzing the interaction of the receptor with either its G protein or arrestin 3. If depolarization only altered ligand affinity, depolarization and washout deactivation kinetics should be similar. This was shown to be the case for the α_{2A}-AR stimulated with noradrenaline (Rinne et al., 2013). But as this was not the case for β_1-AR, the faster deactivation during depolarization pointed towards an alteration in ligand efficacy. Therefore, deactivation rates of the three FRET assays were analyzed in detail in order to identify the contribution of agonist efficacy to the phenomenon of voltage-dependence.

Altered efficacy underlying voltage-dependence has been postulated for some GPCRs before (Martinez-Pinna et al., 2005; Gurung et al., 2008; Navarro-Polanco et al., 2011; Sahlholm et al., 2011; Rinne et al., 2013). Most of these studies used indirect methods hardly suitable to detect alterations in efficacy because either receptor numbers or receptor coupling affected the measurements (Lohse et al., 2003). Only measurements with α_{2A}-AR-cam, the intramolecular FRET-based fusion protein of the α_{2A}-AR, activated by clonidine provided direct evidence for a change in efficacy of this ligand (Rinne et al., 2013).

Deactivation kinetics of data obtained with the β_1-AR sensor (Figure 8C, D) and the FRET-assays measuring receptor-G protein interaction (Figure 11C, D) or receptor-arrestin 3 interaction (Figure 12C, D) were analyzed. Dark gray and light gray boxes in the normalized average trace of the β_1-AR-sensor indicate were off-kinetics induced by depolarization or ligand withdrawal were calculated, respectively (Figure 14A, data of Figure 8C). Mono-exponential functions were fit to the indicated sections of the average traces of Iso- and Adr-stimulated cells. A poor signal-to-noise ratio did not allow fitting of individual experiments. The quantification of k_{off}-values yielded a 100-fold accelerated

deactivation by depolarization compared to washout-induced deactivation (k_{off} voltage=1.7±0.5 s^{-1}; k_{off} washout=0.017±0.003 s^{-1}) in cells stimulated with Iso (Figure 14B). Compared to Iso the affinity of Adr towards β_1-AR is lower. This caused faster washout kinetics and therefore an only about 8-fold but yet significant difference between deactivation kinetics by washout or by depolarization (k_{off} voltage=0.98±0.2 s^{-1}; k_{off} washout=0.13±0.006 s^{-1}) in Adr-stimulated cells.

To visualize the difference in deactivation kinetics of the protein-interaction studies, the data corresponding to the sections indicated in Figure 14A where normalized to the maximal FRET effect in each individual experiment, averaged and overlaid (Figure 14C, E). To increase clearness, the error bars only point to one direction. The arrows mark the time-points at which either the cell was depolarized or the agonist was withdrawn. Already from these overlays it is visible, that the interaction of β_1-AR either with its G protein (Figure 14C, 10 µM Adr) or with arrestin 3 (Figure 14E, 100 nM Iso) is disrupted more rapidly by depolarization than by ligand withdrawal. The quantification was done by fitting a mono-exponential function to the average traces as described above. The dissociation rate of the G protein from β_1-AR upon depolarization was comparable in both Iso- and Adr-stimulated cells (Iso: k_{off}voltage=2.2±1.0 s^{-1}; Adr: k_{off}voltage=2.3±0.5 s^{-1}) (Figure 14D) despite their different washout dissociation rates (Adr: k_{off}washout=0.21±0.006 s^{-1}; Iso: k_{off}washout=0.033±0.003 s^{-1}). This pointed towards a similar mechanism underlying voltage-dependence of Iso- and Adr-stimulated β_1-AR. An 11-fold and a 70-fold difference in dissociation rate during depolarization compared to agonist withdrawal was calculated for Adr and Iso, respectively. Quantification of the arrestin 3 dissociation from β_1-AR yielded 10-fold (k_{off}voltage=0.32±0.02 s^{-1}; k_{off}washout=0.031±0.001 s^{-1}) and about 14-fold (k_{off}voltage=1.37±0.1 s^{-1}; k_{off}washout=0.099±0.002 s^{-1}) differences in Iso- and Adr-stimulated cells, respectively (Figure 14F). Note, the half-times of the measurements of G protein-receptor interaction and the β_1-AR-Arr3-interaction under Adr stimulation were close to the detection limit of the sampling frequency used (G protein: $t_{1/2}$=0.3 s, frequency: 5 Hz; arrestin 3: $t_{1/2}$=0.5 s (Adr), frequency: 2.5 Hz). Measurement accuracy for the fast deactivation and disruption of interaction is therefore limited.

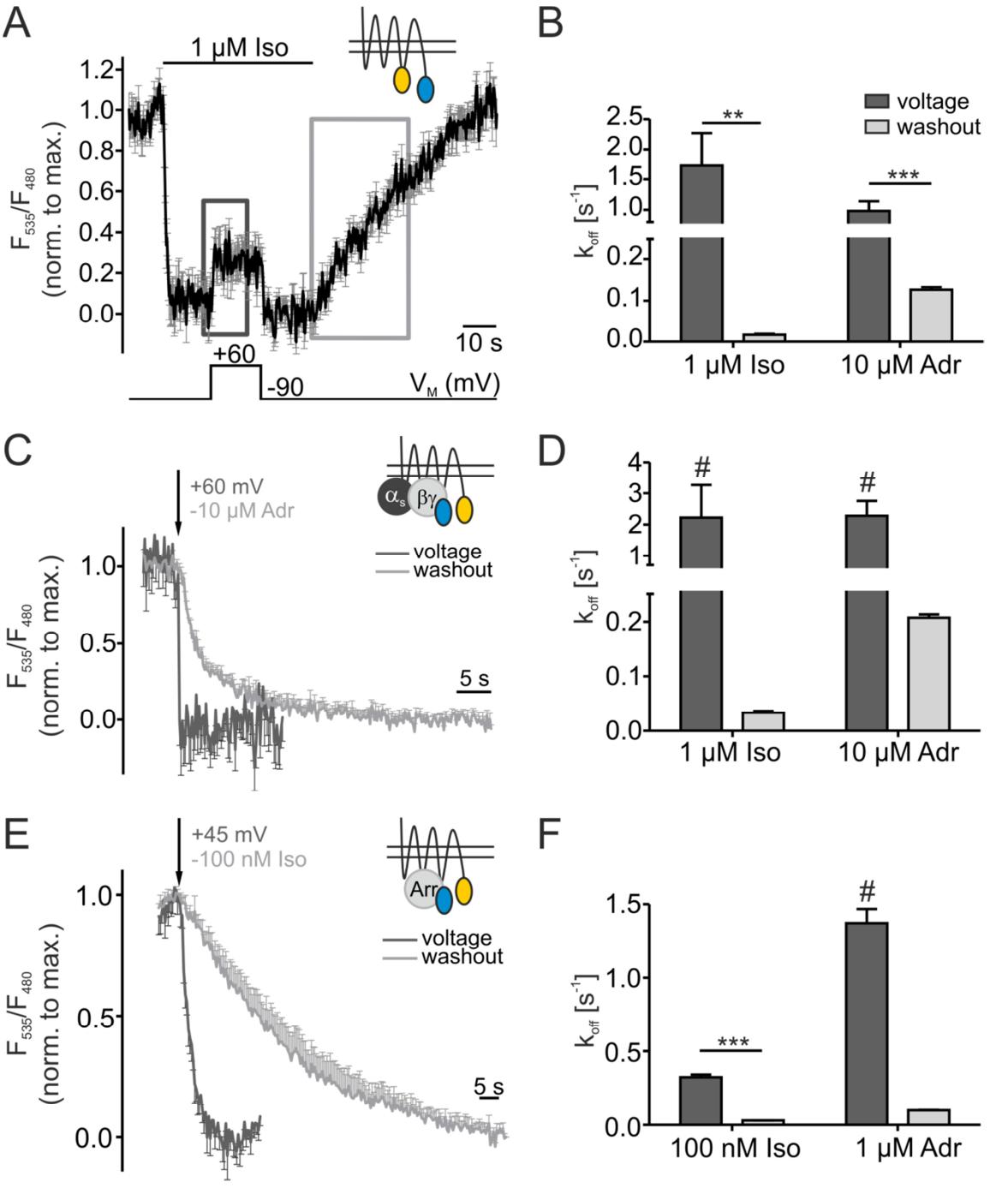

Figure 14: Deactivation kinetics suggests agonist efficacy to be the major target of voltage-dependence. Deactivation kinetics by agonist withdrawal or depolarization were compared for the β_1-AR-sensor (*A and B*), for the interaction of receptor and G protein (*C and D*) and for the interaction of receptor and arrestin (*E and F*) (see insets). *A*: Light gray and dark gray boxes in the average trace taken from Figure 8*C* mark the sections in which off-rates were determined by fitting a mono-exponential function to the average trace. *C and E*: The data sections of Figure 11*D* and Figure 12*C* corresponding to the gray boxes in *A* were normalized to the maximal FRET amplitude and overlaid. Mono-exponential functions were fit to the averages to determine washout- and depolarization-induced deactivation kinetics. To maintain clearness, the error bars only point in one direction. Arrows in both graphs indicate the time point at which agonists were withdrawn or at which the membrane was depolarized. *B, D, F*: Summary of washout- and depolarization-mediated k_{off} values and statistical analysis (B: n≥8; D: n=7, F:n≥8). Statistical significance was determined using F-test for fit comparison. **: p<0.01, ***: p<0.001. #: Sampling rates in measurements analyzed for *D* and *F* were 5 Hz and 2.5 Hz, respectively. The k_{off} values were close to the detection limit of 200 ms in *D* (both agonists) and of 400 ms in *F* (Adr stimulation).

Especially the measurements at the receptor level, but also those of the downstream effectors clearly showed that alterations in efficacy are involved in the phenomenon of voltage-dependent regulation of β_1-AR activity. Furthermore, this reduction in agonist efficacy during depolarization exceeded the reduction in affinity (compare to results of Figure 9A, B and Figure 12E) and therefore seemed to be the major player in voltage-dependent fine-tuning of the β_1-AR activity.

6.1.5 Measurements of deactivation kinetics under constant membrane potential show a moderate reduction in agonist affinity at depolarization

According to the law of mass action a change in off-rate of a reaction has to be due to an alteration in agonist affinity provided that the on-rate of this reaction is unchanged. Thus, I analyzed deactivation kinetics to compare agonist affinities at a constant potential of either -90 mV or +45 mV. Cells were transfected with the arrestin FRET assay constructs, stimulated with either 100 nM Iso (Figure 15A) or 1 µM Adr (Figure 15C) and measured twice, once at each potential. The order of the potentials was alternated between measurements. Upon Iso withdrawal, Arr3 dissociated significantly faster from the receptor at depolarization compared to the dissociation at -90 mV (Figure 15A, B) but the difference in k_{off}-values was less than two-fold (+45 mV: k_{off}=0.044±0.005 s^{-1}; -90 mV: k_{off}=0.027±0.003 s^{-1}) (Figure 15B). Accumulation of receptor-arrestin complexes, presumably in clathrin-coated pits (CCPs), again prevented a full reversibility of the FRET signal after prolonged washout in these measurements (Figure 15A).

From the previous experiments with Adr a larger reduction in affinity in cells stimulated with Adr would be expected compared to the results obtained with Iso. But due to the fast dissociation of Adr from the β_1-AR upon agonist washout and the therefore fast dissociation of Arr3 from the receptor, the additional increase in the dissociation rate during depolarization was hardly visible (Figure 15C). The analysis of k_{off}-values also only yielded a small but significant acceleration in the dissociation rate at depolarization which was less than two-fold (-90 mV: k_{off}=0.1375±0.011 s^{-1}; +45 mV: k_{off}=0.2044±0.030 s^{-1}) (Figure 15D). Note that the FRET signal almost reversed back to baseline after Adr washout. This is likely due to the shorter stimulation time which led to less accumulation in CCPs.

In principle, it is possible to deduce changes in agonist affinities from the evaluation of deactivation or dissociation kinetics if the on-rate of the reaction is unaltered (law of mass action). The analysis showed a slight reduction in affinity for Iso during depolarization but

this experiment did not prove well suited to deduce changes in Adr affinities due to its fast dissociation from the β_1-AR even at the resting potential.

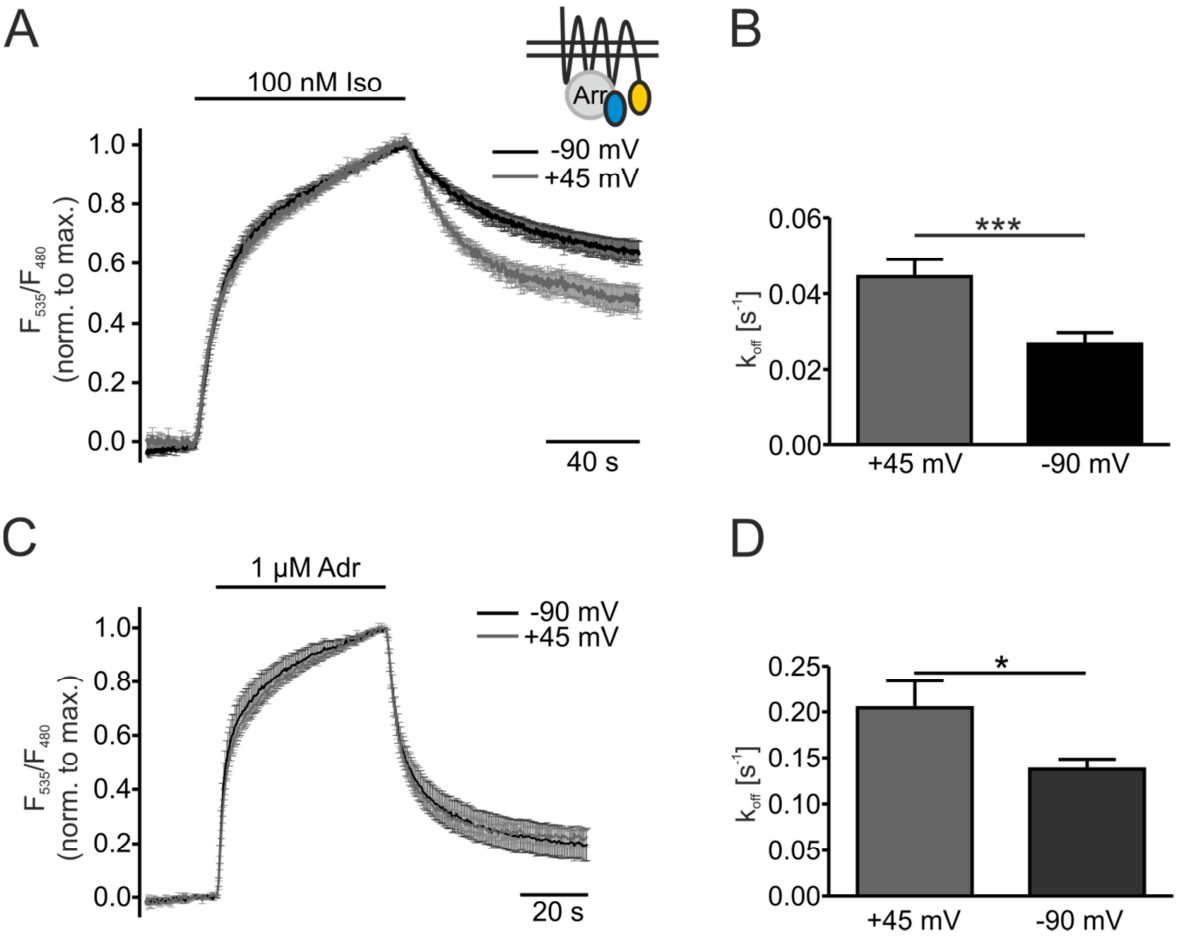

Figure 15: Analysis of deactivation kinetics reveals minor reduction in agonist affinity during depolarization.
A and *C*: Cells transfected with the arrestin FRET assay were measured twice under constant membrane potential of -90 mV and +45 mV in an alternating order and stimulated with 100 nM Iso (*A*) or 1 µM Adr (*C*). Individual measurements were normalized to the maximal agonist-evoked FRET response (average±SEM, *A*: n=9; *C*: n=10). *B* and *D*: Comparison of deactivation kinetics (k_{off}) during depolarization and at rest of the measurements stimulated with Iso (*B*) and Adr (*D*). Statistical analysis was performed with paired student's t-tests. ***: $p<0.001$, *: $p<0.05$.

6.1.6 Efficacy essentially contributes to Iso-stimulated β_1-adrenoceptor voltage-sensitivity: A concentration-response curve

In order to compare the involvement of alterations in affinity and efficacy to voltage-dependence of the β_1-AR activity directly in a classical pharmacological way, data were collected to plot concentration-response curves for Iso at the resting potential (-90 mV) and at depolarization (+45 mV). Because of its good signal-to-noise ratio and the reliably large amplitudes, the arrestin FRET assay was used for this task. Transfected cells were stimulated twice: first with an Iso test concentration and after washout with the reference concentration of 10 µM Iso. During both stimulations the membrane potential was switched between -90 mV and +45 mV (Figure 16A). Two-point interpolations (dashed

lines) were used to adjust the baselines, which increased due to accumulation of receptor-arrestin-complexes. Amplitudes were measured between the dashed lines and the FRET trace at depolarization (A_{+45}) or at rest (A_{-90}) during stimulation with the test concentration. These amplitudes were normalized to the reference amplitude (A_{ref}) at -90 mV during stimulation with 10 µM Iso in each cell (A_{+45}/A_{ref} or A_{-90}/A_{ref}) to allow the comparison of FRET amplitudes between cells independently of the absolute agonist-induced FRET response of individual measurements. The averages of these normalized FRET responses were plotted against the Iso concentration (Figure 16B). Data for 10 µM Iso were collected in the same way as for the other test concentrations: First, 10 µM Iso were applied and withdrawn as the test concentration before the second application of 10 µM Iso was administered as a reference. Note, that the data points at concentrations of 1 µM Iso and higher exceed the 100% reference value. These high concentrations of Iso induced a fast accumulation of arrestin-receptor complexes. As a result, the fraction of available arrestins and receptors for the second stimulation was reduced which resulted in a steep rise of the curve during the first stimulation and comparatively smaller amplitudes during the second one. Paired student's t-tests confirmed significant differences in the FRET response at +45 mV compared to -90 mV of each test concentration except 10^{-10} M Iso. Sigmoidal functions allowing a variable Hill slope were fit to the data collected at -90 mV and at +45 mV. The difference between EC_{50}-values of the curves at -90 mV ($EC_{50}=2.5*10^{-8}$ M) and at +45 mV ($EC_{50}=4.8*10^{-8}$ M) did not reach statistical significance. In contrast, the maximal FRET response at depolarization was significantly lower than the maximal response at the holding potential ($Max_{+45}=1.02$, $Max_{-90}=1.17$; $p=0.0066$, F-test for fit comparison).

This concentration-response curve for Iso confirmed the findings described previously: Mostly a reduction in efficacy underlies the voltage-dependent regulation of Iso-induced β_1-AR activity whereas a reduction in affinity is only a minor contributor.

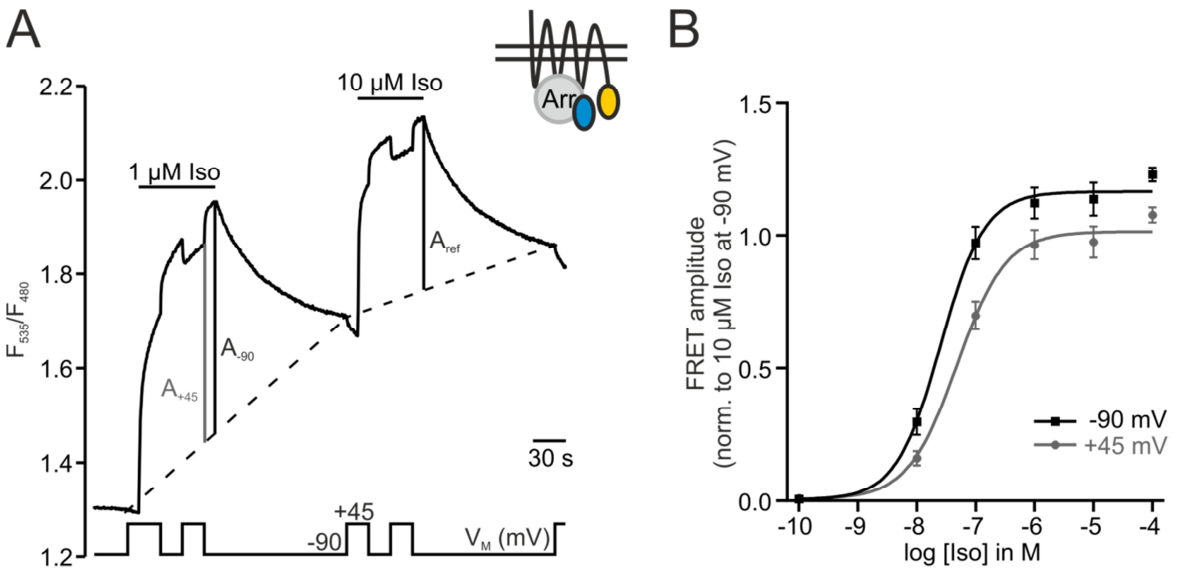

Figure 16: Comparison of concentration-response curves for Iso at two potentials identifies efficacy as the major contributor of voltage-dependence.
A: A representative arrestin FRET assay measurement shows how data for the concentration-response curves were collected. Cells were stimulated with a test concentration of Iso (here 1 µM). After washout of the test concentration, a second stimulation with the reference concentration of 10 µM followed. The membrane potential was switched from -90 mV to +45 mV during both stimulations. A two-step interpolation between data points at rest before and after stimulation was used to adjust the baseline for data analysis (dashed lines). Amplitudes A_{+45} and A_{-90} of each test concentration were set in relation to A_{ref} of the same measurement. *B*: The normalized FRET amplitudes at both potentials were plotted against the Iso concentrations and fit to a concentration-response function (n=3-9 per data point, -90 mV: $EC_{50}=2.5*10^{-8}$ M; +45 mV: $EC_{50}=4.8*10^{-8}$M; $Max_{-90}=1.17$, $Max_{+45}=1.02$,; p=0.0066) Paired student's t-tests or F-test were used to determine statistical differences in FRET amplitudes at rest and depolarization at the tested Iso concentrations or in EC_{50}s and the maximal values of the fit curves, respectively.

6.1.7 β_1-adrenoceptor voltage-dependence is agonist specific

The data collected so far suggested agonist specific differences between Iso and Adr regarding β_1-AR voltage-sensitivity: A reduction in agonist affinity by depolarization seemed more pronounced in Adr- than in Iso-stimulated cells at the receptor level whereas the change in efficacy was comparable for both agonists (Figure 9A, B). A differential voltage-sensitivity depending on the agonist used for stimulation has also been reported for example for the M_2AChR (Navarro-Polanco et al., 2011) and D_{2S}R (Sahlholm et al., 2008b). While pilocarpine-activated M_2AChRs were further activated during depolarization, the activity of receptors activated by acetylcholine was reduced at a positive membrane potential. GIRK currents induced by dopamine-stimulation of D_{2S}Rs decreased during depolarization. However, when the receptors were stimulated with agonists like β-phenethylamine, p- or m-tyramine, depolarization did not alter agonist-evoked GIRK currents.

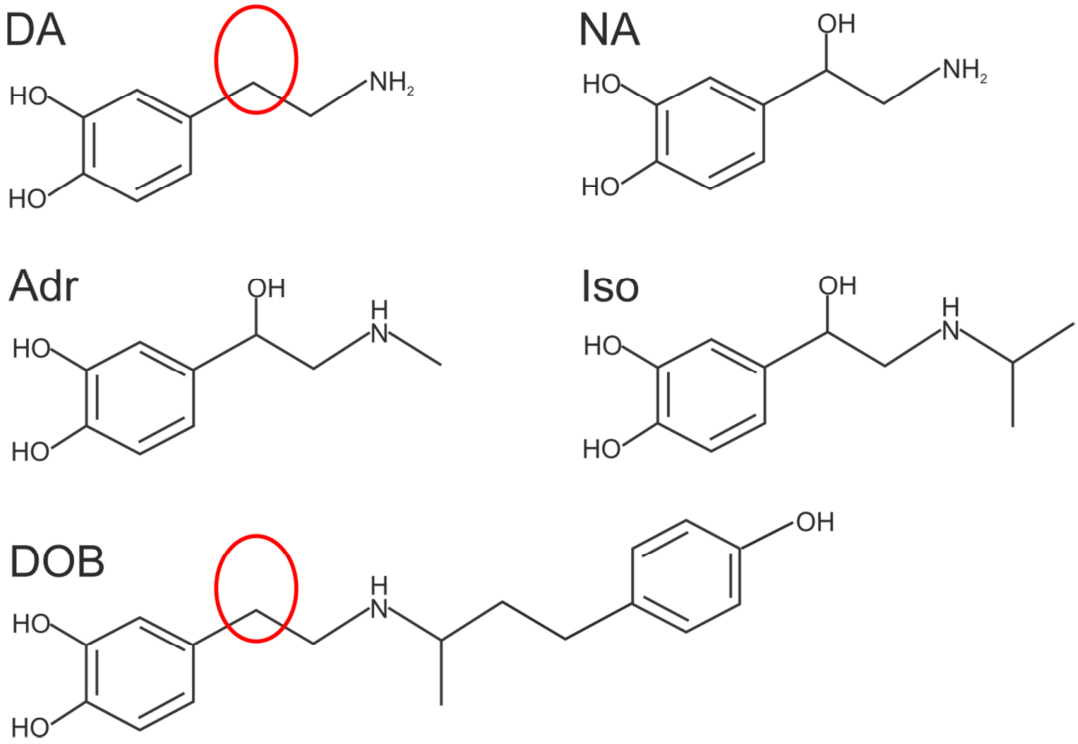

Figure 17: Chemical structure of the natural and synthetic full and partial agonists of β_1-AR used in this study.
The red circles in the dopamine and dobutamine structures mark the lack of a β-hydroxyl-group. DA: dopamine, NA: noradrenaline, Adr: adrenaline, Iso: isoprenaline, DOB: dobutamine.

In order to investigate agonist-specificity of voltage-dependence more closely for the β_1-AR, we used two different partial agonists to stimulate cells transfected with the arrestin FRET assay constructs. The first partial agonist was dobutamine (DOB), a structural analogue of isoprenaline which was developed to selectively increase cardiac contractility (Tuttle and Mills, 1975). The second was dopamine (DA), the simplest catecholamine and a precursor in the synthesis of NA and Adr. Both partial agonists lack the β-OH-group present in the endogenous agonists Adr and NA and the synthetic catecholamine Iso (red circle, Figure 17).

Cells were stimulated with dobutamine and adrenaline in order to estimate the maximal effect that can be induced by this partial agonist. Stimulation with 10 µM and 100 µM dobutamine induced β_1-AR-Arr3-interaction to almost the same degree which was, as expected, smaller than the full activation by 100 µM Adr (Figure 18A). The maximal dobutamine effect was 38±1% of the maximal Adr-evoked FRET response. Depolarization of dobutamine-stimulated cells reversibly diminished β_1-AR-Arr3-interaction as seen in cells stimulated with Adr, NA or Iso (Figure 18B).

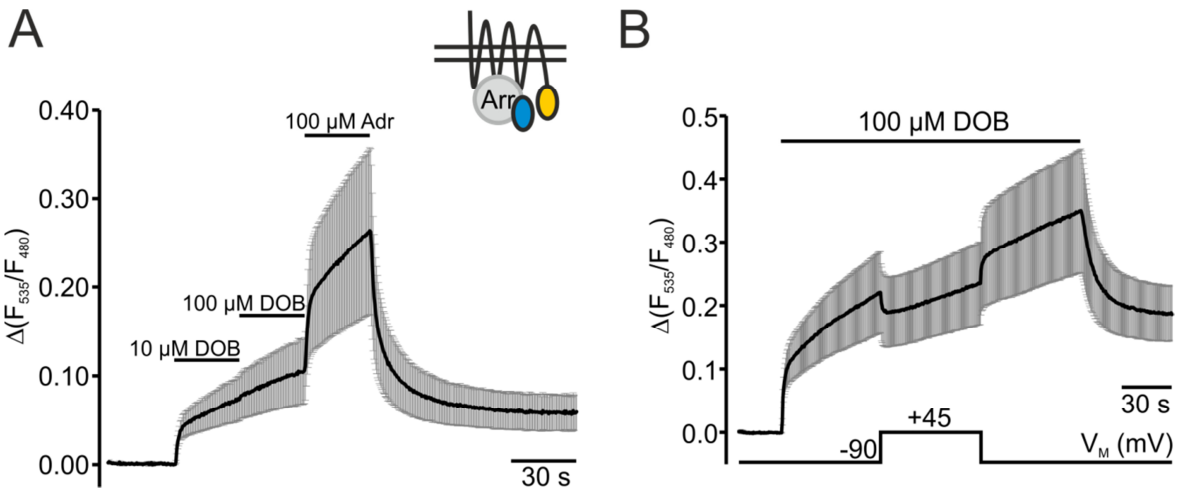

Figure 18: Voltage-dependence of the partial agonist dobutamine.
The arrestin FRET assay was used to investigate voltage-dependence of dobutamine-activated β_1-AR. Individual experiments were normalized to the initial FRET value prior to the first stimulation before averaging. *A*: The maximal FRET response by dobutamine (10 µM and 100 µM) relative to full stimulation with Adr (100 µM) was determined in unpatched cells (average±SEM, n=4, one transfection only). *B*: Voltage-dependence of dobutamine-induced β_1-AR-Arr3-interaction was measured in cells stimulated with 100 µM dobutamine (average±SEM, n=8).

In unpatched cells, FRET measurements were performed to estimate an EC_{50}-value for the β_1-AR-arrestin 3 interaction induced by dopamine in the context of a *Wahlpflichtpraktikum*. Cells were stimulated with increasing concentrations of dopamine ranging from 1 µM to 1 mM without washout between the applications. Individual measurements were normalized to their initial value prior to stimulation with the first concentration of dopamine and then averaged (Figure 19A). It can nicely be appreciated from this overlay that the FRET signal increased stepwise in a concentration-dependent manner. The very fast disruption of interaction upon dopamine withdrawal indicated its low affinity to the β_1-AR. Agonist-evoked FRET responses were normalized to the maximal FRET response induced by 1 mM dopamine in each measurement and plotted against the dopamine concentration (Figure 19B). A sigmoidal curve fit to the data yielded an EC_{50} of $4.2*10^{-4}$ M dopamine. This result was similar to earlier reports of the affinity of dopamine towards β_1-ARs obtained from whole-cell binding experiments on CHO cells stably expressing β_1-AR in which a K_D value of -3.57±0.02 ($EC_{50}=2.7*10^{-4}$ M) was determined (Baker, 2010). To estimate the maximal FRET response which can be induced by the partial agonist dopamine compared to the full agonist Adr, cells were stimulated with increasing concentrations of dopamine. Following application of the highest dopamine concentration, 100 µM Adr were applied (Figure 19C). The dopamine-induced FRET response with 300 µM DA reached a maximum at about 37% of the maximal FRET response induced by 100 µM Adr.

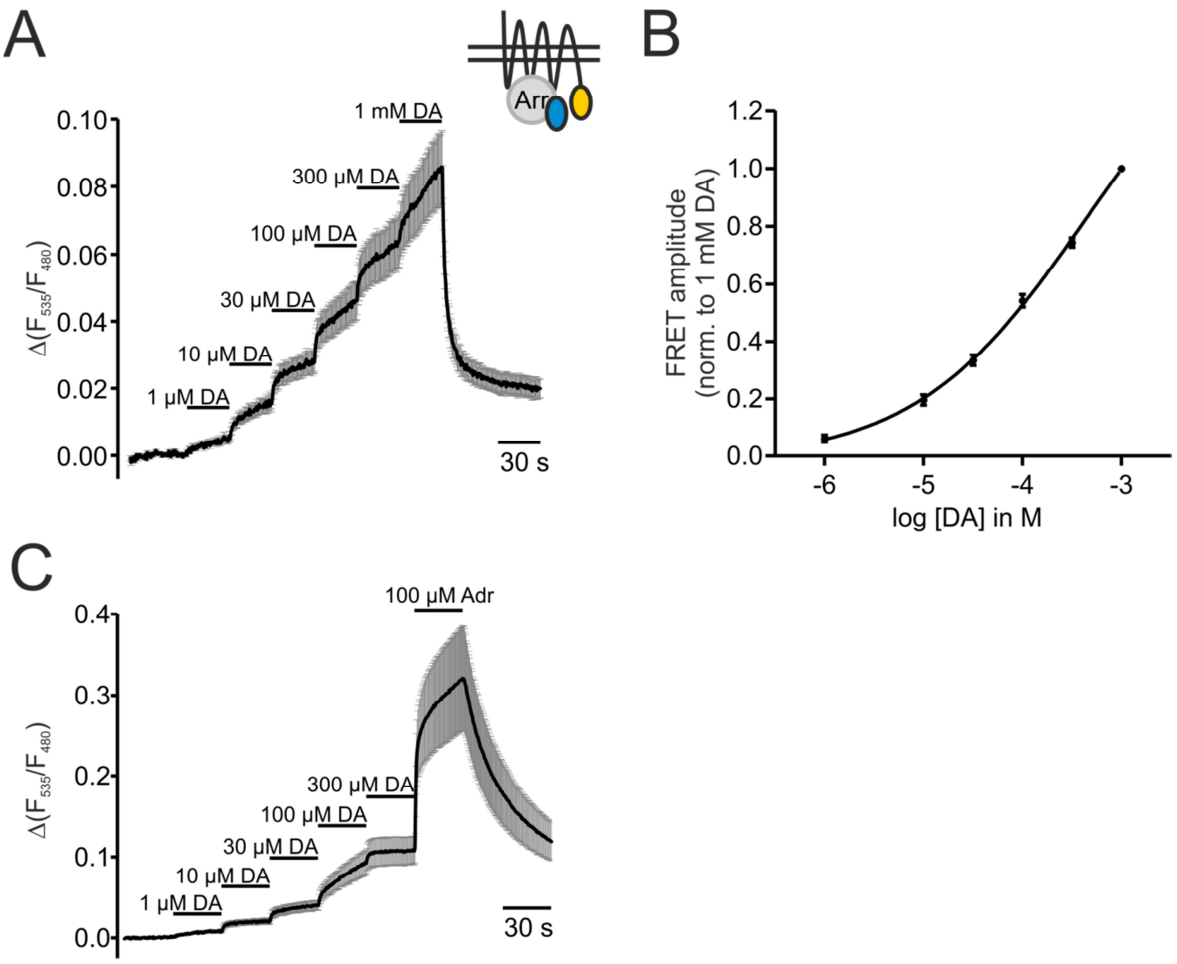

Figure 19: Concentration-dependent activation of β_1-AR by dopamine.
Cells were transfected with constructs of the arrestin FRET assay to investigate dopamine-mediated activation of β_1-AR. All individual measurements were normalized to the FRET value prior to stimulation before averaging. *A*: Data for a concentration-response curve were collected in FRET measurements with dopamine concentrations ranging from 1 µM to 1 mM (average±SEM, n=11). *B*: FRET amplitudes were normalized to the maximal FRET amplitude at 1 mM DA in each measurement, plotted against the DA concentration and fit to a concentration-response function (EC_{50}=4.2*10^{-4} M). *C*: Cells were stimulated with increasing concentrations of DA followed by stimulation with 100 µM Adr to estimate the maximal inducible FRET response by the partial agonist DA (average±SEM, n=5, one transfection only).

With a concentration of 100 µM dopamine the voltage-dependence of dopamine-induce β_1-AR-arrestin 3 interaction was determined. During stimulation with 100 µM dopamine the membrane potential was switched to +45 mV and back to the holding potential before ligand washout (Figure 20A). Interestingly, depolarization further enhanced β_1-AR-Arr3 interaction indicated by an increase in ratio during depolarization which was reversible upon repolarization. A predicted difference in binding of dopamine (Figure 20B) to β_2-AR compared to Iso (Figure 20C) (Katritch et al., 2009) could underlie this difference in direction of voltage-sensitivity. The Iso β-OH group is engaged in a hydrogen bond with the conserved $D^{3.32}$ (D113 in β_2-AR) in TM3 which is important for ligand binding (Figure 20C, indicated by cyan dotted lines). As dopamine lacks this β-hydroxyl group and does not interact with the $D^{3.32}$ at this position, it is slightly rotated within the binding pocket

compared to Iso (Figure 20B). This results in a binding mode that does not involve a hydrogen bond between the catechol meta-OH-group and $N^{6.55}$ (N293 in β_2-AR) in TM6 which is present when Iso is docked into β_2-AR (compare Figure 20B and C, (Katritch et al., 2009)). Similarly, in muscarinic receptors the binding mode of a ligand within the binding pocket also influenced direction of voltage-dependence (Rinne et al., 2015). M_3AChR activity induced by ligands like carbachol (CCh) or ACh interacting with a TM6 asparagine ($N^{6.52}$) was reduced during depolarization. When the receptor was stimulated with pilocarpine which favors an orientation towards $D^{3.32}$, depolarization further enhanced receptor activity (Rinne et al., 2015).

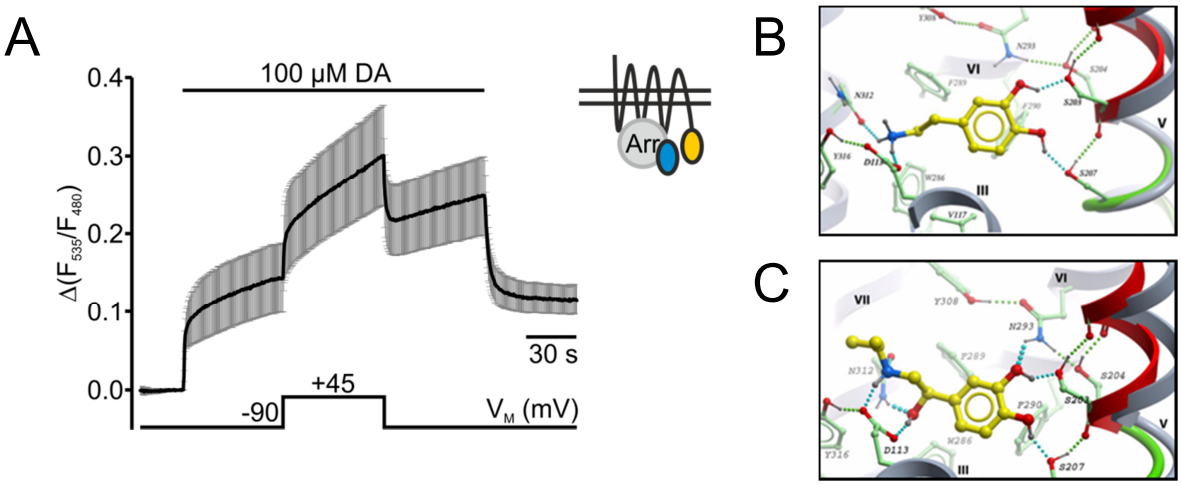

Figure 20: Depolarization increases the interaction between β_1-AR and arrestin 3 in the presence of dopamine.
A: Cells were transfected with constructs of the arrestin FRET assay to investigate voltage-dependence of dopamine-activated β_1-AR. Individual measurements were normalized to the FRET value prior to stimulation before averaging. Voltage-dependence of DA-induced receptor-arrestin interaction was assessed in cells stimulated with 100 µM DA and depolarized to +45 mV (average±SEM, n=9). *B and C*: Representations of the predicted binding modes of dopamine (*B*) and Iso (*C*) to a flexible side chain β_2-AR model were extracted and slightly modified from (Katritch et al., 2009). Agonists are depicted as yellow sticks and carbon atoms. Cyan dotted lines indicate hydrogen bonds between the ligands and the receptor. Oxygen and nitrogen atoms of the ligands are colored red and blue, respectively.

Similar to Iso, dobutamine binding to the structure of β_1-AR also involves a hydrogen bond between the catechol meta-hydroxyl group and the TM6 aspartic acid $N^{6.55}$ (Warne et al., 2011) which could explain the same direction of voltage-dependence despite a lack of the β-OH group.

Taken together these data show that the activity of β_1-AR induced by the partial agonists dopamine and dobutamine was voltage-dependent. This voltage-dependence, however, was of opposite direction. The interaction of β_1-AR and Arr3 was weakened in the presence of dobutamine whereas it was strengthened in the presence of dopamine during depolarization. Different binding modes of these agonists within the binding pocket favoring an orientation towards $N^{6.55}$ or $D^{3.32}$ might account for agonist-specificity of

voltage-dependence and would be in agreement with the data published for muscarinic receptors.

6.2 Voltage-dependence of β_2-adrenoceptors

An over 70% sequence homology in the transmembrane regions exists between the human β_1-AR and the human β_2-AR (Frielle et al., 1989). It was therefore interesting to investigate whether the activity of human β_2-ARs can also be modulated by the membrane potential.

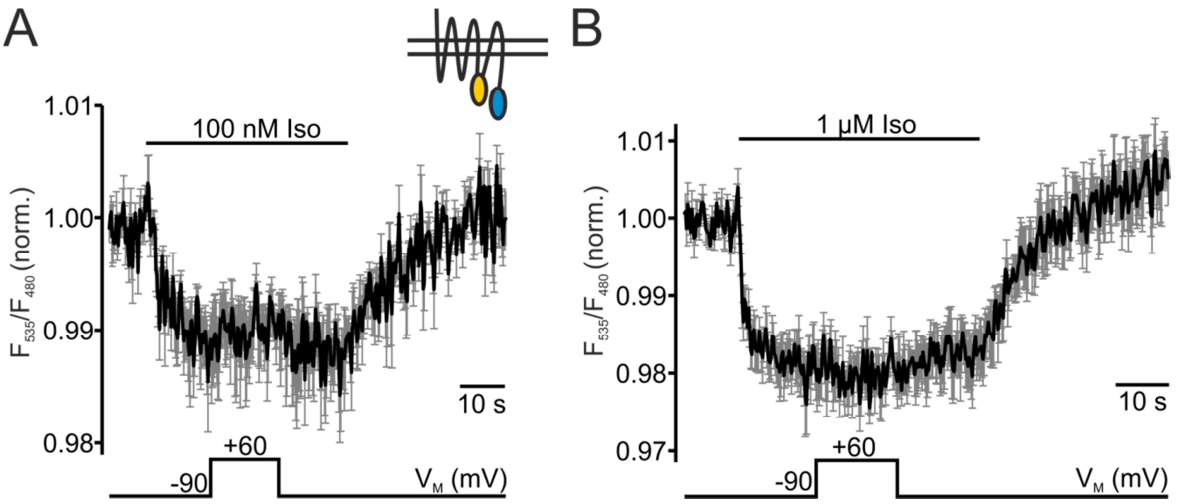

Figure 21: Voltage-dependence of β_2-AR activity is less pronounced than in β_1-AR.
A and *B*: A HEK 293 cell line stably expressing an intramolecular FRET-based β_2-AR fusion protein (β_2-AR-sensor) (Ahles et al., 2011) was stimulated with 100 nM Iso (*A*) or 1 µM Iso (*B*) to investigate its voltage-dependence. Single experiments were corrected for bleaching, normalized to the initial FRET value prior to agonist application and smoothed. A depolarizing step to +60 mV was performed during stimulation with Iso (average±SEM, *A*: n=4, *B*: n=4).

With a human β_2-AR FRET-based intramolecular fusion protein (β_2-AR sensor) similar to the β_1-AR sensor, I aimed to explore β_2-AR voltage-sensitivity. This construct and HEK 293 cells stably expressing it were kindly provided by Prof. Dr. Stefan Engelhardt (cloning of the construct is described in (Ahles et al., 2011)). An eYFP is inserted into the β_2-AR third intracellular loop and CFP is fused to its C-terminus which enables monitoring of receptor conformational changes as a ratio decrease. Stimulation of the stably transfected HEK 293 cells with 100 nM Iso decreased the initial ratio indicating receptor activation. This decrease was reversible after agonist washout (Figure 21A). Due to photobleaching and a poor signal-to-noise ratio, the individual experiments were corrected for bleaching and smoothed before averaging. Depolarization to +60 mV only slightly reduced the Iso-evoked FRET response by an extent hardly above the noise of the average trace (Figure 21A). When cells were stimulated with 1 µM Iso, depolarization was not able to induce any deactivating conformational changes (Figure 21B).

These initial experiments suggested that the voltage-dependence of β_2-AR is difficult to detect with this intramolecular FRET sensor and voltage-dependence seemed to be less pronounced than in β_1-AR. Due to the better signal-to-noise ratio, experiments measuring arrestin 3 interaction with β_2-AR by means of FRET seemed more suitable to investigate β_2-AR voltage-dependence.

6.2.1 Minor reduction of agonist-induced β_2-AR-Arr 3-interaction by depolarization

To elaborate on the voltage-sensitivity of β_2-AR by means of a FRET assay with consistently large FRET responses and a good signal-to-noise ratio, cells were transfected with the plasmids encoding for a human YFP-labeled β_2-AR (β_2-AR-YFP), CFP-Arr3 and unlabeled GRK2 (Krasel et al., 2005).

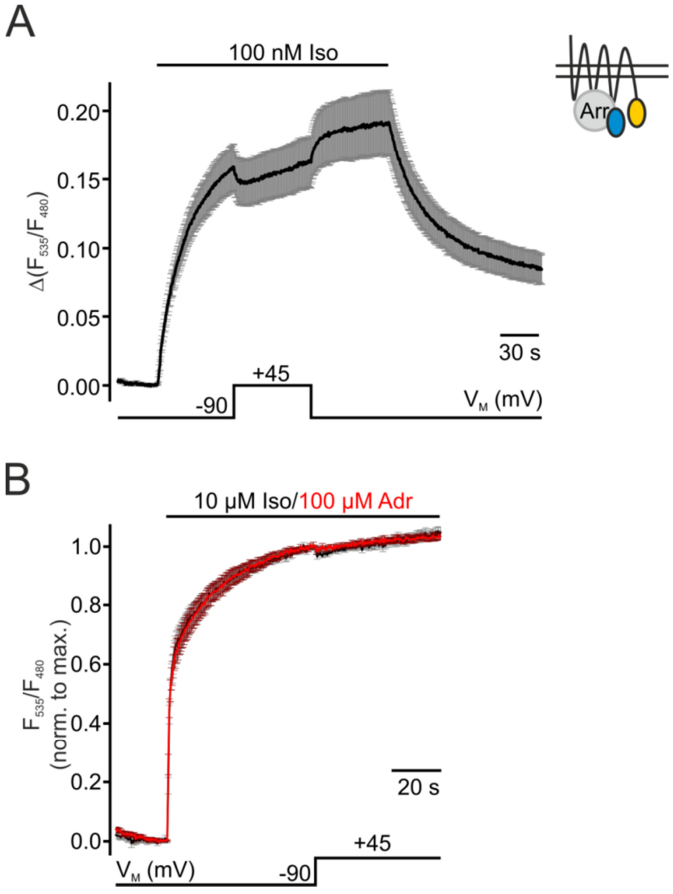

Figure 22: β_2-AR-arrestin 3-interaction is slightly decreased during depolarization.
A and *B*: Cells transfected with β_2-AR-YFP, CFP-Arr and non-fluorescent GRK2 were stimulated with non-saturating (*A*) or saturating (*B*) concentrations of agonist. *A*: Single experiments were normalized to the value prior to stimulation with 100 nM Iso (average±SEM, n=9). *B*: For better comparison of the depolarization effect on receptor-arrestin-interactions induced by 100 µM Adr (red) or 10 µM Iso (black), individual measurements were normalized to the maximal agonist-evoked FRET amplitude before the depolarizing step (average±SEM, Adr: n=8; Iso: n=7).

Stimulation with 100 nM Iso activated the β_2-AR which led to its phosphorylation by GRK2 followed by the recruitment of and interaction with Arr3 which could be monitored by an increase in FRET. A depolarizing pulse to +45 mV only slightly reduced the Iso-

induced FRET amplitude (Figure 22A). The average reduction of interaction by depolarization was 9.9±1.1%. In cells stimulated with saturating concentrations of Iso (10 µM) or Adr (100 µM), depolarization-induced disruption of receptor-arrestin-interaction was hardly visible or absent, respectively (Figure 22B). To compare the effects in Iso- and Adr-stimulated cells, the individual experiments were normalized to the maximal agonist-induced FRET response before the depolarizing pulse.

These data indicate that voltage-dependence of β_2-AR activity is less pronounced than β_1-AR voltage-dependence. The absence of a depolarization-dependent inhibition of β_2-AR-Arr3-interaction in agonist saturation suggests that the β_2-AR voltage-dependence is likely achieved through a reduction in agonist affinity.

6.3 Voltage-dependence of α_{2A}-adrenoceptor

Voltage-dependence of α_{2A}-AR activity at the receptor level as well as its transmission to G protein activation, arrestin 3 interaction and GIRK channel activation has been described thoroughly (Rinne et al., 2013). In the same study, concentration-response curves for noradrenaline were measured with an intramolecular FRET-based α_{2A}-AR fusion protein (α_{2A}-cam) at a holding potential of -90 mV and at depolarization (+60 mV). An about six-fold increase in the EC_{50}-value at depolarization suggested a reduction in affinity underlying voltage-dependence of NA-stimulated α_{2A}-AR.

6.3.1 Determination of voltage-dependent radio-ligand binding to α_{2A}-adrenoceptors expressed in *Xenopus laevis* oocytes

In order to show reduced agonist binding to the receptor at depolarization, I measured direct binding of tritium-labeled noradrenaline ([^{3}H]-NA) to α_{2A}-AR at two different potentials in *X. laevis* oocytes in the laboratory of Dr. Hanna and the late Dr. Itzchak Parnas. Oocytes were injected with cRNA encoding for α_{2A}-AR together with cRNA for the GIRK-channel subunits 1 and 2 one day after oocyte preparation. Control oocytes, which were used to measure unspecific binding of the radio-ligand, were not injected with cRNA. Four to five days after injection, noradrenaline-dependent GIRK currents were measured using standard two-electrode voltage-clamp to ensure sufficient expression of α_{2A}-AR. If the basal GIRK current was enhanced by NA-stimulation, the remaining injected oocytes were used for radio-ligand binding measurements. One oocyte at a time was first incubated in [^{3}H]-NA solution for 30 s or 60 s, then washed for two seconds in a specialized washing chamber to remove the unbound hot ligand and then transferred into vials containing scintillation liquid (5.3.1.4 or (Ben-Chaim et al., 2003)). Oocytes were

either incubated with hot ligand in solutions containing high potassium concentrations (high K^+, HK, about 5 mV) to mimic depolarization or solutions resembling the extracellular solution (ND96, about -88 mV) for the resting state of the membrane potential. Oocytes for specific and unspecific binding were measured alternately.

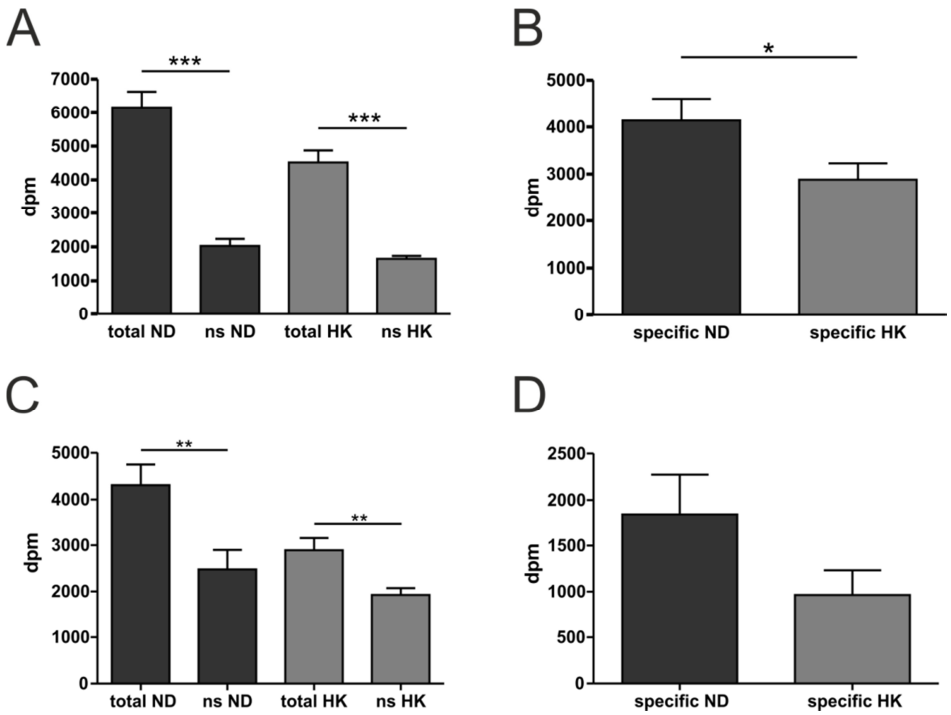

Figure 23: Binding of [^{3}H]-NA to Xenopus laevis oocytes expressing α_{2A}-AR.
X. laevis oocytes were injected with cRNA for α_{2A}-ARs and the subunits 1 and 2 of GIRK channels 4-5 days before the experiment. Control oocytes to detect non-specific binding (ns) were injected with GIRK subunits only. Two different membrane potentials were achieved using buffers with different potassium concentrations (see methods). *A*: Oocytes were incubated with 300 nM [^{3}H]-NA in either ND or HK buffer for 60 s before washing and measuring in a scintillation counter (ND: n=6 (total); n=7 (ns); HK: n=8(total), n=6 (ns)). *B*: Specific binding was determined as the difference between total (total ND, total HK) and unspecific binding (ns ND, ns HK) at both potentials. *C*: Oocytes were incubated with 700 nM [^{3}H]-NA in either ND or HK buffer for 30 s before washing and measuring in a scintillation counter (ND: n=8 (total); n=8 (ns); HK: n=6(total), n=6 (ns)). *D*: Quantification of the specific binding calculated as in *B*. Statistical significance within the ND and HK groups and between columns of specific binding was tested with unpaired student's t-tests. ***: $p<0.001$, **: $p<0.01$, *: $p<0.05$, ns=non-specific binding.

Unfortunately, only in two experiments a significant difference between total and unspecific binding at rest and at depolarization could be detected (Figure 23). The first experiment was performed with a 300 nM [^{3}H]-NA solution and an incubation time of 60 s. The total binding at rest was of 6161±470 dpm and of 4520±350 dpm in the high potassium solution, i.e. at depolarization (Figure 23A). Both conditions showed low unspecific binding to uninjected control oocytes. Specific binding, i.e. the difference between total and unspecific binding, was calculated to be 4137±470 dpm for cells in ND96 solution, i.e. at rest, and 2876±350 dpm at depolarization. These count numbers at rest and depolarization were significantly different (Figure 23B). A second set of data with

significant differences between total and unspecific binding in the conditions at rest and at depolarization was measured with a NA concentration of 700 nM and an incubation time of 30 s (Figure 23C). Calculation of specific binding showed a tendency of lower specific binding at depolarization, however, the difference between 1834±440 dpm (ND96) and 963±270 dpm was not statistically significant (p=0.146) (Figure 23D).

To depolarize the cells in the binding assay without the need of electrophysiological equipment, the potassium concentration was increased on the expense of the sodium concentration in order to maintain the same osmolarity in both the ND and the HK solutions. Measurements by Prof. Andreas Rinne, however, showed that the concentration of sodium is critical for the agonist affinity at the α_{2A}-AR. The EC_{50} increased from 0.8 µM NA in the presence to 19 µM NA in the absence of sodium (unpublished data by Prof. Rinne). These findings concur with measurements on the sodium-dependence of agonist binding to cell homogenates of mouse mammary tumor cells stably expressing the human α_{2A}-AR (Pihlavisto et al., 1998).

Whether the decrease in radio-ligand binding measured in the oocytes resulted from depolarization of the plasma membrane or the reduction in sodium concentration from 96 mM (ND solution) to 2 mM (HK solution) is therefore difficult to answer.

6.3.1.1 Measurement of α_{2A}-adrenoceptor densities in cell membranes of transiently transfected HEK 293 cells

For a different project I measured α_{2A}-AR densities in cell membranes of HEK 293 cells transiently transfected with cDNAs for α_{2A}-AR along with the cDNA for adenylyl cyclase type 5 and for the epac1-camps FRET-sensor (Nikolaev et al., 2004; Reddy et al., 2015). Binding of [^{3}H]-clonidine (700 nM) to membranes prepared from three different transfections were measured in triplicates against binding to membranes of transfected cells in the presence of yohimbine and to untransfected control cells. A slower off-rate of clonidine from α_{2A}-AR due to its higher affinity towards the receptor compared to NA (Jasper et al., 1998) facilitated the measurements. Untransfected controls did not show any specific radio-ligand binding. The average density of the α_{2A}-AR in three preparations was 10.98±0.9 pmol/mg membrane protein.

6.3.2 Depolarization reduced α_{2A}-adrenoceptor-arrestin 3-interaction evoked by adrenaline but not by noradrenaline in saturation

The former studies on the voltage-dependence of α_{2A}-AR activity have been conducted with the ligands noradrenaline or clonidine (Figure 23, radio-ligand binding on HEK cells

and (Rinne et al., 2013)). As there were agonist-specific differences at the β_1-AR and between NA- and clonidine-stimulated α_{2A}-AR (Rinne et al., 2013), I also tested for voltage-dependent regulation of adrenaline-evoked α_{2A}-AR activity. Cells were either stimulated with a saturating concentration of NA (100 µM) or Adr (100 µM). While depolarization did not disrupt receptor-arrestin interaction induced by NA, it was able to reduce the interaction in Adr-stimulated cells (Figure 24A). For better visualization of the depolarizing-effect on NA- and Adr-stimulated cells, the experiments were normalized to the maximal agonist-evoked FRET response before the depolarizing step. To make sure that stimulation with 100 µM Adr fully saturated the receptor, unpatched cells were stimulated with 100 µM and 300 µM Adr in FRET measurements (Figure 24B). No additional recruitment of and interaction with arrestin 3 was induced in the presence of the higher Adr concentration.

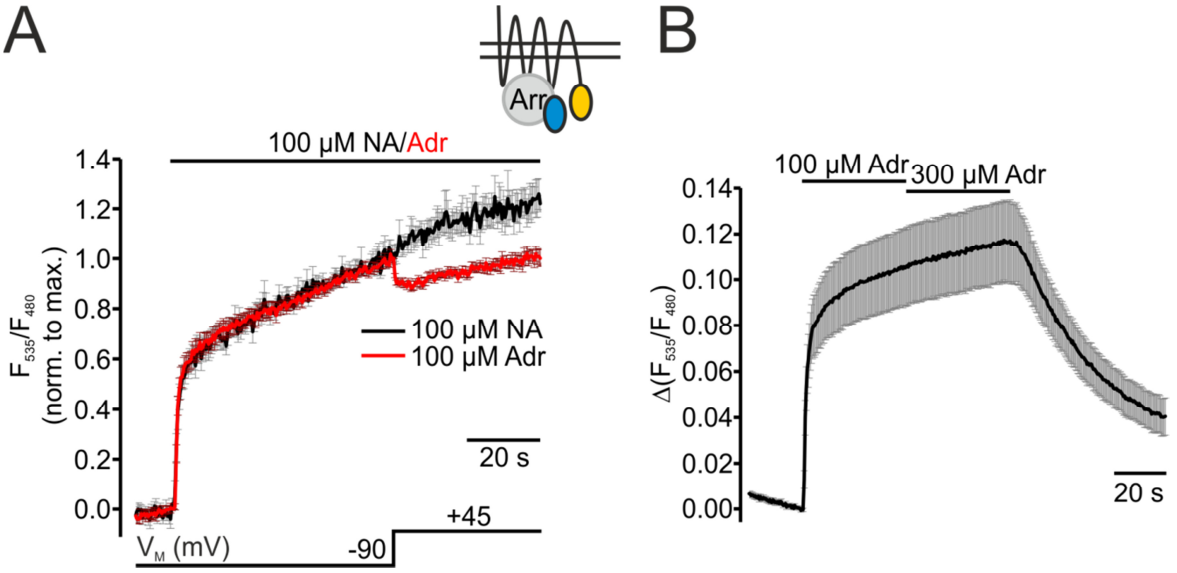

Figure 24: Voltage-dependence of α_{2A}-AR-arrestin 3-interaction shows agonist-specificity.
The interaction of α_{2A}-AR and arrestin 3 was monitored using the following FRET constructs: α_{2A}-AR-YFP, CFP-Arr, GRK2. *A*: Measurements of receptor-arrestin interaction stimulated with 100 µM NA (black, n=6) or 100 µM Adr (red, n=10) were normalized to the maximal agonist-evoked FRET response before depolarization to +45 mV before averaging (average±SEM). *B*: To ensure that 100 µM Adr in *A* fully saturated the FRET assay, unpatched cells expressing the same constructs were stimulated with 100 µM Adr followed by the stimulation with 300 µM Adr (average±SEM, n=12).

Depolarization-mediated differences between NA- and Adr-activated cells also argue in favor of agonist-specificity of α_{2A}-AR voltage-dependence. Voltage-dependence of NA-induced receptor activity seemed to be purely dependent on a reduction in agonist affinity consistent with the earlier report (Rinne et al., 2013). However, an alteration in agonist efficacy could play a role in the voltage-dependence of Adr-activated α_{2A}-AR. But the contribution of reduction in Adr affinity *versus* efficacy during depolarization remains to be determined.

6.4 How do G protein-coupled receptors "sense" changes in the membrane potential?

During the last decade, more and more GPCRs of different classes have been shown to be voltage-dependent (for example (Ben-Chaim et al., 2003; Martinez-Pinna et al., 2005, 2010; Ohana et al., 2006; Sahlholm et al., 2008c; Rinne et al., 2013)). However, the mechanism how the membrane potential alters receptor conformation and thereby its activation remains unidentified. Two approaches have been used in this study in the attempt to elucidate the underlying mechanism: First, via changes in extracellular surface charge and second, via site directed mutagenesis.

6.4.1 Increase in extracellular surface charge did not alter voltage-dependent behavior of α_{2A}-adrenoceptor activity

One possibility of how the membrane potential could influence receptor conformation would be via an alteration of the ion composition on the outer or inner surface of the plasma membrane. In order to alter the extracellular surface charge and composition, normal FRET buffer was replaced by a FRET buffer containing 20 mM $MgCl_2$ (high Mg^{2+} buffer) instead of the usual 1 mM. To be able to compare measurements with high and normal Mg^{2+}-concentration, FRET buffer was supplemented with 60 mM glucose (glucose buffer) to adjust the osmolarity and served as the control buffer.

Stably expressed α_{2A}-AR-cam was stimulated with 10 µM NA dissolved either in the glucose or the high Mg^{2+} buffer (Figure 25). In the absence of noradrenaline neither the high Mg^{2+} nor the glucose buffer induced any changes in the ratio. The degree of agonist-induced reduction in the ratio and its recovery after NA withdrawal was similar in cells measured in either buffer condition (Figure 25A). Depolarization-induced reduction of the NA-evoked FRET response in the presence of high or normal extracellular Mg^{2+} concentrations was virtually identical (Figure 25B). Also hyperpolarization from -90 mV to -120 mV did not change the agonist-evoked FRET response regardless of the extracellular Mg^{2+} concentration (Figure 25C).

Changes in the extracellular surface charge by addition of a high concentration of $MgCl_2$ did not alter voltage-dependence of NA-activated α_{2A}-ARs.

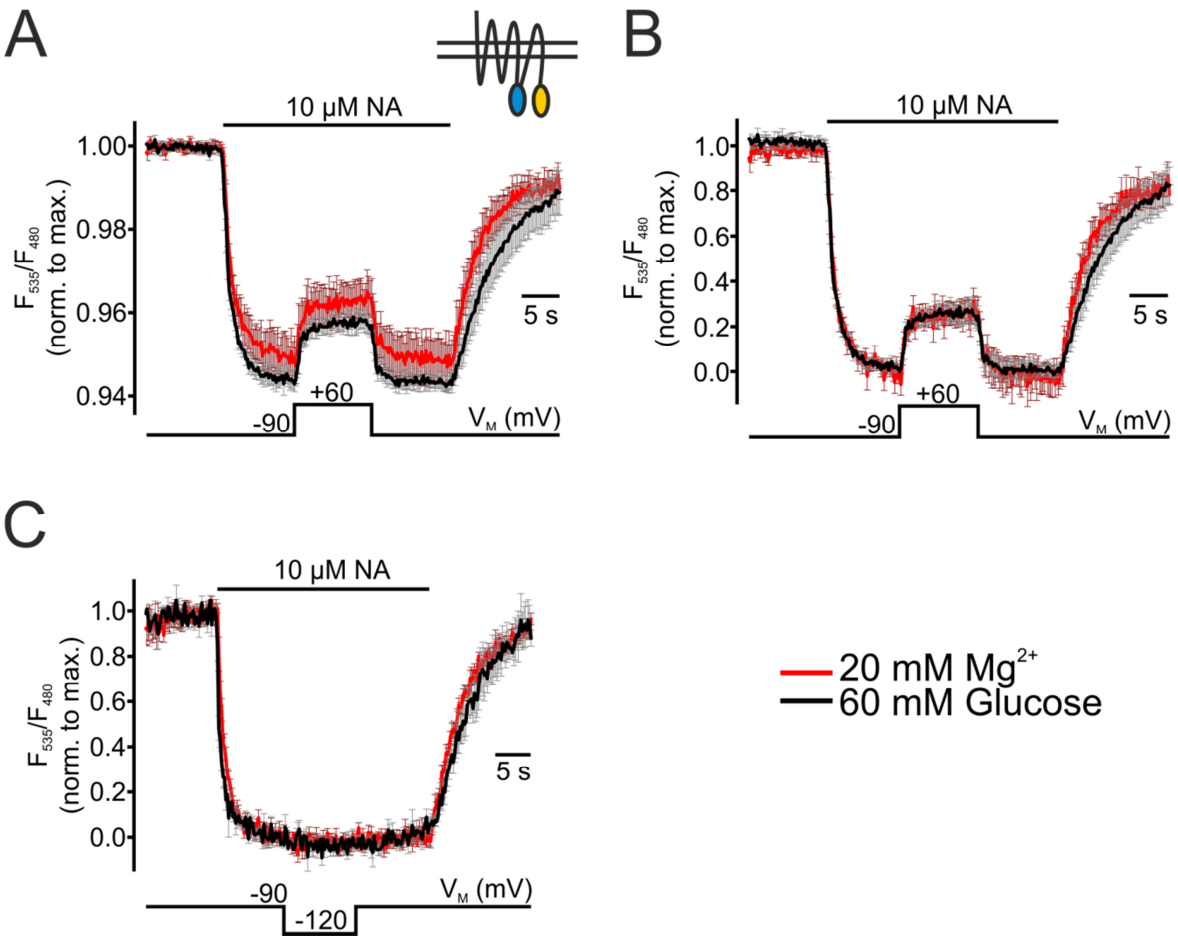

Figure 25: Manipulation of the outer surface charge does not alter voltage-sensitivity of α_{2A}-AR-cam. The outer environment of HEK 293 cells stably expressing an intramolecular FRET-based α_{2A}-AR-fusion protein (α_{2A}-cam, (Vilardaga et al., 2003)) was altered with an external buffer containing a high Mg^{2+} concentration (20 mM). As a control normal FRET buffer was augmented with 60 mM glucose to equalize osmolarity of the two buffers. *A*: The same protocol was used for measurements with high external magnesium (red, n=6) and normal FRET buffer with glucose (black, n=5). Individual traces were corrected for bleaching and normalized to the initial FRET value prior to stimulation with 10 µM NA. In measurements either magnesium concentration, noradrenaline was solved in the same buffer (averages±SEM). *B*: Normalization of the data in *A* to the maximal agonist-evoked response facilitates the comparison of the degree of depolarization-induced receptor deactivation. *C*: Cells were stimulated with 10 µM NA in either high or normal magnesium concentration containing buffer and hyperpolarized from the holding potential of -90 mV to -120 mV. Individual experiments were normalized to the maximal NA-induced FRET response prior to the hyperpolarizing step (average±SEM; red: high magnesium, n=5; black: normal magnesium, n=4).

6.4.2 Site-directed mutagenesis was used to identify amino acids involved in voltage-sensing

Voltage-gated ion channels sense changes in the membrane potential with a voltage-sensor containing several basic amino acids, the S4-segment (Bezanilla, 2000). However, a voltage-sensor similar to the S4-domains in voltage-sensitive ion channels is not present in GPCRs. Several mutational studies have been performed but the GPCR voltage sensor has not yet been identified (see for example (Ben-Chaim et al., 2006; Navarro-Polanco et al., 2011; Sahlholm et al., 2012)). In this study, the α_{2A}-AR has been mutated by the QuickChange site-directed mutagenesis method in order to find the GPCR voltage-sensor.

6.4.2.1 Mutation of an amino acid involved in ligand binding

A point mutation has been inserted into the wild-type α_{2A}-AR-cam at an important position for ligand binding. The replacement of serine $204^{5.46}$ by alanine (S204A), a residue involved in ligand binding through its interactions with the para-hydroxyl group of the phenyl ring of catecholamines (Figure 20B and C, (Wang et al., 1991), was supposed to abolish receptor activation by noradrenaline. Receptor activation upon binding of the agonist UK1403 should remain intact. However, stimulation with a high concentration of noradrenaline (100 µM) still induced an agonist-dependent conformational change in the α_{2A}-AR-cam in a pilot experiment (Figure 26). Due to the high concentration of agonist, a reduction of the NA-induced FRET amplitude by depolarization was not likely. As this mutant preserved its ability to bind NA, it was not investigated further.

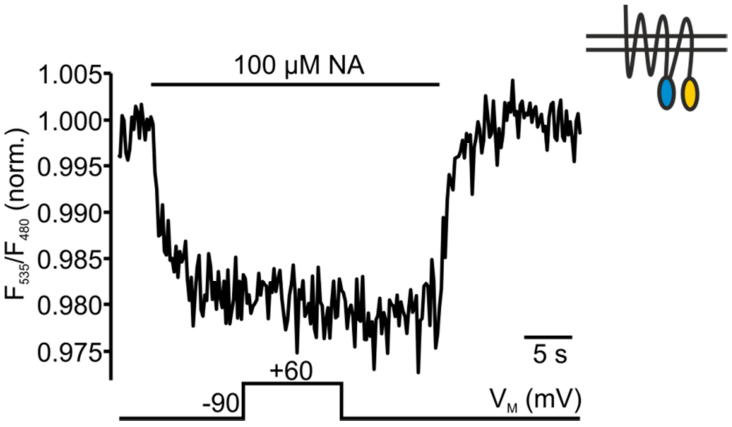

Figure 26: Mutagenesis of an amino acid involved in ligand binding.
The α_{2A}-AR-S204A-cam was constructed using site-directed mutagenesis. Stimulation with 100 µM NA of three cells transiently transfected with the construct activated the receptor mutant reversibly represented in this individual experiment (one of three measurement performed). The acceptor-over-donor ratio was corrected for bleaching and normalized to the initial values before agonist stimulation. A depolarizing step to +60 mV was performed during NA-stimulation.

6.4.2.2 Neutralizing mutations of charged amino acids

Ben-Chaim and colleagues were first able to measure 'gating currents' in M_1AChR- and M_2AChR-expressing Xenopus oocytes (Ben-Chaim et al., 2006). It is therefore plausible that charged amino acids could function as voltage-sensors and move through the electrical field of the membrane during depolarization generating gating currents. About 10% of the amino acids residing in the TM domains of the α_{2A}-AR are charged at physiological pH (Vroling et al., 2011) and only few of these charged amino acids within the TM domains are highly conserved among class A GPCRs (Suwa et al., 2011).

One aspartic acid conserved among biogenic amine receptors is $D^{3.32}$ (Gether, 2000) which is also important for ligand binding. Its mutation to alanine (D113A) in the α_{2A}-AR-cam resulted in the loss of NA-induced receptor activation and could therefore not be

investigated in terms of voltage-dependence (unpublished data acquired during my diploma thesis).

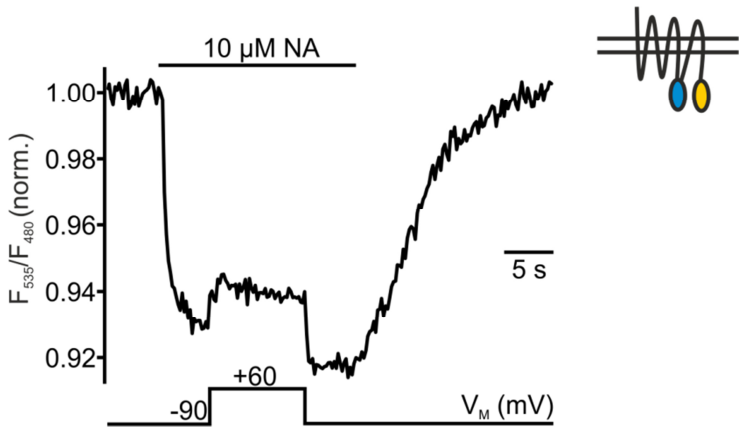

Figure 27: Charge neutralization of lysine 103 does not alter voltage-dependence of α_{2A}-AR activity. Lysine 103 in the extracellular half of TM3 was replaced by alanine to neutralize the positive charge using site-directed mutagenesis. The resulting α_{2A}-AR-K103A-cam construct was expressed transiently and stimulated with 10 µM NA and depolarized to +60 mV during the stimulation. The resulting single experiment was corrected for bleaching and normalized to its initial FRET value prior to stimulation.

A charged amino acid, lysine 103, in the vicinity of this important aspartic acid was then mutated (K103A). It is located within the extracellular half of TM3 and points towards the cytoplasm (Vroling et al., 2011). Stimulation of the α_{2A}-AR-K103A-cam with 10 µM NA activated the receptor which was reversible upon withdrawal of the agonist (Figure 27). In this pilot experiment the depolarization-induced deactivation of the α_{2A}-AR-K103A-cam was comparable to the wild-type α_{2A}-AR-cam. No further measurements were conducted with this mutant as the lysine at position 103 did not seem to be a part of a voltage-sensor in α_{2A}-adrenoceptors.

6.4.2.3 Introduction of an additional charge near the highly conserved $D^{2.50}$ increased agonist affinity

Another highly conserved aspartic acid among class A GPCRs is $D^{2.50}$ in TM2 (D79 in α_{2A}-AR) (Gether, 2000). It is involved in a hydrogen bond network that connects transmembrane domains one, two and seven (Okada et al., 2002; Angel et al., 2009) and is also involved in the coordination of a sodium ion (Liu et al., 2012). This aspartic acid has been mutated to an alanine in M_2AChR which then failed to exhibit gating currents likely due to a low expression of the mutant receptor (Navarro-Polanco et al., 2011).

When the corresponding aspartic acid (D79) was mutated to alanine in the α_{2A}-AR-cam, voltage-dependence was not detectable and the affinity for NA was reduced by more than 10-fold (unpublished data by Prof. Rinne).

As the mutation of the conserved D79 resulted in a dramatic reduction in agonist affinity, we introduced a positive charge in close proximity to the negatively charged D79 as a countercharge. We aimed to alter voltage-dependence without losing agonist affinity due to the removal of D79. Anna-Lena Krett mutated leucine 75, a residue one helical turn beneath D79 in TM2 (Figure 28A), to lysine (L75K) by site-directed mutagenesis. Depolarization deactivated both wild-type α_{2A}-AR-cam and α_{2A}-AR-L75K-cam but to a different degree which was nicely visible after normalization to the maximal agonist-evoked FRET response (Figure 28B). The overlay also showed a pronounced difference in receptor deactivation after NA withdrawal. The mutant receptor sensor deactivated very slowly compared to the wild-type α_{2A}-AR-cam indicating that the introduction of the positive charge near $D^{2.50}$ increased the affinity for NA. To confirm this increase in agonist affinity, unpatched cells expressing either the wild-type or the mutant α_{2A}-AR-L75K-cam were stimulated with increasing concentrations of noradrenaline in order to plot concentration-response curves (Figure 28C). NA-evoked responses were normalized to the reference concentration of 100 µM NA and plotted against the NA concentration. The concentration-response curve for the L75K-cam showed a left shift compared to the wild-type receptor by a factor of approximately five (EC_{50}L75K=0.22 µM; EC_{50}wt=1.04 µM) (Figure 28C). In addition, deactivation kinetics after withdrawal of 100 µM NA were analyzed in unpatched cells expressing either wild-type or mutant α_{2A}-AR-cam. Also here deactivation of the mutant receptor was clearly slower than wt α_{2A}-AR-cam deactivation (Figure 28D). On average, k_{off}-values of mono-exponential curves fit to the individual traces were about 3-fold lower in the mutant (k_{off}=0.06±0.01 s^{-1}) compared to the wild-type receptor (k_{off}=0.16±0.02 s^{-1}).

When cells expressing wild-type-α_{2A}-AR-cam were stimulated with 10 µM NA, the depolarizing effect on receptor deactivation was reduced compared to the stimulation with lower concentrations as reported (compare black traces in Figure 28B and E; (Rinne et al., 2013)). The α_{2A}-AR-L75K-cam could not be deactivated by depolarization anymore during stimulation with 10 µM NA (Figure 28E).

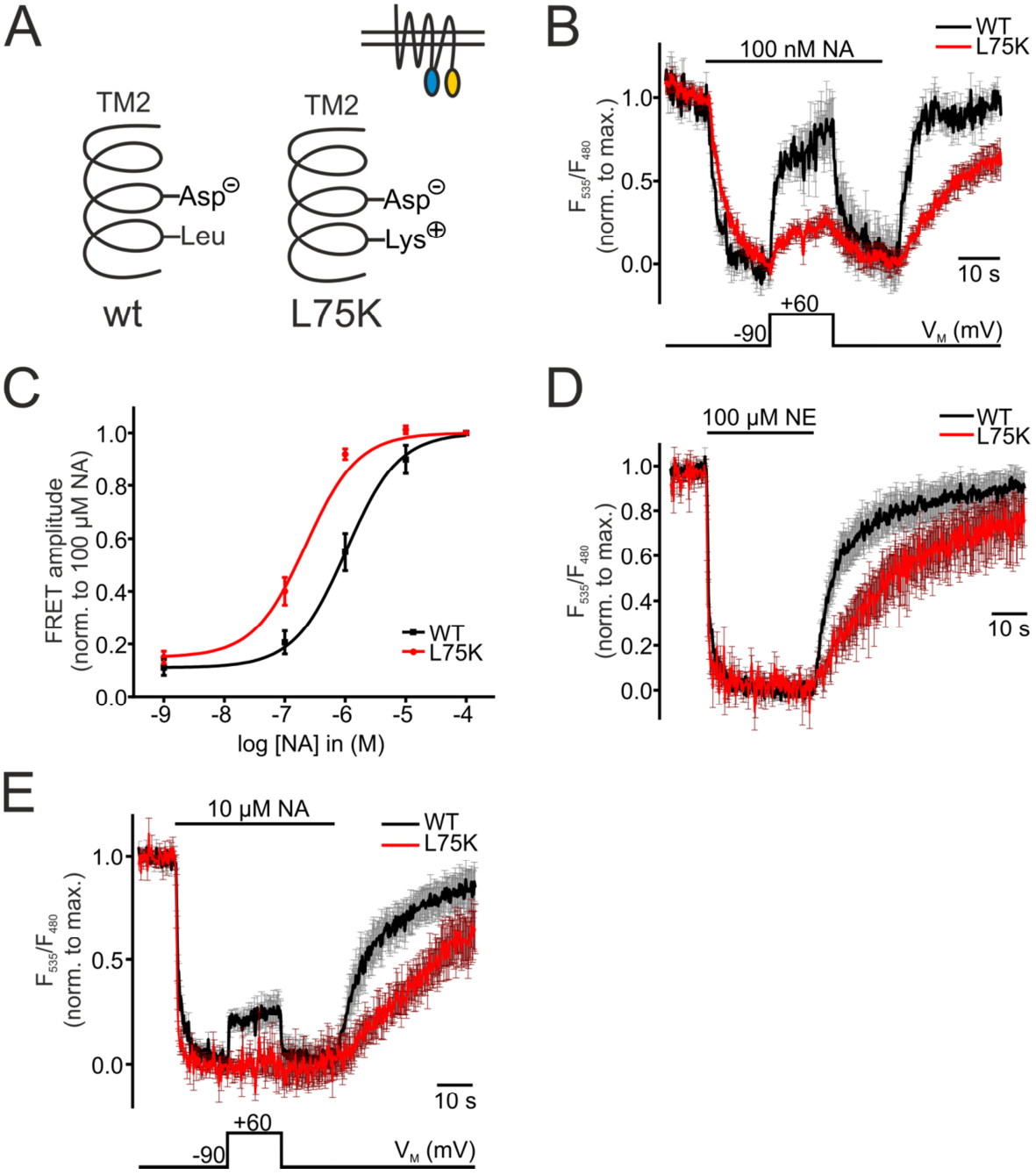

Figure 28: Insertion of an additional charge near $D^{2.50}$ increases receptor affinity towards NA.
A: The schematic shows the highly conserved D79 in TM2 and the site of mutation from the wild-type (wt) residue leucine (left) to a lysine (right) in the α_{2A}-AR-L75K-cam. The black backbone structure depicts the TM2 α-helix. Measurements were conducted in cells transiently expressing either the wt- or the L75K-cam variant of the α_{2A}-AR. All individual experiments were corrected for photo bleaching. *B*: To compare the effect of depolarization on receptor activity of wt or mutant α_{2A}-AR, cells were stimulated with 100 nM NA and subjected to a depolarizing step to +60 mV. Individual measurements were normalized to the maximal agonist-induced FRET response prior to depolarization (average±SEM; wt: black, n=5; L75K: red, n=8). *C*: To collect data for a concentration-response curve wt- and L75K-cam were stimulated with different concentrations of NA. The NA-evoked FRET response was normalized to the FRET response evoked by 100 µM NA in individual experiments. The normalized responses were plotted against the noradrenaline concentrations and fit to a sigmoidal curve (wt-cam: black, n=7, EC_{50}=1.04 µM; L75K-cam: red, n=11, EC50=0.22 µM). *D*: Individual measurements in unpatched cells stimulated with 100 µM NA were normalized to the maximal NA-mediated FRET response to compare off-kinetics (average±SEM; wt-cam: black, n=10; L75K-cam: red, n=7). *E*: Measurements of mutant- and wt-cam stimulated with 10 µM NA were normalized to the maximal FRET response prior to the depolarizing step (average±SEM; wt-cam: black, n=4; L75K-cam: red, n=6).

Introduction of the L75K mutant into α_{2A}-AR-YFP resulted in a receptor construct unable to interact with arrestin in an arrestin FRET assay despite good plasma membrane localization. It was not investigated, however, whether the absence of a FRET increase upon stimulation with NA resulted from a lack of receptor phosphorylation by GRK2, failed translocation of arrestin to the plasma membrane, missing interaction between α_{2A}-AR-YFP and CFP-arrestin per se or any unspecific effect of depolarization for example on the orientation of the fluorophores towards one another. Introduction of a negative charge in the vicinity of $D^{2.50}$ (A83D) into the α_{2A}-AR-cam and –YFP resulted in receptor mutants which were not expressed in HEK 293 cells.

Taken together, the left shift in concentration-response curve and slow deactivation kinetics seen in Figure 28B, D and E indicate an increase in affinity towards NA induced by the mutation of L75 to K75. Compensation of the shift in agonist affinity did not equal the degree of depolarization-induced receptor deactivation: Depolarization deactivated wild-type α_{2A}-AR-cam during stimulation with 1 µM NA (Figure 29C (black trace), more than factor five-fold higher suggested by the concentration-response curve) to a greater extent than during stimulation of the α_{2A}-AR-L75K-cam with 100 nM (Figure 28B, red trace). This suggests that the introduction of a countercharge near $D^{2.50}$ altered voltage-dependence of the construct and that $D^{2.50}$ could supposedly be a residue of the voltage-sensor of α_{2A}-AR. This conclusion, however, needs to be strengthened by further experiments (7.2).

6.4.2.4 An L75K/D79A α_{2A}-AR-cam double mutant did not reverse voltage-sensitivity

As seen in the concentration-response curve and the analysis of deactivation kinetics, the replacement of leucine 75 by lysine increased the affinity for noradrenaline at the α_{2A}-AR and reduced voltage-dependence. If $D^{2.50}$ were the voltage-sensor and caused a voltage-dependent conformational change in the receptor by a movement of TM2 in one direction, we wondered whether an opposite charge would reverse the direction of TM movement and of voltage-dependence or would reduce voltage-dependence. Taking the α_{2A}-AR-L75K-cam as a template the additional D79A-mutation was inserted by site-directed mutagenesis (Figure 29A). Cells expressing the resulting receptor double mutant (α_{2A}-AR-L75K/D79A-cam) were stimulated with 1 µM NA and subjected to a depolarizing pulse to +60 mV (Figure 29B). Noradrenaline activated the mutant receptor resulting in an average ratio decrease of just above 1%. This agonist-induced FRET amplitude was slightly reduced during depolarization to +60 mV (Figure 29B). Comparison of conformational

changes induced by stimulation with 1 µM NA of wildtype-, L75K- and L75K/D79A-cam revealed large differences especially for the double mutant receptor construct which seemed restricted in its ability to undergo an activating conformational change upon NA-stimulation (Figure 29C). Single mutation of leucine 75 hardly reduced the NA-induced FRET response compared to the wild-type α_{2A}-AR-cam.

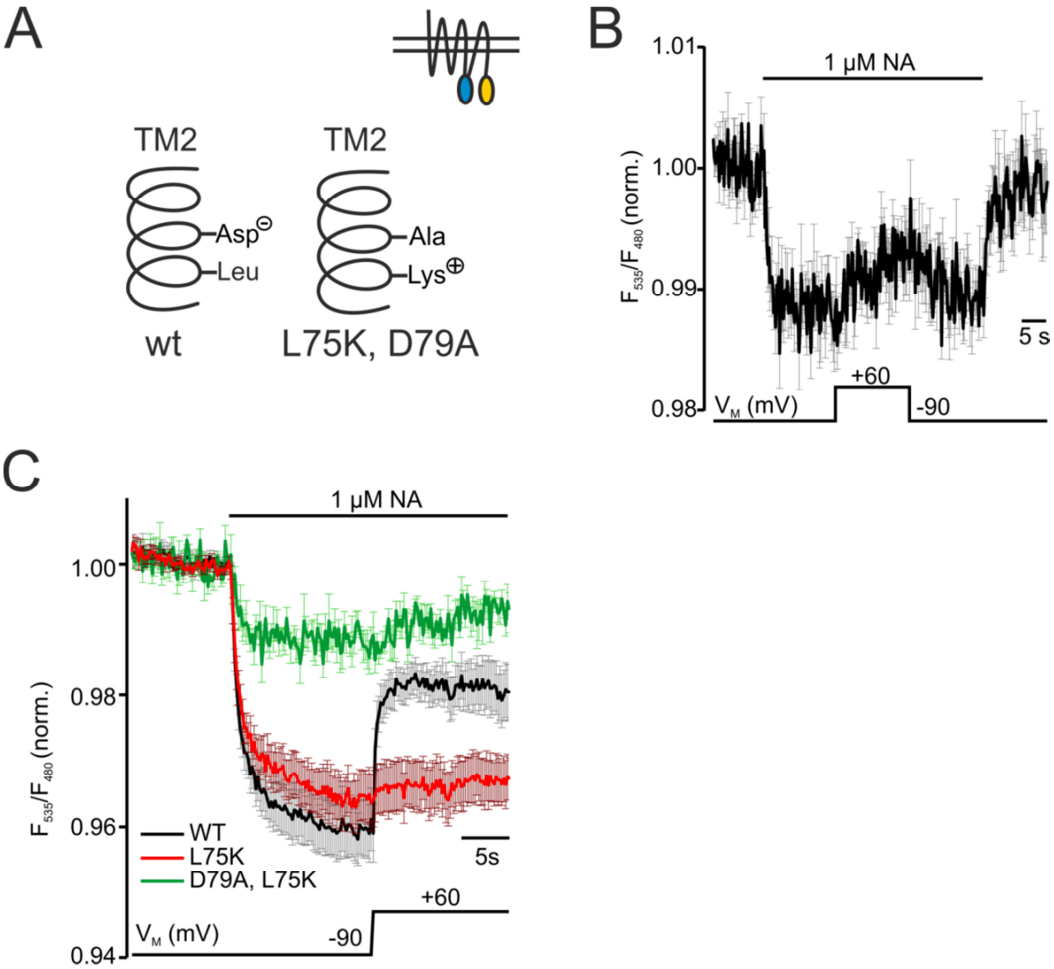

Figure 29: Double mutation of the α_{2A}-AR-cam: Insertion of K75 and charge removal by mutation of D79 to A79

A: The schematic shows the double mutation compared to the wt-residues at positions 75 and 79. *B*: The transiently expressed L75K/D79A double mutant was activated with 1 µM NA and depolarized to +60 mV (average±SEM, n=3). *C* and *D*: Comparison of the depolarizing effect on transiently transfected wt-, L75K- and L75K/D79A-cam constructs activated with 1 µM NA. Normalization to the initial FRET values prior to NA application allows comparison of the degree of agonist-induced conformational change in the receptor molecules (*C*). For the comparison of depolarization-induced receptor inactivation the same data was normalized to the maximal NA-induced FRET response before the depolarizing step (*D*). Average±SEM; wt-cam: black, n=3; L75K-cam: red, n=8; D79A/L75K-cam (data of *B*): green, n=3.

Introduction of the two point mutations into α_{2A}-AR-cam (α_{2A}-AR-L75K/D79A-cam) reduced its activity, did not invert voltage-dependence but responded only poorly to depolarization. $D^{2.50}$ seemed to be part of the voltage-sensor in α_{2A}-AR among other yet unidentified residues. Whether these findings are transferable to other voltage-dependent GPCRs remains to be tested.

7 Discussion

About 3% of all genes in the human genome encode for GPCRs (Takeda et al., 2002). They can be activated by small molecules, peptides, proteins or photons and transduce extracellular signals across the membrane into intracellular responses (Gether, 2000). Fairly recent findings showed that the activity of several G_i- and G_q-coupled GPCRs was sensitive to alterations in the membrane potential (Ben-Chaim et al., 2003; Martinez-Pinna et al., 2005, 2010; Sahlholm et al., 2008c, 2012; Rinne et al., 2013). Voltage-dependence has first been identified as altered agonist affinity at depolarization in radio-ligand binding experiments (Ben-Chaim et al., 2003). Alterations in the membrane potential were induced with buffers of different potassium concentration. A direct control of the membrane potential by voltage-clamp electrophysiology to measure G_i-mediated GIRK currents or acetylcholine-induced potassium currents (I_{KACh}) in atrial myocytes to address voltage-dependence of the corresponding receptors was an advantage compared to measurements that relied on altered potentials by different potassium concentrations (e.g. (Moreno-Galindo et al., 2011; Navarro-Polanco et al., 2011; Sahlholm et al., 2012). However, inward rectification of GIRK channels has been shown to be altered in a concentration-dependent manner (Hommers et al., 2003). Strong receptor activation led to a reduction in inward rectification. This indirect effect could be misinterpreted as a voltage-dependent reduction of receptor activity. The combination of patch-clamp electrophysiology and measurements of Ca^{2+}-signals identified voltage-dependence of certain G_q-coupled receptors (Martinez-Pinna et al., 2004, 2005). Conclusions from these measurements involved statements of altered agonist efficacy due to changes in the membrane potential. However, these indirect measurements are unsuited for efficacy measurements as they are affected by receptor expression, coupling of effectors and amplification steps in the signaling cascade (Lohse et al., 2003). A suitable tool to directly measure the influence of membrane depolarization on agonist efficacy and/or affinity are fluorescence-based assays monitoring receptor conformational changes or direct receptor-effector interactions (Lohse et al., 2003; Rinne et al., 2013, 2015). Such a direct assay was applied to investigate depolarization-dependent conformational changes within the binding pocket of M_2AChR using site-directed fluorescence labeling (Dekel et al., 2012).

By means of different intramolecular and intermolecular FRET-based assays in combination with direct control of the membrane potential with patch-clamp electrophysiology led to the following key findings in this study: 1) The activity of the G_s-coupled β_1-AR and to a smaller extent of β_2-AR is voltage-dependent. 2) This voltage-

dependence was an intrinsic property of the two receptors and occurred within the physiological range of membrane potential. 3) Measurements of effectors of both β_1-AR and β_2-AR revealed transmission of the voltage-sensitivity to downstream signaling. 4) Stimulation of β_1-AR with different ligands also showed an agonist-specific component of β_1-AR voltage-sensitivity. 5) Most importantly, voltage-dependence was mainly mediated via a reduction in agonist efficacy during depolarization at β_1-ARs activated by isoprenaline or adrenaline. A depolarization-induced reduction in agonist affinity contributed only to a minor extent to β_1-AR voltage-dependence and appeared to be stronger for Adr than Iso.

7.1 Voltage-dependence of adrenoceptors

By means of a combination of FRET measurements and whole-cell patch-clamp in voltage-clamp mode voltage-dependence of G_s-coupled receptors β_1-AR and β_2-AR was determined (Birk et al., 2015). Even though the molecular mechanism by which the membrane potential induces a conformational change in the ligand binding pocket remains unclear, it could ultimately alter either agonist affinity, agonist efficacy or both. Voltage-dependence of agonist binding has been measured for M_1AChR, $mGluR_1$, M_2AChR and $mGluR_3$. Depolarization increased the binding of the former two and decreased agonist binding of the latter two (Ben-Chaim et al., 2003; Ohana et al., 2006). I also intended to investigate voltage-dependent binding of [^{3}H]-noradrenaline to α_{2A}-AR expressed in *Xenopus* oocytes to directly show reduced noradrenaline affinity which has been demonstrated with the α_{2A}-AR-cam (Rinne et al., 2013). In two sets of experiments specific binding could be detected at rest and at depolarization induced by high external K^+ (Figure 23). In one of the two experiments specific binding was significantly lower during depolarization whereas the other only showed a tendency towards reduced binding. Several problems occurred and made it difficult to interpret the data: Expression of α_{2A}-AR was low in most batches of injected oocytes which resulted in low total binding of the radio-ligand. Depolarization of cells using buffers of high K^+-concentrations is also difficult. High external K^+ might by itself influence GPCR activity as described for P2Y receptors (Pitt et al., 2005). In addition, noradrenaline affinity was reduced when the external solution was depleted of sodium indicating a sodium-dependence of noradrenaline binding to α_{2A}-AR (unpublished data of Prof. Rinne and (Pihlavisto et al., 1998)). Although we think that binding of noradrenaline should be decreased during depolarization as indicated by the right-shift in the concentration-response curve measured for α_{2A}-AR-cam, it was not possible to definitively show it in a ligand binding assay.

Alterations in agonist affinity were also apparent in the measurements of β_1-AR and β_2-AR and α_{2A}-AR. Stimulation of β_1-AR with saturating concentrations of Iso or Adr reduced the depolarization effect on receptor activity and receptor-arrestin interaction indicating a depolarization-mediated decrease in agonist affinity (Figure 9, Figure 12E). Adr-stimulated cells showed higher sensitivity towards depolarization-induced receptor deactivation in non-saturating conditions and thereby a larger reduction of depolarization-effect with increasing concentrations of agonist. Nevertheless, a reduced deactivating effect by depolarization remained during saturation with Iso, Adr and NA (Figure 9 and Figure 12E and F). Agonist affinity was therefore not the only target of voltage-dependence in β_1-AR. This finding was especially surprising for Adr because so far voltage-dependence of receptors stimulated by endogenous ligands has been attributed to alterations in agonist affinity (Navarro-Polanco et al., 2013; Rinne et al., 2013). Voltage-dependence of β_2-AR seemed to be purely mediated by a change in agonist affinity given that saturation of the receptor with either Iso or Adr prevented disruption of receptor-arrestin interaction during depolarization (Figure 22). Depolarization-mediated reduction of α_{2A}-AR-Arr3 interaction was abolished under saturation with NA whereas some reduction remained under saturation with Adr (Figure 24A). As described above reduction of NA affinity during depolarization at the α_{2A}-AR was in line with earlier work (Rinne et al., 2013).

Receptor number and coupling to effectors are tissue and cell type specific wherefore measurement of agonist efficacy should be direct through detection of receptor conformational changes. FRET-based intramolecular receptor fusion proteins are therefore an ideal tool to measure intrinsic efficacy (Lohse et al., 2003). A reduction in clonidine efficacy during depolarization has been directly demonstrated in this manner with the α_{2A}-AR-cam construct (Rinne et al., 2013). Reports on voltage-dependent alteration of agonist efficacy at the M_2AChR activated by pilocarpine, the P_2Y_1 or the $D_{2S}R$, however, were based on indirect efficacy measurements (Gurung et al., 2008; Navarro-Polanco et al., 2011; Sahlholm et al., 2011). Using FRET assays measuring β_1-AR activation as well as assays detecting receptor-effector interaction the depolarizing effect on agonist efficacy was analyzed directly. Deactivation kinetics in all three assays showed a substantial acceleration (up to 100-fold in Iso-stimulated receptors at the receptor level) during depolarization compared to deactivation by agonist withdrawal. Interestingly, although Iso and Adr exhibited agonist-specificity with regard to voltage-dependent reduction in agonist affinity, deactivation kinetics during depolarization yielded a comparable degree of

depolarization-mediated reduction in agonist efficacy (Figure 14B and D). The differences between deactivation kinetics by depolarization and by agonist washout exceeded the only minor reduction in agonist affinity for both Iso and Adr. Therefore alterations in efficacy seem to mainly underlie voltage-dependence of Iso- and Adr-stimulated β_1-AR. This conclusion was also corroborated by a classical concentration-response experiment of β_1-AR-arrestin 3 interaction induced by isoprenaline: Whereas the about two-fold right-shift of the curve at depolarization relative to the curve at rest, representing a reduction in Iso-affinity, did not reach statistical significance, the maximal FRET response at depolarization was significantly smaller, which reflects a reduction in efficacy (Figure 16B). For Adr the right-shift in a concentration-response curve at depolarization would be expected to be more pronounced and the reduction in the maximal FRET response similar or less pronounced as seen for Iso. It would be interesting to do similar measurement with Adr to see whether these predictions would be confirmed.

Voltage-dependence of GPCRs has been suggested to be an intrinsic property of the receptor molecule. Strong evidence supporting this hypothesis arose from measurements of gating charges in M_1AChR and M_2AChR (Ben-Chaim et al., 2006; Navarro-Polanco et al., 2013). Charge movement resulting in currents analogous to gating currents of voltage-gated ion channels also correlated well with voltage-dependent agonist binding in M_2AChR (Ben-Chaim et al., 2006). Additional evidence for an intrinsic voltage-dependence of the receptor molecule was provided by FRET-based measurements of an intramolecular α_{2A}-AR fusion protein (α_{2A}-AR-cam) (Rinne et al., 2013). The activation-induced movement of transmembrane helices relative to each other which is transferred to intracellular loop 3 (IL3) and the c-terminus, enabled FRET measurements with these fusion proteins as they carry FRET donor and acceptor in the c-terminus and IL3 or vice versa (Lohse et al., 2003; Vilardaga et al., 2003). With the α_{2A}-AR-cam a depolarization-mediated receptor deactivation was monitored which was reversible upon repolarization (Rinne et al., 2013). FRET response-V_M relations of NA-activated α_{2A}-AR-cam in the presence and absence of PTX overlay nicely which indicated that voltage-dependence was an intrinsic property of the receptor and was independent of its interaction with G_i proteins (Rinne et al., 2013). This is also corroborated by the fact that insertion of a bulky fluorophore into the third intracellular loop greatly reduces G protein coupling to these intramolecular FRET-based receptors (Vilardaga et al., 2003; Hoffmann et al., 2005). With FRET-based fusion proteins of β_1-AR and β_2-AR cloned analogously to α_{2A}-AR-cam (Rochais et al., 2007; Ahles et al., 2011), depolarization-induced receptor deactivation was

nicely visible for the former and also present but less pronounced in the later (Figure 8 and Figure 21A). Both Iso- and Adr-stimulated cells expressing the β_1-AR-sensor showed reversible receptor deactivation during depolarization. These data confirmed the intrinsic voltage-dependence of the G_s protein-coupled β_1-AR and β_2-AR. As both β_1-AR- and β_2-AR-sensors closely resemble wild-type-like properties (Rochais et al., 2007; Ahles et al., 2011), these findings can also be extrapolated to the wild-type β_1-AR and β_2-AR.

Real-time live-cell FRET measurements are well suited to investigate receptor conformational changes as described above but also to monitor protein interactions along the signaling axes downstream of the receptor molecule (Lohse et al., 2012). FRET assays monitoring receptor-effector interaction and G protein activation demonstrated that voltage-dependence was transmitted from the receptor molecule to downstream effectors. This is a necessity for the voltage-dependence to be of physiological importance as alterations in downstream signaling result in altered cellular responses to extracellular stimuli. For β_1-AR both agonist-induced G protein-receptor interaction as well as G protein activation were reduced by depolarization of the plasma membrane (Figure 10B, C and Figure 11B-C). Arrestin signaling was also decreased during depolarization indicated by a reduction of β_1-AR-arrestin 3 interaction (Figure 12). Interaction of arrestin 3 with the β_2-AR induced by a non-saturating Iso concentration was also decreased during depolarization (Figure 22A). Stimulation with a saturating concentration of Iso and Adr or NA prevented a depolarizing effect on the interaction of arrestin 3 with β_2-AR or α_{2A}-AR, respectively, whereas the interaction of α_{2A}-AR and arrestin 3 induced by a saturating concentration of Adr was still reduced by depolarization (Figure 22B and Figure 24A). Voltage-dependence of downstream signaling is in line with measurements of altered GIRK currents transmitted from voltage-dependent M_2AChR,, α_{2A}-AR, $mGluR_3$, D_2, H_3, H_4, of changes in Cl^- currents of Ca^{2+}-dependent chloride channels through voltage-dependent M_1AChRs or of differences in Ca^{2+} signaling due to voltage-dependence of P_2Y_1, 5-HT_{2A}, TXA_2 or LPA receptors (Ben-Chaim et al., 2003; Martinez-Pinna et al., 2005, 2010; Ohana et al., 2006; Sahlholm et al., 2008c, 2012; Rinne et al., 2013). Another indication that voltage-dependence of β_1-AR could be of physiological relevance is that it occurred within the range of physiological membrane potential (Figure 13). Similar measurements at the α_{2A}-AR yielded a half maximal effective potential of -20 mV (Rinne et al., 2013) compared to -27 mV and -28 mV for Adr- and Iso-stimulated β_1-AR, respectively. The half-point of maximal charge movement was slightly more negative in M_1AChR (V_{50}=-53 mV (Rinne et al., 2015)) and M_2AChR (V_{50}=-44 mV (Ben-Chaim et

al., 2006); V_{50}=-67 mV (Navarro-Polanco et al., 2011)). Number of charges moved across the membrane (z-values) of 0.49 e_0 determined for Adr-stimulated β_1-AR was comparable to the values calculated for M_1AChR (z=0.76 e_0 (Rinne et al., 2015)), M_2AChR (z=0.55/0.85 e_0 (Ben-Chaim et al., 2006; Navarro-Polanco et al., 2011)) and α_{2A}-AR (z=0.5 e_0 (Rinne et al., 2013)). A slightly shallower V_M-FRET response relation of Iso-stimulated cells resulted in a z-score of 0.36 e_0. A third important observation pointing towards physiological relevance was that voltage-induced deactivation of β_1-AR occurred within very fast time scales (Figure 14). The voltage-dependent regulation of agonist efficacy could lead to very fast alterations of receptor signaling because the time-limiting step of agonist dissociation from the receptor is bypassed. Downstream signaling could therefore be altered by the membrane potential even in the presence of agonists. Fast kinetics are consistent with fast voltage-dependent changes in M_2AChR for which it was suggested that even a single action potential would suffice to induce fast gating charges (Ben-Chaim et al., 2006). An indication of the physiological importance of voltage-dependent regulation of receptor activity was suggested by studies on G_i protein-coupled presynaptic M_2AChR autoreceptors which seemed to control kinetics of neurotransmitter release at murine neuromuscular junctions (Kupchik et al., 2011). However, to finally prove a direct involvement of voltage-dependent M_2AChR in the control of vesicle fusion and transmitter release could only derive from measurements with mutant M_2AChR lacking voltage-dependence.

The differential contribution of altered affinity of NA and Adr at α_{2A}-ARs also indicated an agonist-specific component of α_{2A}-AR voltage-dependence. This was also true for Adr and Iso at the β_1-AR but especially obvious during stimulation with the partial agonist dopamine (Figure 20). Very recently it has been shown for muscarinic receptors that the mode of agonist binding would determine the direction of voltage-dependence (Rinne et al., 2015). An asparagine ($N^{6.52}$) in TM6 was crucial for the effect of voltage changes on the signal and its mutation to glutamine was able to reverse the voltage-dependent effect. Agonist orientation towards TM6 correlated with a decrease in receptor activity during depolarization whereas orientation towards TM3 (particularly $D^{3.32}$) correlated with an increased activity during depolarization. An interaction of the β-OH-group present in the catecholamines Adr, NA and Iso with $N^{6.55}$ was suggested based on modeled Iso binding to β_2-AR (Wieland et al., 1996). However, more recent dockings of Iso to β_1-AR or β_2-AR rather proposed an interaction of $N^{6.55}$ with the cathechol meta-OH-group and an interaction of the β-OH-group with the highly conserved $D^{3.32}$ (Katritch et al., 2009; Warne

et al., 2011). Dopamine lacks the β-OH-group altering the interaction with $D^{3.32}$ and dopamine does not interact with TM6. This could cause a different binding mode within the binding pocket of β_1-AR and could therefore result in the opposite voltage-dependent behavior of dopamine-stimulated β_1-AR. Although the β-OH-group is also absent in dobutamine, the binding mode to β_1-AR includes H-bonding between $N^{6.55}$ and the catechol meta-OH group (Warne et al., 2011) thereby probably causing a voltage-dependent behavior more similar to Iso than to dopamine. Agonist-specificity is not limited to the adrenoceptors investigated in this study but was also reported for example for several (clinically used) agonists at the $D_{2S}R$ (Sahlholm et al., 2008b, 2011), for the α_{2A}-AR (Rinne et al., 2013) and for muscarinic receptors (Navarro-Polanco et al., 2011; Rinne et al., 2015).

To enable Förster resonance energy transfer between the donor and acceptor fluorophore, their emission and absorption spectra, respectively, need to overlap, the distance to one another must be 10 nM or less and the orientation of the transition dipoles should ideally be parallel (Förster, 1948; Miyawaki, 2011; Lohse et al., 2012). A combination of FRET and whole-cell patch clamp technique enabled us to directly set the membrane potential to any desired value. Compared to a change in membrane potential by external buffers of high potassium concentrations this method is independent of the expression of potassium conducting channels and thereby favorable on a single cell level. Furthermore, as described before, elevation of the extracellular K^+-concentration was shown to influence GPCR activity independently of the rise in membrane potential and should therefore be avoided (Pitt et al., 2005). It was important to make sure that depolarization-induced alterations in the agonist-evoked FRET response were the result of a specific deactivating conformational change or disruption of receptor-effector interaction. Strong depolarization could also change the energy transfer signal unspecifically via a change in dipole orientation or in acceptor quantum yield. However, evidence arguing in favor of a specific effect of depolarization on receptor conformation and receptor-effector interaction was the following: 1) Depolarization did not change the initial FRET signal of the β_1-AR-sensor in the absence of ligands. It only reduced the agonist-induced FRET response. 2) The effect of depolarization on agonist-evoked FRET responses was similar in amplitude for three different FRET assays even though 3) the direction of agonist-induced FRET amplitudes was opposed in receptor-FRET compared to the interaction assays.

7.2 Investigating the mechanism of voltage-sensing

Despite an increasing number of publications about voltage-sensitive GPCRs the mechanism underlying voltage-dependence has not yet been identified. In the attempt to identify residues involved in voltage-sensing amino acids of α_{2A}-AR were mutated by site-directed mutagenesis in this study. Most mutations did not alter voltage-dependence, however, $D^{2.50}$could be a part of the voltage-sensor in α_{2A}-AR.

In the first years it seemed that a receptor's preferred G protein subtype would determine whether depolarization deactivated a receptor or enhanced its activation. This was based on the observation that G_i-coupled receptors like M_2AChR or D_2 were deactivated whereas activity of G_q-coupled receptors like M_1AChR or P_2Y_1R increased during depolarization (summarized in (Mahaut-Smith et al., 2008)). An exchange of intracellular loop three (IL3), the main G protein coupling part of M_1AChR and M_2AChR, between the two receptors reversed direction of voltage-dependence during ACh stimulation. Therefore a mechanism was suggested in which voltage-dependent alteration in receptor activity was induced via altered G protein binding which in turn led to conformational rearrangements in the orthosteric binding pocket. However, gating currents in these chimeric constructs remained similar to wild-type M_1AChR and M_2AChR. In addition stimulation of M_2AChR by two different ligands, ACh and pilocarpine, led to opposing depolarization effects (Navarro-Polanco et al., 2011). These findings suggested that IL3 rather functions as an effector of voltage-sensor movement than acting as a voltage-sensor itself. It is now believed that voltage-induced conformational changes directly act on the orthosteric binding site (Ben-Chaim et al., 2006; Bezanilla, 2008; Navarro-Polanco et al., 2011). As described above, treatment of the α_{2A}-AR with PTX did not alter depolarization-induced receptor deactivation which also supports the hypothesis of a G protein-independent mechanism underlying voltage-dependence.

A current task in the research field of GPCR voltage-dependence is the identification of a voltage-sensor which detects changes in the membrane potential and translates these changes into conformational changes in the orthosteric binding site and the receptor molecule itself. A possible voltage-sensor could be composed of charged amino acids which would move through the electrical field upon membrane potential changes and which is how voltage-gated ion channel react to different polarization of the membrane. However, sequence analysis showed that a similar structure to voltage-sensors of voltage-gated ion channels does not exist in GPCRs (Bezanilla, 2008). Numbers of charges moved across the membrane of $z=0.36\text{-}0.85$ e_0 measured for β_1-AR, α_{2A}-AR, M_1AChR and

M_2AChR (Ben-Chaim et al., 2006; Navarro-Polanco et al., 2011; Rinne et al., 2013, 2015; Birk et al., 2015) suggest that either one charged residue moves across half the membrane or a number of charged residues undergo small movements. The former is rather unlikely as a movement of one amino acid across half the membrane would cause a large movement of its TM domain which would certainly hamper receptor function. The membrane potential in GPCRs is therefore presumably sensed by more than one residue.

In fact only few charged amino acids reside within the TM domains were the electrical field is strongest. Mutation of a charged lysine in the extracellular half of TM3 did not alter voltage-dependence of α_{2A}-AR (Figure 27). Mutation of $S^{5.46}$ involved in agonist binding (Figure 26) most likely did not help to identify a voltage-sensor but would need to be investigated in more detail before a conclusive evaluation can be done.

Alterations in the membrane potential could also be transmitted via the movement of dipoles through the electrical field. Another possibility of sensing the membrane potential is by free ions associated in cavities within the receptor molecules (Bezanilla, 2008). As crystal structures of β_1-AR and $A_{2A}R$ identified a sodium ion binding site within the TM bundle, mutation of the coordinating residues $D^{2.50}$ or $S^{3.39}$ seemed reasonable (Liu et al., 2012; Miller-Gallacher et al., 2014). Mutation of the corresponding aspartic acid in M_2AChR to alanine resulted in a construct with low membrane expression and no conclusive results on voltage-dependence of this mutant could be obtained (Navarro-Polanco et al., 2011). Introduction of the $D^{2.50}$A mutation into α_{2A}-AR greatly reduced agonist affinity and a depolarization-induced receptor deactivation was not detectable (unpublished data of Prof. Rinne). Via the introduction of a positive counter charge in the direct vicinity of the aspartic acid we hoped to create a receptor mutant lacking voltage-dependence but with otherwise wild-type-like properties (Figure 28). The resulting α_{2A}-AR-L75K-cam increased agonist affinity but showed reduced voltage-dependence compared to wild-type α_{2A}-AR stimulated with noradrenaline. This was not only due to the higher affinity of the mutant and a resulting left-shift of voltage-dependence as wild-type α_{2A}-AR-cam showed a stronger deactivation during depolarization when activated with a noradrenaline concentration which balanced the differences in agonist affinity. Combination of both mutations to α_{2A}-AR-L75K/D79A-cam generated a mutant of little agonist-evoked FRET responses and some depolarization-dependent deactivation. If $D^{2.50}$ were the only residue involved in voltage-sensing, one would expect a reversed voltage-dependence of this double mutant due to the removal of a negative and insertion of a positive charge, but was not detected in the FRET measurements. Nevertheless, $D^{2.50}$

seemed to be involved in voltage-sensing of the α_{2A}-AR but the exact course of voltage-dependence of this receptor mutant needs to be investigated in more detail in the future. A shift in the Boltzmann curve or an alteration of its steepness would be hints on altered voltage-sensitivity of the mutant and an involvement of $D^{2.50}$ in the voltage-sensor.

In summary I was able to demonstrate, for the first time, that also the activity of G_s-coupled receptors displays voltage-dependence. Voltage-dependence of β_1-AR is mainly mediated by an alteration in efficacy of both Adr and Iso and occurs within the time scale of cardiac action potentials. The activity of β_1-AR could therefore be modulated even without dissociation of the endogenous ligand adrenaline from the receptor. Rhythmic alterations in the membrane potential of myocytes occurring physiologically could reversibly deactivate the receptors resulting in reduced receptor desensitization via a reduced interaction of receptors and arrestins.

The highly conserved aspartic acid in TM2 of *Rhodopsin*-family GPCRs could be involved in voltage-sensing in the α_{2A}-AR. However, its contribution needs to be verified in further experiments. Similar mutations in other receptors would be necessary to test whether this involvement is an α_{2A}-AR-specific phenomenon or whether $D^{2.50}$ is part of a common GPCR voltage-sensor. Besides $D^{2.50}$ the search for other components of a GPCR voltage-sensor which directly react to changes in the membrane potential is still ongoing.

8 References

Aggarwal SK, MacKinnon R (1996) Contribution of the S4 segment to gating charge in the Shaker K+ channel. Neuron 16:1169–1177.

Ahles A, Engelhardt S (2014) Polymorphic variants of adrenoceptors: pharmacology, physiology, and role in disease. Pharmacol Rev 66:598–637.

Ahles A, Rochais F, Frambach T, Bünemann M, Engelhardt S (2011) A Polymorphism-Specific "Memory" Mechanism in the β2 -Adrenergic Receptor. Sci Signal 4:ra53.

Ahles A, Rodewald F, Rochais F, Bünemann M, Engelhardt S (2015) Interhelical interaction and receptor phosphorylation regulate activation kinetics of different human beta1-adrenoceptor variants. J Biol Chem 290:1760–1769.

Angel TE, Chance MR, Palczewski K (2009) Conserved waters mediate structural and functional activation of family A (rhodopsin-like) G protein-coupled receptors. Proc Natl Acad Sci U S A 106:8555–8560.

Baker JG (2010) The selectivity of β-adrenoceptor agonists at human β1-, β2- and β3-adrenoceptors. Br J Pharmacol 160:1048–1061.

Baldwin JM (1994) Structure and function of receptors coupled to G proteins. Curr Opin Cell Biol 6:180–190.

Ballesteros JA, Weinstein H (1995) Integrated methods for the construction of three-dimensional models and computational probing of structure-function relations in G protein-coupled receptors. In: Methods in Neurosciences (Sealfon SC, ed), pp.366–428. Elsevier.

Barak LS, Ferguson SS, Zhang J, Caron MG (1997) A beta-arrestin/green fluorescent protein biosensor for detecting G protein-coupled receptor activation. J Biol Chem 272:27497–27500.

Ben-Chaim Y, Chanda B, Dascal N, Bezanilla F, Parnas I, Parnas H (2006) Movement of "gating charge" is coupled to ligand binding in a G-protein-coupled receptor. Nature 444:1–13.

Ben-Chaim Y, Tour O, Dascal N, Parnas I, Parnas H (2003) The M2 muscarinic G-protein-coupled receptor is voltage-sensitive. J Biol Chem 278:22482–22491.

Benovic JL, Regan JW, Matsui H, Mayor F, Cotecchia S, Leeb-Lundberg LM, Caron MG, Lefkowitz RJ (1987) Agonist-dependent phosphorylation of the alpha 2-adrenergic receptor by the beta-adrenergic receptor kinase. J Biol Chem 262:17251–17253.

Berney C, Danuser G (2003) FRET or no FRET: A quantitative comparison. Biophys J 84:3992–4010.

Bezanilla F (2000) The voltage sensor in voltage-dependent ion channels. Physiol Rev 80:555–592.

Bezanilla F (2008) How membrane proteins sense voltage. Nat Rev Mol Cell Biol 9:323–332.

Birk A, Rinne A, Bünemann M (2015) Membrane Potential Controls the Efficacy of Catecholamine-induced β1-Adrenoceptor Activity. J Biol Chem 290:27311–27320.

Birnboim HC, Doly J (1979) A rapid alkaline extraction procedure for screening recombinant plasmid DNA. Nucleic Acids Res 7:1513–1524.

Bockaert J, Dumuis A, Fagni L, Marin P (2004) GPCR-GIP networks: a first step in the discovery of new therapeutic drugs? Curr Opin Drug Discov Devel 7:649–657.

Bond RA, Bylund DB, Eikenburg DC, Hieble JP, Hills R, Minneman KP, Parra S (2015) Adrenoceptors: β1-adrenoceptor. IUPHAR/BPS Guid to Pharmacol Available at: http://www.guidetopharmacology.org/GRAC/ObjectDisplayForward?objectId=28.

Braman J, Papworth C, Greener A (1996) Site-directed mutagenesis using double-standed plasmid DNA templates. Methods Mol Biol 57:31–44.

Bünemann M, Frank M, Lohse MJ (2003) Gi protein activation in intact cells involves subunit rearrangement rather than dissociation. Proc Natl Acad Sci U S A 100:16077–16082.

Chen CY, Dion SB, Kim CM, Benovic JL (1993) Beta-adrenergic receptor kinase. Agonist-dependent receptor binding promotes kinase activation. J Biol Chem 268:7825–7831.

Christopoulos A (2002) Allosteric binding sites on cell-surface receptors: novel targets for drug discovery. Nat Rev Drug Discov 1:198–210.

Dekel N, Priest MF, Parnas H, Parnas I, Bezanilla F (2012) Depolarization induces a conformational change in the binding site region of the M2 muscarinic receptor. Proc Natl Acad Sci U S A 109:285–290.

Docherty JR (1998) Subtypes of functional α1- and α2-adrenoceptors. Eur J Pharmacol 361:1–15.

Dror RO, Mildorf TJ, Hilger D, Manglik A, Borhani DW, Arlow DH, Philippsen A, Villanueva N, Yang Z, Lerch MT, Hubbell WL, Kobilka BK, Sunahara RK, Shaw DE (2015) Structural basis for nucleotide exchange in heterotrimeric G proteins. Science 348:1361–1365.

Ferguson SSG (2001) Evolving concepts in G protein-coupled receptor endocytosis: the role in receptor desensitization and signaling. Pharmacol Rev 53:1–24.

Förster T (1948) Zwischenmolekulare Energiewanderung und Fluoreszenz. Ann Phys 2:55–57.

Frank M, Thümer L, Lohse MJ, Bünemann M (2005) G Protein activation without subunit dissociation depends on a Gαi-specific region. J Biol Chem 280:24584–24590.

Fredriksson R, Lagerström MC, Lundin L-G, Schiöth HB (2003) The G-protein-coupled receptors in the human genome form five main families. Phylogenetic analysis, paralogon groups, and fingerprints. Mol Pharmacol 63:1256–1272.

Frielle T, Caron MG, Lefkowitz RJ (1989) Properties of the beta1- and beta2-adrenergic receptor subtypes revealed by molecular cloning. Clin Chem 35:721–725.

Frishman WH (2013) β-Adrenergic blockade in cardiovascular disease. J Cardiovasc Pharmacol Ther 18:310–319.

Galés C, Van Durm JJJ, Schaak S, Pontier S, Percherancier Y, Audet M, Paris H, Bouvier M (2006) Probing the activation-promoted structural rearrangements in preassembled receptor-G protein complexes. Nat Struct Mol Biol 13:778–786.

Gether U (2000) Uncovering molecular mechanisms involved in activation of G protein-coupled receptors. Endocr Rev 21:90–113.

Goodman OB, Krupnick JG, Santini F, Gurevich V V, Penn RB, Gagnon AW, Keen JH, Benovic JL (1996) Beta-arrestin acts as a clathrin adaptor in endocytosis of the β2-adrenergic receptor. Nature 383:447–450.

Gurevich E V, Tesmer JJG, Mushegian A, Gurevich V V (2012) G protein-coupled receptor kinases: more than just kinases and not only for GPCRs. Pharmacol Ther 133:40–69.

Gurung IS, Martinez-Pinna J, Mahaut-Smith MP (2008) Novel consequences of voltage-dependence to G-protein-coupled P2Y1 receptors. Br J Pharmacol 154:882–889.

Gutiérrez-De-Terán H, Massink A, Rodríguez D, Liu W, Han GW, Joseph JS, Katritch I, Heitman LH, Xia L, Ijzerman AP, Cherezov V, Katritch V, Stevens RC (2013) The role of a sodium ion binding site in the allosteric modulation of the A2A adenosine G protein-coupled receptor. Structure 21:2175–2185.

Hamill OP, Marty A, Neher E, Sakmann B, Sigworth FJ (1981) Improved patch-clamp techniques for high-resolution current recording from cells and cell-free membrane patches. Pflugers Arch 391:85–100.

Heim R, Tsien RY (1996) Engineering green fluorescent protein for improved brightness, longer wavelengths and fluorescence resonance energy transfer. Curr Biol 6:178–182.

Hein L (2006) Adrenoceptors and signal transduction in neurons. Cell Tissue Res 326:541–551.

Hein L, Altman JD, Kobilka BK (1999) Two functionally distinct α2-adrenergic receptors regulate sympathetic neurotransmission. Nature 402:181–184.

Hein P, Frank M, Hoffmann C, Lohse MJ, Bünemann M (2005) Dynamics of receptor/G protein coupling in living cells. EMBO J 24:4106–4114.

Hein P, Rochais F, Hoffmann C, Dorsch S, Nikolaev VO, Engelhardt S, Berlot CH, Lohse MJ, Bünemann M (2006) Gs activation is time-limiting in initiating receptor-mediated

signaling. J Bol Chem 281:33345–33351.

Hoffmann C, Gaietta G, Bünemann M, Adams SR, Oberdorff-Maass S, Behr B, Vilardaga J-P, Tsien RY, Ellisman MH, Lohse MJ (2005) A FlAsH-based FRET approach to determine G protein-coupled receptor activation in living cells. Nat Methods 2:171–176.

Hofmann KP, Scheerer P, Hildebrand PW, Choe H-W, Park JH, Heck M, Ernst OP (2009) A G protein-coupled receptor at work: the rhodopsin model. Trends Biochem Sci 34:540–552.

Hommers LG, Lohse MJ, Bünemann M (2003) Regulation of the inward rectifying properties of G-protein-activated inwardly rectifying K+ (GIRK) channels by βγ subunits. J Biol Chem 278:1037–1043.

Huber T, Menon S, Sakmar TP (2008) Structural Basis for Ligand Binding and Specificity in Adrenergic Receptors : Implications for GPCR-Targeted Drug Discovery. Biochemistry 47:11013–11023.

Irannejad R, Tomshine JC, Tomshine JR, Chevalier M, Mahoney JP, Steyaert J, Rasmussen SGF, Sunahara RK, El-Samad H, Huang B, von Zastrow M (2013) Conformational biosensors reveal GPCR signalling from endosomes. Nature 495:534–538.

Jasper JR, Lesnick JD, Chang LK, Yamanishi SS, Chang TK, Hsu SA., Daunt DA, Bonhaus DW, Eglen RM (1998) Ligand Efficacy and Potency at Recombinant α2 Adrenergic Receptors. Biochem Pharmacol 55:1035–1043.

Katritch V, Cherezov V, Stevens RC (2013) Structure-function of the G protein-coupled receptor superfamily. Annu Rev Pharmacol Toxicol 53:531–556.

Katritch V, Fenalti G, Abola EE, Roth BL, Cherezov V, Stevens RC (2014) Allosteric sodium in class A GPCR signaling. Trends Biochem Sci 39:233–244.

Katritch V, Reynolds KA, Cherezov V, Hanson MA, Roth CB, Yeager M, Abagyan R (2009) Analysis of Full and Partial Agonists Binding to β2-Adrenergic Receptor Suggests a Role of Transmembrane Helix V in Agonist-Specific Conformational Changes. J Mol Recognit 22:307–318.

Kenakin TP (1984) The Classification of Drugs and Isolated Tissues Drug Receptors in. Pharmacol Rev 36:165–222.

Kirstein SL, Insel PA (2004) Autonomic nervous system pharmacogenomics: a progress report. Pharmacol Rev 56:31–52.

Knaus AE, Muthig V, Schickinger S, Moura E, Beetz N, Gilsbach R, Hein L (2007) α2-Adrenoceptor subtypes-Unexpected functions for receptors and ligands derived from gene-targeted mouse models. Neurochem Int 51:277–281.

Kobilka BK, Deupi X (2007) Conformational complexity of G-protein-coupled receptors.

Trends Pharmacol Sci 28:397–406.

Krasel C, Bünemann M, Lorenz K, Lohse MJ (2005) β-arrestin binding to the β2-adrenergic receptor requires both receptor phosphorylation and receptor activation. J Biol Chem 280:9528–9535.

Krupnick JG, Goodman OB, Keen JH, Benovic JL (1997) Arrestin/clathrin interaction: Localization of the Clathrin binding domain of nonvisual arrestins to the carboxyl terminus. J Biol Chem 272:15011–15016.

Kupchik YM, Barchad-Avitzur O, Wess J, Ben-Chaim Y, Parnas I, Parnas H (2011) A novel fast mechanism for GPCR-mediated signal transduction--control of neurotransmitter release. J Cell Biol 192:137–151.

Laporte S a, Oakley RH, Zhang J, Holt J a, Ferguson SS, Caron MG, Barak LS (1999) The β2-adrenergic receptor/βarrestin complex recruits the clathrin adaptor AP-2 during endocytosis. Proc Natl Acad Sci U S A 96:3712–3717.

Laporte S a., Oakley RH, Holt J a., Barak LS, Caron MG (2000) The interaction of β-arrestin with the AP-2 adaptor is required for the clustering of β2-adrenergic receptor into clathrin-coated pits. J Biol Chem 275:23120–23126.

Li J, Edwards PC, Burghammer M, Villa C, Schertler GFX (2004) Structure of bovine rhodopsin in a trigonal crystal form. J Mol Biol 343:1409–1438.

Li L, Homan KT, Vishnivetskiy SA, Manglik A, Tesmer JJG, Gurevich V V., Gurevich E V. (2015) G protein-coupled receptor kinases of the GRK4 subfamily phosphorylate inactive GPCRs. J Biol Chem:jbc.M115.644773.

Liu W, Chun E, Thompson A a, Chubukov P, Xu F, Katritch V, Han GW, Roth CB, Heitman LH, IJzerman AP, Cherezov V, Stevens RC (2012) Structural basis for allosteric regulation of GPCRs by sodium ions. Science 337:232–236.

Lohse MJ (1993) Molecular mechanisms of membrane receptor desensitization. Biochim Biophys Acta 1179:171–188.

Lohse MJ, Nuber S, Hoffmann C (2012) Fluorescence/Bioluminescence Resonance Energy Transfer Techniques to Study G-Protein-Coupled Receptor Activation and Signaling. Pharmacol Rev 64:299–336.

Lohse MJ, Vilardaga J-P, Bünemann M (2003) Direct optical recording of intrinsic efficacy at a G protein-coupled receptor. Life Sci 74:397–404.

Luttrell LM, Ferguson SS, Daaka Y, Miller WE, Maudsley S, Della Rocca GJ, Lin F, Kawakatsu H, Owada K, Luttrell DK, Caron MG, Lefkowitz RJ (1999) β-arrestin-dependent formation of β2 adrenergic receptor-Src protein kinase complexes. Science 283:655–661.

Lymperopoulos A, Rengo G, Koch WJ (2013) Adrenergic Nervous System in Heart Failure: Pathophysiology and Therapy. Circ Res 113:739–753.

Mahaut-Smith MP, Martinez-Pinna J, Gurung IS (2008) A role for membrane potential in regulating GPCRs? Trends Pharmacol Sci 29:421–429.

Marrero MB, Schieffer B, Paxton WG, Heerdt L, Berk BC, Delafontaine P, Bernstein KE (1995) Direct stimulation of Jak/STAT pathway by the angiotensin II AT1 receptor. Nature 375:247–250.

Martinez-Pinna J, Gurung IS, Mahaut-Smith MP, Morales A (2010) Direct voltage control of endogenous lysophosphatidic acid G-protein-coupled receptors in Xenopus oocytes. J Physiol 588:1683–1693.

Martinez-Pinna J, Gurung IS, Vial C, Leon C, Gachet C, Evans RJ, Mahaut-Smith MP (2005) Direct voltage control of signaling via P2Y1 and other Gαq-coupled receptors. J Biol Chem 280:1490–1498.

Martinez-Pinna J, Tolhurst G, Gurung IS, Vandenberg JI, Mahaut-Smith MP (2004) Sensitivity limits for voltage control of P2Y receptor-evoked Ca2+ mobilization in the rat megakaryocyte. J Physiol 555:61–70.

McCudden CR, Hains MD, Kimple RJ, Siderovski DP, Willard FS (2005) G-protein signaling: back to the future. Cell Mol Life Sci 62:551–577.

Miller-Gallacher JL, Nehmé R, Warne T, Edwards PC, Schertler GFX, Leslie AG, Tate CG (2014) The 2.1 Å resolution structure of cyanopindolol-bound β1-adrenoceptor identifies an intramembrane Na+ ion that stabilises the ligand-free receptor. PLoS One 9:e92727.

Milligan G, Kostenis E (2006) Heterotrimeric G-proteins: a short history. Br J Pharmacol 147 Suppl :S46–S55.

Mirzadegan T, Benkö G, Filipek S, Palczewski K (2003) Sequence Analyses of G-Protein-Coupled Receptors: Similarities to Rhodopsin. Biochemistry 42:2759–2767.

Miyawaki A (2011) Development of probes for cellular functions using fluorescent proteins and fluorescence resonance energy transfer. Annu Rev Biochem 80:357–373.

Molleman A (2003) Patch Clamping: An Introductory Guide To Patch Clamp Electrophysiology, 1st ed. Chichester, England: John Wiley & Sons, Ltd.

Moreno-Galindo EG, Sánchez-Chapula JA, Sachse FB, Rodriguez-Paredes JA, Tristani-Firouzi M, Navarro-Polanco R a (2011) Relaxation gating of the acetylcholine-activated inward rectifier K+ current (IKACh) is mediated by intrinsic voltage-sensitivity of the muscarinic receptor. J Physiol 7:1755–1767.

Navarro-Polanco R a, Moreno-Galindo EG, Ferrer-Villada T, Arias M, Rigby JR, Sánchez-Chapula JA, Tristani-Firouzi M (2011) Conformational changes in the M2 muscarinic receptor induced by membrane voltage and agonist binding. J Physiol 7:1741–1753.

Navarro-Polanco RA, Aréchiga-Figueroa IA, Salazar-Fajardo PD, Benavides-Haro DE, Rodríguez-Elías JC, Sachse FB, Tristani-Firouzi M, Sánchez-Chapula JA, Moreno-

Galindo EG (2013) Voltage sensitivity of M2 muscarinic receptors underlies the delayed rectifier-like activation of ACh-gated K(+) current by choline in feline atrial myocytes. J Physiol 591:4273–4286.

Nikolaev VO, Bünemann M, Hein L, Hannawacker A, Lohse MJ (2004) Novel single chain cAMP sensors for receptor-induced signal propagation. J Biol Chem 279:37215–37218.

Ohana L, Barchad O, Parnas I, Parnas H (2006) The metabotropic glutamate G-protein-coupled receptors mGluR3 and mGluR1a are voltage-sensitive. J Biol Chem 281:24204–24215.

Okada T, Fujiyoshi Y, Silow M, Navarro J, Landau EM, Shichida Y (2002) Functional role of internal water molecules in rhodopsin revealed by X-ray crystallography. Proc Natl Acad Sci U S A 99:5982–5987.

Okada T, Sugihara M, Bondar A-N, Elstner M, Entel P, Buss V (2004) The retinal conformation and its environment in rhodopsin in light of a new 2.2 A crystal structure. J Mol Biol 342:571–583.

Oldham WM, Hamm HE (2007) How do receptors activate G proteins? In: Advances in protein chemistry, pp.67–93.

Oldham WM, Hamm HE (2008) Heterotrimeric G protein activation by G-protein-coupled receptors. Nat Rev Mol Cell Biol 9:60–71.

Ortega VE (2014) Pharmacogenetics of β2 adrenergic receptor agonists in asthma management. Clin Genet 86:12–20.

Palczewski K (2000) Crystal Structure of Rhodopsin: A G Protein-Coupled Receptor. Science (80-) 289:739–745.

Pierce KL, Lefkowitz RJ (2001) Classical and new roles of beta-arrestins in the regulation of G-protein-coupled receptors. Nat Rev Neurosci 2:727–733.

Pierce KL, Premont RT, Lefkowitz RJ (2002) Seven-transmembrane receptors. Nat Rev Mol Cell Biol 3:639–650.

Pihlavisto M, Sjöholm B, Scheinin M, Wurster S (1998) Modulation of agonist binding to recombinant human alpha2-adrenoceptors by sodium ions. Biochim Biophys Acta 1448:135–146.

Pitcher JA, Fredericks ZL, Stone WC, Premont RT, Stoffel RH, Koch WJ, Lefkowitz RJ (1996) Phosphatidylinositol 4,5-Bisphosohate (PIP2)-enhanced G Protein-coupled Receptor Kinase (GRK) Activity. J Bol Chem 271:24907–24913.

Pitcher JA, Inglese J, Higgins JB, Arriza JL, Casey PJ, Kim C, Benovic JL, Kwatra MM, Caron MG, Lefkowitz RJ (1992) Role of beta gamma subunits of G proteins in targeting the beta-adrenergic receptor kinase to membrane-bound receptors. Science 257:1264–1267.

Pitt SJ, Martinez-Pinna J, Barnard E a, Mahaut-Smith MP (2005) Potentiation of P2Y receptors by physiological elevations of extracellular K+ via a mechanism independent of Ca2+ influx. Mol Pharmacol 67:1705–1713.

Prasher DC, Eckenrode VK, Ward WW, Prendergast FG, Cormier MJ (1992) Primary structure of the Aequorea victoria green-fluorescent protein. Gene 111:229–233.

Rask-Andersen M, Almén MS, Schiöth HB (2011) Trends in the exploitation of novel drug targets. Nat Rev Drug Discov 10:579–590.

Rasmussen SGF et al. (2011a) Crystal structure of the β2 adrenergic receptor–Gs protein complex. Nature 477:549–555.

Rasmussen SGF, Choi H-J, Fung JJ, Pardon E, Casarosa P, Chae PS, Devree BT, Rosenbaum DM, Thian FS, Kobilka TS, Schnapp A, Konetzki I, Sunahara RK, Gellman SH, Pautsch A, Steyaert J, Weis WI, Kobilka BK (2011b) Structure of a nanobody-stabilized active state of the β2 adrenoceptor. Nature 469:175–180.

Rasmussen SGF, Choi H-J, Rosenbaum DM, Kobilka TS, Thian FS, Edwards PC, Burghammer M, Ratnala VRP, Sanishvili R, Fischetti RF, Schertler GFX, Weis WI, Kobilka BK (2007) Crystal structure of the human β2 adrenergic G-protein-coupled receptor. Nature 450:383–387.

Reddy GR, Subramanian H, Birk A, Milde M, Nikolaev VO, Bünemann M (2015) Adenylyl cyclases 5 and 6 underlie PIP3-dependent regulation. FASEB J 29:3458–3471.

Reiter E, Ahn S, Shukla AK, Lefkowitz RJ (2012) Molecular Mechanism of beta-Arrestin-Biased Agonism at Seven-Transmembrane Receptors. Annu Rev Pharmacol Toxicol 52:179–197.

Ribas C, Penela P, Murga C, Salcedo A, García-Hoz C, Jurado-Pueyo M, Aymerich I, Mayor F (2007) The G protein-coupled receptor kinase (GRK) interactome: Role of GRKs in GPCR regulation and signaling. Biochim Biophys Acta 1768:913–922.

Ribeiro FM, Ferreira LT, Paquet M, Cregan T, Ding Q, Gros R, Ferguson SSG (2009) Phosphorylation-independent regulation of metabotropic glutamate receptor 5 desensitization and internalization by G protein-coupled receptor kinase 2 in neurons. J Biol Chem 284:23444–23453.

Rinne A, Birk A, Bünemann M (2013) Voltage regulates adrenergic receptor function. Proc Natl Acad Sci 110:1536–1541.

Rinne A, Mobarec JC, Mahaut-Smith MP, Kolb P, Bünemann M (2015) The mode of agonist binding to a G protein-coupled receptor switches the effect that voltage changes have on signaling. Sci Signal 8:ra110.

Rochais F, Vilardaga J-P, Nikolaev VO, Bünemann M, Lohse MJ, Engelhardt S (2007) Real-time optical recording of β1-adrenergic receptor activation reveals supersensitivity of the Arg389 variant to carvedilol. J Clin Invest 117:229–235.

Sahlholm K, Barchad-Avitzur O, Marcellino D, Gómez-Soler M, Fuxe K, Ciruela F, Arhem P (2011) Agonist-specific voltage sensitivity at the dopamine D2S receptor - molecular determinants and relevance to therapeutic ligands. Neuropharmacology 61:937–949.

Sahlholm K, Marcellino D, Nilsson J, Fuxe K, Arhem P (2008a) Differential voltage-sensitivity of D2-like dopamine receptors. Biochem Biophys Res Commun 374:496–501.

Sahlholm K, Marcellino D, Nilsson J, Fuxe K, Arhem P (2008b) Voltage-sensitivity at the human dopamine D2S receptor is agonist-specific. Biochem Biophys Res Commun 377:1216–1221.

Sahlholm K, Nilsson J, Marcellino D, Fuxe K, Arhem P (2008c) Voltage-dependence of the human dopamine D2 receptor. Synapse 62:476–480.

Sahlholm K, Nilsson J, Marcellino D, Fuxe K, Arhem P (2012) Voltage sensitivities and deactivation kinetics of histamine H3 and H4 receptors. Biochim Biophys Acta 1818:3081–3089.

Saunders C, Limbird LE (1999) Localization and trafficking of α2-adrenergic receptor subtypes in cells and tissues. Pharmacol Ther 84:193–205.

Seoh SA, Sigg D, Papazian DM, Bezanilla F (1996) Voltage-sensing residues in the S2 and S4 segments of the Shaker K+ channel. Neuron 16:1159–1167.

Shenoy SK, Lefkowitz RJ (2003) Multifaceted roles of β-arrestins in the regulation of seven-membrane-spanning receptor trafficking and signalling. Biochem J 375:503–515.

Shenoy SK, Lefkowitz RJ (2005) Seven-Transmembrane Receptor Signaling Through β-Arrestin. Sci STKE signal Transduct Knowl Environ 308:cm10.

Simon MI, Strathmann MP, Gautam N (1991) Diversity of G Proteins. Science 252:802–808.

Stoffel RH, Randall RR, Premont RT, Lefkowitz RJ, Inglese J (1994) Palmitoylation of G Protein-coupled Receptor Kinase, GRK6. J Bol Chem 269:27791–27794.

Sun Y, Huang J, Xiang Y, Bastepe M, Jüppner H, Kobilka BK, Zhang JJ, Huang X-Y (2007) Dosage-dependent switch from G protein-coupled to G protein-independent signaling by a GPCR. EMBO J 26:53–64.

Suwa M, Sugihara M, Ono Y (2011) Functional and structural overview of G-protein-coupled receptors comprehensively obtained from genome sequences. Pharmaceuticals 4:652–664.

Takeda S, Kadowaki S, Haga T, Takaesu H, Mitaku S (2002) Identification of G protein-coupled receptor genes from the human genome sequence. FEBS Lett 520:97–101.

Tate CG, Schertler GFX (2009) Engineering G protein-coupled receptors to facilitate their

structure determination. Curr Opin Struct Biol 19:386–395.

Tuteja N (2009) Signaling through G protein coupled receptors. Plant Signal Behav 4:942–947.

Tuttle RR, Mills J (1975) Dobutamine: development of a new catecholamine to selectively increase cardiac contractility. Circ Res 36:185–196.

Vilardaga J-P, Bünemann M, Krasel C, Castro M, Lohse MJ (2003) Measurement of the millisecond activation switch of G protein-coupled receptors in living cells. Nat Biotechnol 21:807–812.

Violin JD, Ren X-R, Lefkowitz RJ (2006) G-protein-coupled receptor kinase specificity for beta-arrestin recruitment to the beta2-adrenergic receptor revealed by fluorescence resonance energy transfer. J Biol Chem 281:20577–20588.

Vroling B, Sanders M, Baakman C, Borrmann A, Verhoeven S, Klomp J, Oliveira L, de Vlieg J, Vriend G (2011) GPCRDB: information system for G protein-coupled receptors. Nucleic Acids Res 39:D309–D319.

Wang C-D, Buck MA, Fraser CM (1991) Site-directed mutagenesis of α2A-adrenergic receptors: identification of amino acids involved in ligand binding and receptor activation by agonists. Mol Pharmacol 40:168–179.

Warne T, Moukhametzianov R, Baker JG, Nehmé R, Edwards PC, Leslie AG, Schertler GFX, Tate CG (2011) The structural basis for agonist and partial agonist action on a β1-adrenergic receptor. Nature 469:241–244.

Wettschureck N, Offermanns S (2005) Mammalian G Proteins and Their Cell Type Specific Functions. Physilological Rev:1159–1204.

Wieland K, Zuurmond HM, Krasel C, IJzerman AP, Lohse MJ (1996) Involvement of Asn-293 in stereospecific agonist recognition and in activation of the β2-adrenergic receptor. Proc Natl Acad Sci U S A 93:9276–9281.

Winstel R, Freund S, Krasel C, Hoppe E, Lohse MJ (1996) Protein kinase cross-talk: membrane targeting of the beta-adrenergic receptor kinase by protein kinase C. Proc Natl Acad Sci U S A 93:2105–2109.

Wolters V (2014) Rekrutierung der G-Protein-gekoppelten Rezeptorkinase 2 zum M3-ACh-Rezeptor - Identifizierung des Einflusses von Gaq und Erstellung eines kinetischen Modells.

9 Figure index

10 Publications

10.1 Published Abstracts

Birk, A, Rinne, A, Bünemann, M (2014). β_1-adrenergic receptors exhibit voltage-dependence of agonist efficacy. Proceedings of the British Pharmacological Society 12(1): abst023P

Birk A, Rinne A, Ahles A, Engelhardt S and Bünemann M (2013). β_1-adrenergic receptor activation is voltage-sensitive. Naunyn-Schmiedebergs Arch Pharmacol 386: S9

Rinne A, **Birk A**, Bünemann M (2013). The membrane potential acts as an allosteric modulator of the α_{2A} adrenergic receptor. Naunyn-Schmiedebergs Arch Pharmacol 386: S66

Rinne A, **Birk A**, Bünemann M (2012). Voltage-dependent modulation of α_{2A} adrenergic receptor signaling. Naunyn-Schmiedebergs Arch Pharmacol 385: S75

Rinne A, **Birk A**, Bünemann M (2012). Voltage-dependent modulation of α_{2A} adrenergic receptor conformations. Biophysical Journal 102(3):517a

10.2 Journal Articles

Birk A, Rinne A, Bünemann M (2015). Membrane Potential Controls the Efficacy of Catecholamine-Induced β_1-Adrenoceptor Activity. J. Biol. Chem. 290 (45): 27311-27320

Reddy GR, Subramanian H, **Birk A**, Milde M, Nikolaev VO, Bünemann M (2015). Adenylyl cyclases 5 and 6 underlie PIP3-dependent regulation. FASEB J. 8:3458-3471

Rinne A, **Birk A**, Bünemann M (2013). Voltage regulates adrenergic receptor function. Proc Natl Acad Sci USA. 110(4):1536-1541

11 Curriculum Vitae

This page contains personal information. It is therefore excluded from online publication.

Diese Seite enthält persönliche Daten. Sie ist daher nicht Bestandteil der Online-Veröffentlichung

12 Erklärung

Ich versichere, dass ich meine Dissertation

Voltage-dependence of adrenoceptor activity:
Mechanisms and signal transduction

selbstständig, ohne unerlaubte Hilfe angefertigt habe und mich dabei keiner anderen als den von mir ausdrücklich bezeichneten Quellen bedient habe. Alle vollständig oder sinngemäß übernommenen Zitate sind als solche gekennzeichnet.

Die Dissertation wurde in der jetzigen oder einer ähnlichen Form noch bei keiner anderen Hochschule eingereicht und hat noch keinen sonstigen Prüfungszwecken gedient.

Marburg, den 6. November 2015

_____

Alexandra Birk

13 Danksagung

Ich möchte mich ganz herzlich bei Herrn Bünemann dafür bedanken, dass ich die Arbeit an diesem spannenden Thema nach der Diplomarbeit weiterführen konnte. Für die Unterstützung, die vielen guten Ratschläge, das große Engagement und das Vertrauen in mich war und bin ich sehr dankbar. Besonders bedanken möchte ich mich auch dafür, dass ich die Möglichkeit bekommen habe, für einen Forschungsaufenthalt nach Israel zu reisen und dass ich auf vielen nationalen und internationalen Konferenzen meine Forschungsergebnisse vorstellen durfte. Vielen Dank für diese schönen und prägenden Erfahrungen.

Bei allen derzeitigen und ehemaligen Mitgliedern der Arbeitsgruppe möchte ich mich besonders für die gute Zusammenarbeit und das angenehme Arbeitsklima bedanken. An unsere gemeinsamen Ausflüge in den Kletterwald, den Zoo, auf den Klettersteig, nach Göteborg, etc. erinnere ich mich immer sehr gerne zurück. Ich werde Euch vermissen!

Herzlich bedanken möchte ich mich bei Andreas Rinne für die Einarbeitung in die Welt der Elektrophysiologie und die große Unterstützung in technischen und inhaltlichen Fragen.

Vielen Dank, Cornelius, dass Deine Tür für unzählige Fragen immer offen stand und Du auf jede eine Antwort hattest. Vielen Dank auch für die vielen Tipps und Tricks fürs Labor, für diverse Datenbanken, für die Benutzung von Prism und für Vieles mehr.

Liebe Eva-Lisa, es war sehr schön, dass wir solange gemeinsam Rücken an Rücken in diesem tollen Labor gearbeitet haben und dass wir uns auch außerhalb der Arbeit wunderbar verstehen.

Danke liebe Änna, für die schöne gemeinsame Zeit in unserem „royal office“, das wir gerne mit Kate und William geteilt haben. Ich hoffe, mein Nachfolger teilt unsere Freude am englischen Königshaus.

Vielen Dank Michael für den neuen Schwung, den Du mit der Laufgruppe, den Kochabenden und mit Deiner guten Laune in die Gruppe gebracht hast. Vielen Dank auch für die vielen Male, die Du mich nach Hause gefahren hast und für die gemeinsamen Arbeitswochenenden mit Avanti-Essensbestellung.

Vielen Dank Katharina, Susen und Emma für die vielen kleinen Schwätzchen zwischendurch, die Versorgung mit Süßigkeiten und für die aufbauenden Worte, wenn es mal nicht so lief.

I am also very grateful, that Itzchak and Hanna Parnas gave me the opportunity to work in their lab, learn new techniques and meet very helpful and charming people. My special

thanks go to Yair, Ofra and Noa who taught me the methods I needed for my experiments, helped me with them, answered all my questions, showed me the city with its amazing sites and people and made me feel very welcome. Thank you very much for this wonderful experience!

Den vielen lieben Menschen, die ich in meiner Zeit in Marburg kennen und schätzen gelernt habe, möchte ich für die wunderbare Zeit, das gemeinsame Lachen und die gemeinsamen Aktivitäten danken. Auch wenn es mit der Arbeit mal nicht so lief, habt ihr es immer geschafft, meine Stimmung wieder aufzuhellen. Ihr werdet mir sehr fehlen!

Ganz besonders möchte ich Daniel und meiner Familie für die uneingeschränkte Unterstützung danken, die Ihr mir entgegen bringt. Ihr habt immer an mich geglaubt. Vielen Dank dafür!